SOME ASPECTS OF SOIL PHYSICS APPLICABLE TO TRICKLE IRRIGATION

A thesis presented in partial fulfillment
of the requirements for the Degree of
Master of Science
in Soil Science at
Massey University

EWAN RODERICK HARPER

1983

ABSTRACT

Irrigation of crops is one of the more widely used techniques to increase yeilds. Trickle irrigation is one such method and is more suited to horticultural crops. In New Zealand, with horticulture assuming more importance, appropriate methods of design and operation of trickle irrigation systems are required. In this study a simple approximation to Wooding's solution for steady infiltration from a shallow ponded source, much like that found under trickle emitters is examined. This may aid in irrigation design and practice. The approximation also allowed for the development of a method to concurrently measure the saturated hydraulic conductivity and sorptivity from simple field infiltration measurements with a minimum of soil disturbance. Saturated hydraulic conductivities and sorptivities are of great use in soil water studies in general.

A commercial trickle irrigation system was also examined to determine the suitability of such irrigation systems to particular soils, and to examine the present irrigation scheduling. The approximation to Wooding's solution was found to perform well in the field in many respects, particularly in determining steady ponded zone sizes. Ponded zone sizes are important in that they control the volume of soil wetted by irrigation to a large degree. Much of this agreement is due to the use of parameters determined by the simple field method developed from this theory. Sorptivities and saturated hydraulic conductivities obtained by this method were found to be more realistic for trickle irrigation than those determined by other existing methods. Systematic errors in these other methods, mainly soil disturbance and the concomitant creation of continuous flow paths for water, as well as soil smearing, are thought to be the main cause of this difference.

Temporal and spatial variation in soil physical properties are however, found to hinder the use of soil physics theory in the field. Macropores (due to soil biological activity) were found to profoundly influence infiltration processes and soil-water distribution. These effects were particularly marked for the site with a commercial trickle irrigation system. Here the efficiency of the present system is thought to be low, and evidence indicates that irrigation was in excess of plant requirements. The utility of Wooding's solution, and the method to measure soil physical parameters developed from this, is further demonstrated in this orchard.

ACKNOWLEDGEMENTS

I express my sincere thanks to my supervisors Dave Scotter and Brent Clothier for their encouragement, direction and friendship over the considerable period of time it has taken for this study. Also to my parents for their support and unstinting attitude with cheque books. Thanks to John Kirkman for his efforts on my behalf, and the staff of Plant Physiology Division, DSIR, for their help and use of facilities.

Thanks also to F.Z., Sir Henry and Marty for the inspiration necessary.

For the typing (above and beyond the call of normal duty, in a precarious state) I wish to thank Liz Wills.

TABLE OF CONTENTS

Page

Page

LIST OF FIGURES

Page

Page

Page

Page

Page

Page

LIST OF TABLES

LIST OF SYMBOLS

		UNITS
a	dimensionless parameter (equation 1.13)	-
C	correction for mercury depression in capillary tube	kPa
C_k	dimensionless parameter (equation 2.5)	-
C_ϕ	dimensionless parameter (equation 2.7)	-
CV	coefficient of variation	-
d	drainage rate	mm day^{-1}
D	soil-water diffusivity	$m^2 s^{-1}$
D_*	constant soil-water diffusivity	$m^2 s^{-1}$
Ep	pan evaporation	mm day^{-1}
ET	evapotranspiration	mm day^{-1}
f	empirical constant	-
F	dimensionless flux (equation 1.13)	-
G	probability density function	-
h	mercury height in capillary tube	m
H	ponding height in auger hole	m
I	irrigation rate	mm day^{-1}
J	drainage flux (equation 4.1)	mm day^{-1}
k	hydraulic conductivity function	m s^{-1}
k_n	hydraulic conductivity at the antecedent water content	m s^{-1}
k_s	saturated hydraulic conductivity	m s^{-1}
n	sample size	-
N	sample size required to be within a set interval of the mean	-
p	porosity	-
PWP	permanent wilting point	mm
q	soil-water flux density	m s^{-1}
q	steady-state soil-water flux density	m s^{-1}
Q	flow or discharge rate	$m^3 s^{-1}$
Q_B	buffered flow rate	$m^3 s^{-1}$
r	radial distance	m
r_e	radius at which two terms of equation (1.14) are equal	m
r_{max}	maximum ponded radius when flow is due solely to gravity	m
r_o	cavity radius	m
r_p	ponded radius	m

		UNITS
r_u	steady-state ponded radius	m
r_w	wetted radius	m
r_{xy}	correlation coefficient	-
R	dimensionless radius	-
RF	rainfall rate	mm day^{-1}
s	standard deviation	-
s_e	standard error	-
s_{ln}	log-normal distribution standard deviation	-
$S(\theta_s, \theta_n)$	sorptivity	m $s^{-\frac{1}{2}}$
St(n)	soil-water storage on day n	mm
ΔSt	change in soil water storage	mm day^{-1}
t	time	s
t_*	calculated characteristic time toward steady-state	s
T	time to steady-state	s
TWHC	total water holding capacity of soil	mm
W	water content increment from irrigation	m^3
x	horizontal distance	m
x	mean value	-
y	horizontal distance (normal to x)	m
z	depth	m
z_w	wet front depth	m
Z	dimensionless depth	-
α	slope of the exponential conductivity function (equation 1.7)	m^{-1}
θ	volumetric water content	-
θ_{FC}	volumetric water content at field capacity	-
θ_n	antecedent water content	-
θ_s	satiated water content	-
$\Delta\theta$	change in profile water content	mm
ρ_b	dry bulk density	kg m^{-3}
ρ_s	particle density	kg m^{-3}
ϕ	matric flux potential (equation 1.5)	$m^2 s^{-1}$
ϕ_s	satiated matric flux potential (equation 1.10)	$m^2 s^{-1}$

		UNITS
Ψ	soil-water potential	kPa
Ψ_t	total soil-water potential	kPa

CHAPTER 1

TRICKLE IRRIGATION: BACKGROUND AND THEORY

1.1 INTRODUCTION

Irrigation, either to increase existing yields, or to allow development of previously barren areas has been practiced since at least 4000 B.C. (Jensen, 1980). Traditional methods, such as flood and furrow irrigation comprise most of the world's irrigated area, estimated in 1977 to be 223 million ha (FAO, 1977). These traditional methods supply water to plants in such a way that often 40 to 60% of applied water may drain from the root zone (Raats, 1974). In such cases soil storage capacity and plant drought tolerance are of prime importance (Rawlins, 1973). Technological developments over the last century have resulted in "high frequency irrigation" systems, which supply small amounts of water regularly to the root zone. Examples of such systems are trickle or trickle-drip systems, and mini-sprinkler systems. These systems may result in reduced drainage losses and reduce dependence on soil and plant characteristics.

In areas where intensive horticulture is practiced, such as in New Zealand, trickle irrigation is one of the more commonly used high frequency irrigation systems. The total global area estimated to be irrigated by this method in 1979 was 130,000 ha (Bresler, 1977). With the increasing importance of horticulture, techniques of design and operation, and methods of assessing the suitability of such systems are required. In the following sections of this chapter the principles and benefits of high frequency irrigation are discussed. Soil physics theory applicable to trickle irrigation is also introduced.

1.2 IRRIGATION

1.2.1 GENERAL INTRODUCTION

Surface irrigation imposes two fundamental constraints on irrigation management (Rawlins and Raats,1975). Firstly flow over the soil surface is required to distribute water, and so a minimum depth of water is needed simply to achieve uniform coverage. The large spatial

variability in infiltration rates, even over a small area (e.g. Nielsen et al. 1973; Vieira et al. 1981), also results in large amounts of water being necessary to recharge the soil evenly over the total irrigated area. Those areas with the lowest infiltration rate then determine the total depth of water needed. Secondly fixed labour and material costs are associated with each application. Both these constraints make it economically advantageous to decrease the number of applications, by increasing the time between irrigations. This method of irrigation scheduling, commonly used for flood, furrow and hand portable sprinkler systems, is termed low frequency irrigation. Use of this method requires a substantial soil-water storage capacity and may often rely on the drought tolerance of the crop (Rawlins, 1973). The major process within the irrigation cycle is plant (root) extraction of water.

More recently developed irrigation systems (e.g. trickle, basin, solid-set and centre-pivot spray irrigation systems) have little or no additional cost associated with each application, and may result in a more uniform distribution of water to the root zone. These systems can be operated more frequently so as to match plant water usage. This method of irrigation scheduling, termed high frequency irrigation (HFI), lessens the dependence on crop drought tolerance and soil storage capacity. The irrigation process is "infiltration dominated", in contrast to the "extraction dominated" low frequency irrigation systems discussed previously. The consequences of this fundamental change in irrigation method, with emphasis on trickle irrigation, are covered in the following sections.

1.2.2. HIGH FREQUENCY IRRIGATION: THEORETICAL CONSIDERATIONS

The physical basis of the advantages (and disadvantages) obtained using HFI are discussed below. Specific advantages and disadvantages of trickle irrigation are discussed in the following sections.

High frequency irrigation has been examined, using simple one-dimensional analyses by Rawlins (1973), Raats (1974) and Rawlins and Raats (1975). The basis of these studies is that high frequency pulses of water (of the order of one per day) are dampened within a few centimeters of the source (Gardner, 1964; Zur and Savaldi, 1977). Steady flow can reasonably then be assumed to exist. The simplest of these analyses is that of Rawlins (1973), which assumes steady downward flow in a homogeneous soil, due solely to gravity (i.e. matric potential gradients are neglected). Steady evaporative demands are represented by a root water extraction pattern that is considered to decrease exponentially with depth. Exponential decreases in root density are frequently found in the field (Scotter, 1976). As water is extracted by roots, the volumetric water content (θ) decreases. Thus the flux downwards, which is considered numerically equal to the hydraulic conductivity (k), also decreases. If the flux at the surface is far in excess of transpiration, there will be extensive drainage beyond the root zone (at some arbitrary depth of the exponential function). However, if the surface flux is matched to the transpiration demands, drainage losses can be small. Although θ in the root zone can be high, k often decreases rapidly with decreasing θ, so consequently drainage can be kept to a minimum. This is shown clearly in Figure 3 of Rawlins (1973), and is also demonstrated by Raats (1974) and Rawlins and Raats (1975).

These latter two analyses, although still assuming both steady surface fluxes and transpirational demands, as well as an exponential root water extraction function, also account for matric potential gradients. Both these analyses examine the effect of salts in the irrigation water as well. Effects such as active exclusion of solutes by roots, and soil-solute interactions which may be important (Nye, 1979) are however not included. It is found that soil solution salt concentrations can be kept low, in the order of 2 to 3 times the concentration of the irrigation water, by adjusting surface fluxes to allow

drainage of the concentrated salt solution. While salinity control is of little importance in New Zealand, the implications of this theory to root-zone fertilizer concentration are of significance. This is discussed briefly in later sections.

1.2.3 BENEFITS AND DISADVANTAGES OF HIGH FREQUENCY IRRIGATION

(a) Benefits:

The following list of benefits can accrue from HFI.

(i) High soil-water potential: As the frequency of irrigation increases, the time average soil-water potential increases. (Note that dry soils have more negative potentials.) Thus HFI eliminates the large fluctuations in soil-water potential (Ψ) of low frequency irrigation (Bresler and Yaron,1972). While some early studies indicate transpiration does not appear to decrease until the "Permanent Wilting Point" is reached (e.g. Veihmeyer and Hendrickson, 1927), these should be treated with caution. Evidence indicates that lowering of θ, even at the wet end of the range, may lead to a reduction of photosynthesis and eventually in growth (Gardner and Millar, 1973). It is now generally accepted that crop growth only proceeds unimpaired when θ is reasonably high (Bresler, 1977). Plant yield, and possibly product quality are only maximal when θ is continually high (Slatyer, 1969; Hsiao, 1973), unless a stress period is necessary for differentiation or fruit set (Salter and Goode, 1967). High time average soil water contents may also lead to improved yields through extreme temperature fluctuations being reduced (Freeburg et al. 1974).

(ii) Reduced water usage: HFI techniques when properly managed can reduce water usage. As application rates can be kept low, drainage beyond the root zone can be restricted. Although the wetted soil volume is often restricted for some HFI methods (e.g. trickle and small spray systems), reducing water usage, this may have little or no detrimental effect on plant yield. Transpiration and

growth rates decline little with large decreases in wetted root volumes, (e.g. Black and West, 1974; Frith and Nichols, 1974). Water savings can also be made by irrigating at rates less than the soils ability to absorb free water. By maintaining unsaturated flow runoff is minimized and flow down macropores and its deleterious consequences (e.g. Thomas and Phillips, 1979) are reduced.

(iii) Use of otherwise unsuitable soils: As application rates can be tailored to meet evapotranspirative demands with little drainage, soils with low water holding capacities (e.g. coarse textured soils) can be irrigated. Saline soils can also be irrigated if application rates are sufficient to flush salts from the root zone.

(iv) Improved nutrient status: Both the above mentioned analyses and more complex models (e.g. Bresler, 1975) demonstrate that solutes can be either flushed from, or retained within the root zone depending on application rate relative to the soils permeability. With low frequency irrigation leaching may be extensive due to excess drainage during and immediately following irrigation. With high water contents both root penetration and nutrient diffusion to roots are also enhanced. (Rawlins and Raats, 1975).

(b) Disadvantages:

While the disadvantages listed below can be minimized by good management of HFI systems, they deserve consideration.

(i) Poor soil aeration: If water contents are maintained too high oxygen diffusion within the soil may be reduced. Elimination of soil oxygen (i.e. anaerobic root zone conditions) has been found to cause stomatal closure, even at optimal soil water potentials (Sojka and Stolzy, 1980). This can result in fruit drop (Salter and Goode, 1967), impaired yields (e.g. Gur et al. 1979) or possibly plant death.

(ii) Reduced rooting volumes: While reduced root volumes can operate effectively, plant anchorage may suffer as a consequence. With smaller root volumes crop susceptibility to irrigation system breakdown is also increased, and nutrient availability is decreased. Where irrigation is supplementary to rainfall these disadvantages may be negligible, with roots extending throughout large portions of the soil in response to natural water content distributions.

(iii) Salt accumulations: Salts may accumulate at the edge of wetted volumes when solute concentrations in the soil or irrigation water (e.g. when fertilizer is added) are high. In these cases it may be necessary to flush these accumulations at some stage to prevent rain washing them into the root zone, leading to osmotic shock (Bresler, 1977). This will be of more importance when irrigated volumes are small such as for trickle and mini-sprinkler installations.

1.2.4 TRICKLE IRRIGATION

(a) Physical Aspects

Although trickle irrigation was originally developed as a subsurface method in glasshouses in Germany (Howell et al. 1980), it appears to first been applied outdoors in Israel in the early 1960's (e.g. Celestre, 1964). Trickle irrigation involves the slow application of water from an emitter onto the soil surface. As the emitters are attached to supply pipes, this method is more suited to row crops (e.g. orchards and vineyards) than to densely planted crops.

Application of water from a single point onto the soil surface leads to wetted soil volumes being restricted both radially and vertically. Soil surface physical properties are critical in determining the area over which infiltration will take place, and hence the wetted soil volume. While highly permeable soils may have very small ponded zones, infiltration almost occurring from a point source (e.g. Roth, 1974), most soils have a ponded zone

ranging from 10 cm to 1 m in diameter. The shape of this pond is controlled by surface topography. Ponded zones typically increase in size as infiltration proceeds, until a final steady-state is achieved, in response to declining matric potential gradients. An upper limit to the ponded zone size can be found simply by assuming matric potential gradients to be non-existent. In this case fluxes will be due solely to gravity and hence a maximum radius (r_{max}) is given by:

$$r_{max} = (Q/\pi k_s)^{\frac{1}{2}}. \qquad (1.1)$$

Here Q is emitter discharge (in $m^3 s^{-1}$).

In coarser textured soils k_s is frequently large, and the final ponded zone size small (see Figure 1.1). Increasing Q will lead to a larger ponded zone, although longer times are then required to attain a final size (Brandt et al. 1971: Bresler et al. 1971; Levin et al. 1979). In some field cases (Earl and Jury 1977) times to attain a steady ponded zone size are large, in excess of a day. This contrasts with numerical simulations and other field studies. This difference is thought to be due to surface slaking and crusting. Numerical simulations for soils with different textures show coarser soils to obtain steady ponded zone sizes more rapidly than finer soils (see Figure 1.1).

As mentioned, the size of the ponded zone is important in that it controls the wetted volume to a large extent. Adjusting Q, or the length of application will allow lateral flow to be controlled to some extent. Typically wetted zones (and water content distributions) in vertical cross-section are semi-circular at short times, and elliptical at long times when gravity begins to dominate flow patterns at shorter times, the vertical extent of flow is greater than that for finer soils. This is a response to both decreased capillarity and decreased ponded zone sizes for similar discharge rates. Similarly for higher Q

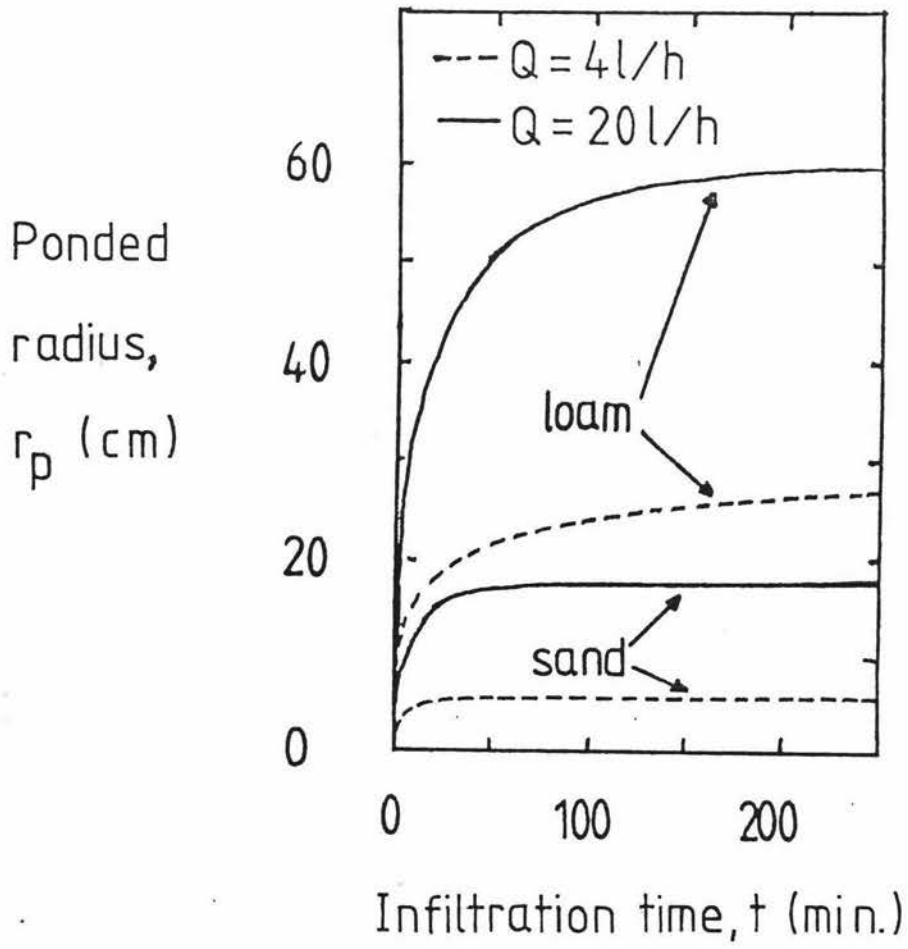

Fig. 1.1 Ponded radius (r_p) as a function of infiltration time for two soils and two discharges. Results are from numerical simulation. After Bresler (1978).

wetted zones are shallower (for a given amount of water applied), due to increased ponded zone sizes. These trends are clearly seen in Figure 1.2. Total wetted soil volumes, however, decrease with decreasing Q, and the water content distribution within that volume tends to be more uniform (Levin et al. 1979).

Pulsing applications has a similar effect to lowering Q (Levin et al. 1979). In this case the steady ponded zone size is rapidly attained by sequential pulses due to a high antecedent water content (θ_n).

At the completion of irrigation, redistribution of the applied water begins. Little research has been carried out on redistribution from trickle sources, due to both the complexity of the process and the greater importance of infiltration. While vertical drainage is sometimes considered (e.g. Tsipori and Shimshi, 1979), the effect of lateral redistribution is generally neglected. While some studies indicate that lateral redistribution is generally neglected. While some studies indicate that lateral redistribution after irrigation is appreciable (e.g. Levin et al. 1979; Bar-Yosef and Sheikholslami, 1976: Mostaghimi et al. 1981), others demonstrate that this phenomonen may be of little consequence (e.g. Curtis and Watson, 1979). It appears likely that lateral redistribution will be of less significance in field situations, since wetted volumes are large, and large volumes of water are required to raise water contents by even small amounts at large distances away from the emitter.

Also in the field irrigation is usually frequent, whereas in many of the above studies irrigation was into an initially dry soil, so steady-state water content distributions may not have been attained. With frequent irrigation steady ponded zone sizes and wetted volumes are likely to be attained quickly.

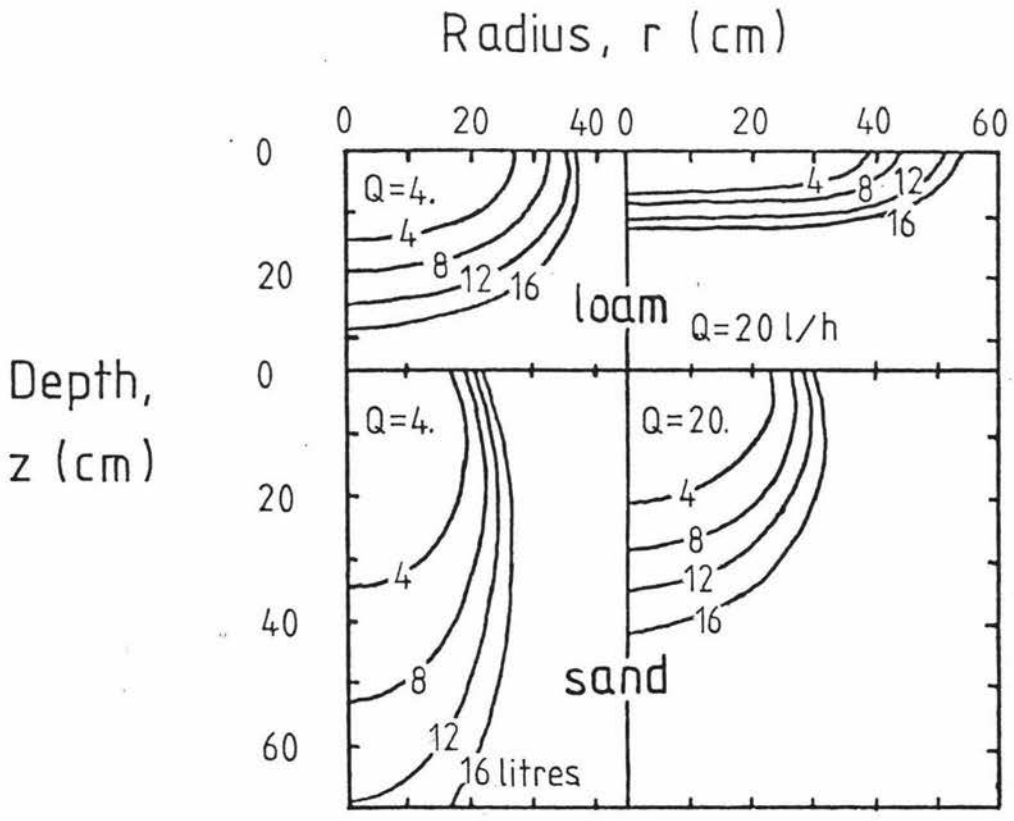

Fig. 1.2 Wetting front position as a function of infiltration time and cumulative infiltration water (in litres) indicated by the numbers labelling the lines, for two soils and two discharges. Results are from numerical simulation. After Bresler (1978).

While trickle irrigation shares the benefits (and drawbacks) of other HFI systems discussed previously, others are unique to this method. Some studies (e.g. Bresler, 1977; Howell et al. 1980; Bucks et al. 1982) have discussed these in detail. Salient points are listed below.

(b) Benefits

(i) Increased yields: While HFI often gives higher yields than low frequency irrigation, crop yields between high frequency irrigation methods, under similar management are comparable (e.g. Bernstien and Francois, 1973; Bucks et al. 1974; Hiler and Howell, 1973; Freeman et al. 1976). With adequate irrigation, increasing trickle irrigation frequency has been found to both increase (Goldberg and Shmueli, 1970; Levin et al. 1974) and to have no effect on yield (Earl and Jury, 1977). The above results highlight the need for efficient management of HFI systems. With efficient management trickle irrigation is one of the most useful methods of increasing crop yields (Tsipori and Shimshi, 1979), the flexibility in design available (Q, length of application, and emitter spacing and number all being variable) allows for a variety of configurations and crop factors to be accommodated.

(ii) Reduced water usage: Trickle irrigation restricts wetted zones horizontally. This can save water through reduced evapotranspiration and drainage from non-cropped areas. Run off and spray wind drift are non-existent (of sprinklers). Water May also be saved when crops are immature by lowering applications to wet smaller soil volumes (Howell et al. 1980).

(iii) Other factors: With trickle irrigation it is possible to fertilize or apply herbicides and fungicides directly to crop roots through the irrigation system. This can result in considerable savings of labour and materials (Bresler, 1977). Foliage is dry with trickle irrigation, and this may help to prevent leaf diseases that

rely on humidity for propagation. When emitters are located in rows, non-irrigated areas may be extensive. This allows freedom of movement for machinery. Labour costs can be reduced with automatic operation, and energy costs can be lower due to the low operational pressures required (Bresler, 1977).

(c) Drawbacks

(i) Emitter clogging: Emitters can be clogged if adequate filtering is not used. When there are few emitters per plant, this may have serious consequences for those plants which are adjacent to the affected emitter.

(ii) Cost: While trickle irrigation may be a low cost option for sparsely planted crops (Levin et al. 1974), the high cost of emitters can make it unsuitable for densely planted crops.

(iii) Small wetted areas: Considering the relatively small soil volume wetted by trickle irrigation, careful monitoring of soil water status is needed to maintain high yields, yet minimize drainage losses. For many crops, especially orchards, lysimeters are impractical due to the volume of soil in the root-zone of each plant (Howell et al. 1980). Techniques such as tensiometry, gravimetric sampling, neutron probing or the use of water balances are necessary. The problems associated with the use of these methods when wetted volumes are restricted are discussed in Chapter 4.

(iv) Design: To obtain the full benefits of trickle irrigation, system design is of paramount importance. The main design problem associated with trickle irrigation is selecting the proper combination of emitter spacing and discharge for a given soil and crop (Bresler, 1977; 1978). While several techniques already exist, it is best to use those based on physical theory, rather than solely on empirical methods, so design methods are more universally applicable. As infiltration is the dominant process in

trickle irrigation, theory describing the infiltration process is important. Existing theory which may be of use in designing and operating trickle irrigation systems is discussed in the following sections.

1.3 SOIL PHYSICS THEORY APPROPRIATE TO TRICKLE IRRIGATION.

1.3.1 INTRODUCTION

Water distribution from a trickle source is best described using a three-dimensional geometry. For homogeneous, stable soil, combination of Darcy's law with a continuity expression gives the flow equation (Philip, 1969);

$$\partial\theta/\partial t = \nabla (k\nabla\Psi) - (\partial k/\partial z). \qquad (1.2)$$

Here θ is the volumetric water content, t is time, k is the unsaturated hydraulic conductivity, Ψ the matric potential, and z the vertical space co-ordinate, taken positive downward. The horizontal space co-ordinates are x and y. Radial co-ordinates, defining $r = (x^2 + y^2)^{\frac{1}{2}}$, can also be used if the flow is axis-symmetric.

Equation (1.2) can also be written in terms of the soil-water diffusivity, D, as;

$$\partial\theta/\partial t = \nabla (D\nabla\theta) - (dk/d\theta).(\partial\theta/\partial z). \qquad (1.3)$$

The diffusivity is defined by;

$$D = k\,(d\Psi/d\theta). \qquad (1.4)$$

Both D and k usually have a strong functional dependence on θ (or Ψ) and impart on equations (1.2) and (1.3) a highly non-linear nature. Unless simplifying assumptions are made, numerical techniques must be used to solve equations (1.2) and (1.3). Solutions which may be of use for trickle irrigation design and management are discussed in the following sections.

1.3.2 NUMERICAL SOLUTIONS

Equations (1.2) and (1.3) when applied to infiltration from a point source and subject to suitable initial conditions, can at present only be completely solved by numerical means. Three-dimensional infiltration was first simulated by Brandt et al. (1971), using both cylindrical and plane flow models, the source being a finite sized ponded zone expanding with time as matric-potential gradients decreased. While few comparisons have been made between numerical results and experimental data (Bresler, 1977), both field and laboratory studies show good agreement with this and similar models, (e.g. Bresler et al. 1971; Ben-Asher et al. 1978). Similar models have also been used (Bresler, 1975) to simulate simultaneous water and solute movement. Experimental evidence (Bresler and Russo, 1975: Levin et al. 1979) also validates this model. Redistribution can also be studied with these models, by simply extending calculations and accounting for hysteresis, so that the wetted portions begin to drain after cessation of irrigation (e.g. Curtis and Watson, 1979). Few, if any, simulations of three-dimensional infiltration with plant uptake have been undertaken. This is most probably due to the complexity of the processes involved. Results from numerical studies have been summarized and presented by Bresler (1977; 1978).

1.3.3 QUASI-ANALYTICAL AND ANALYTICAL SOLUTIONS

(a) Introduction:

Analytical solutions to the flow equation are those where the solution is found completely by mathematical analysis. Quasi-analytical solutions are those which have the basic form found by mathematical analysis, but some numerical means may have to be utilized to evaluate necessary coefficients or impressions (Philip, 1969). Most of the solutions outlined below are analytical (or exact) solutions.

Few, if any, analytical or quasi-analytical solutions for redistribution, root uptake or soil evaporation using three dimensional geometries are to be found in the literature. This may be due to the complexity of these phenomena. Existing one-dimensional solutions for plant uptake (e.g. Lomen and Warrick, 1978), drainage (Sisson et al. 1980), and evaporation (e.g. Gardner, 1958) may be used where emitter spacing and discharge is such that one dimensional flow effectively exists. Commonly used one-dimensional infiltration solutions (e.g. Philip, 1957) along with more recently developed theories such as that for pulsed flow (Zur and Savaldi, 1977) could also be used in such circumstances. However, where emitters are isolated, multi-dimensional infiltration solutions will be of more use. These are discussed below.

(b) Multi- dimensional transient absorption and infiltration solutions:

Much of the early infiltration theory is summarized by Philip (1969). The earliest multi-dimensional solution is that of Philip (1966) which models absorption (i.e. with gravity neglected) and infiltration from buried cavities. An exact series solution is given for absorption as well as two approximate solutions. The approximations concern the shape of the diffusivity function. Both "linear" (diffusivity constant with θ) and delta-function diffusivities (a Green and Ampt (1911) diffusivity) are used. These two diffusivities delineate the envelope of possible behaviour of all soils. Field and laboratory tests (Peck and Talsma, 1968; Talsma, 1969;1970) validate these solutions for short times. Transient and steady long time infiltration solutions using delta-function diffusivities are not given, being complex and of doubtful physical meaning (Philip, 1969). The exact solutions in a series form have not been used to date, as they require complex calculations and may only be useful for short times. Two- and three-dimensional long time steady infiltration solutions also exist (Philip, 1969) but have not been tested to date.

Multi-dimensional absorption for constant flux from a cavity has recently been studied (Parlange, 1973; Philip and Knight, 1974) by quasi-analytical means. The utility of the Philip-Knight technique relies on the definition of a flux-concentration parameter, which is little affected by diffusivity form, or time (White, 1979). Easily evaluated expressions for water content profiles (which are obviously arcs of a circle) for any diffusivity result. Laboratory tests (Clothier and Scotter, 1982) show good agreement with this theory in a fine sand for times up to 100 mins ($Q = 10^{-7} m^3 s^{-1}$). Constant-flux solutions, such as this theory, are more applicable to trickle irrigation than previously mentioned constant-concentration solutions, due to the flux controlled nature of trickle systems. However, this approach cannot account for gravity and so is restricted in its utility.

(c) Linearized infiltration solutions: The linearization procedure, and point and line source solutions.

A large class of multi-dimensional solutions to the flow equation result from a linearization technique developed by Philip (1968a). These solutions are summarized by Merril et al. (1978) and Raats and Warrick (1980). The first step in this procedure is the introduction of the "matric flux potential" (Raats, 1971) defined as:

$$\phi = \int_{\Psi_n}^{\Psi} k d\Psi = \int_{\theta_n}^{\theta} D d\theta. \qquad (1.5)$$

Provided k (and D) is a single-valued function of Ψ, such as during infiltration, then differentiation and substitution of (1.5) into (1.2) gives:

$$\partial\theta/\partial t = \nabla^2\phi - (1/k)(dk/d\Psi)(d\phi/dz). \qquad (1.6)$$

Further simplification is possible if it is assumed that k is given by the exponential function proposed by Gardner (1958):

$$k = k_0 \exp(\alpha\Psi). \qquad (1.7)$$

It follows that;

$$\phi = (k - k_n)/\alpha, \qquad (1.8a)$$

and that if the soil is quite dry (i.e. $\Psi_n \rightarrow -\infty$) then:

$$\phi = k/\alpha. \qquad (1.8b)$$

Equation (1.6) reduces to (Philip, 1969):

$$(d\theta/d\phi)(\partial\theta/\partial t) = \nabla^2\phi - \alpha(d\phi/dz). \qquad (1.9)$$

In equation (1.7) α is the constant in the exponential conductivity function, and for a ponded source k_o is sensibly the saturated hydraulic conductivity k_s.

The constant α indicates the importance of capillarity. Coarse soils, where k declines rapidly with Ψ, have numerically large α values. Measured α values from many studies, as summarized by Bresler (1978), lie between 0.07 and 170 m^{-1}. Large variations in α are found for single texture classes. Correlation coefficients (for goodness of fit of conductivity data to equation (1.7)) are also variable, indicating that the exponential conductivity function does not always describe laboratory and field results. However, with high frequency irrigation Ψ may vary over only a small range, within which k may appear to be exponential.

The first three dimensional solution using this linearization procedure is that of Philip (1968b) for steady-state infiltration. In this case the left hand side of equation (1.6) is zero. Both buried point and buried spherical cavity (approximate) solutions are given. In the latter differences in gravitational head within the cavity were neglected. Analysis by Parlange (1974) shows this omission may be important. Steady infiltration solutions for surface point sources, which are more directly applicable to trickle irrigation, are given by Raats (1971). A general theorem extending any buried source solution to the surface was developed by Philip (1971). More recently point source solutions for steady infiltration in systematically heterogeneous soils

(specifically k varying exponentially with depth) have been presented (Philip, 1972; Philip and Forrester, 1975) and tested Merrill et al. (1978). Many other solutions for steady infiltration from strip and line sources exist, and are listed in Table 1.1. Several of these include phenomena such as uptake of water by plants (e.g. Gilley and Allred, 1974) and layered soils (e.g. Dirksen, 1978).

(d) Linearized infiltration solutions: Disc sources and time dependent infiltration.

Possibly the most useful steady-state infiltration solution for trickle irrigation is that of Wooding (1968), for infiltration from a shallow circular pond. Two boundary conditions are involved in this solution. First, over the region wetted by the shallow pool of negligible hydraulic head, θ is constant and equal to the satiated (following Brutsaert, 1979) water content, θ_s. Hence ϕ becomes ϕ_s, defined by:

$$\phi_s = \int_{\theta_n}^{\theta_s} D d\theta. \qquad (1.10)$$

Secondly over the non-wetted region, assuming evaporation is negligible, the vertical flux at the surface can be taken as zero. For this region the downward flow is given by:

$$k(\partial\Psi/\partial z) = \partial\phi/\partial z = k. \qquad (1.11)$$

Using equation (1.8) then gives:

$$\partial\phi/\partial z = \alpha\phi.$$

Both boundary conditions are then linear in θ.

Wooding's complete solution is in terms of a complex series. Results are shown in Figures 1.2 and 1.3. Here the dimensionless variables are $a = \alpha r_u/2$ where r_u is the steady-state ponded radius, $R = \alpha r/2$ and $Z = \alpha z/2$. Figure 1.2 effectively shows water content distributions, in the form of ϕ/ϕ_s, for two values of a. As a increases, indicative of coarser soils, the region of ϕ/ϕ_s elongates

Table 1.1 Chronological list of Two and Three Dimensional Solutions of the Moisture Flow Equation (1.2) using the Linearizing Assumption of $k = k_s \exp(\alpha \Psi)$.

1. Philip (1968b). Single, buried point sources and spherical cavities.
2. Wooding (1968). Single disc source.
3. Philip (1969). Single buried line source.
4. Raats (1970). Array of surface line sources.
5. Philip (1971). Surface sources.
6. Raats (1971). Single surface point sources.
7. Philip (1972). Buried, surface and perched sources in hetereogeneous soils.
8. Raats (1972). Sources buried at some distance below the soil surface.
9. Maaledj and Malavard (1973). Influence of impermeable layers.
10. Zachmann and Thomas (1973). Array of buried line sources.
11. Gilley and Allred (1974). Array of buried line sources, including influence of uptake of water by plants.
12. Lomen and Warrick (1974). Line Sources (Includes time dependence).
13. Parlange (1974). Correction due to gravity for cavities.
14. Thomas et al. (1974). Array of buried line sources.
15. Warrick (1974). Point sources (Includes time dependence).
16. Philip and Forrester (1975). Buried, surface and perched points in heterogeneous soils.
17. Lomen and Warrick (1976). Summary paper; includes ring sources.
18. Warrick and Lomen (1976). Strip and disc sources (Includes time dependence).
19. Raats (1976). Summary paper; includes flow to line sinks.
20. Thomas et al. (1976). Array of buried line sources; includes comparison with experiment.

20. Thomas *et al.* (1976). Array of buried line sources; includes comparison with experiment.
21. Batu (1977, 1978). Line and strip sources.
22. Warrick and Lomen (1977). Line above a shallow water table.
23. Lomen and Warrick (1978b). Surface flux proportional to k.
24. Raats (1977). Laterally confined flows from sources and to sinks.
25. Warrick and Amoozegar - Fard (1977). Water regimes for porous cup samplers.
26. Thomas *et al.* (1977). Line sources, plant uptake measurements.
27. Merrill *et al.* (1978). Point sources on a heterogeneous column, including cyclic application; includes comparison with experiment.
28. Dirksen (1978). Basically confined, buried line sources in homogeneous and layered soils.
29. Warrick *et al.* (1979). Line sources with extraction and design nomographs.

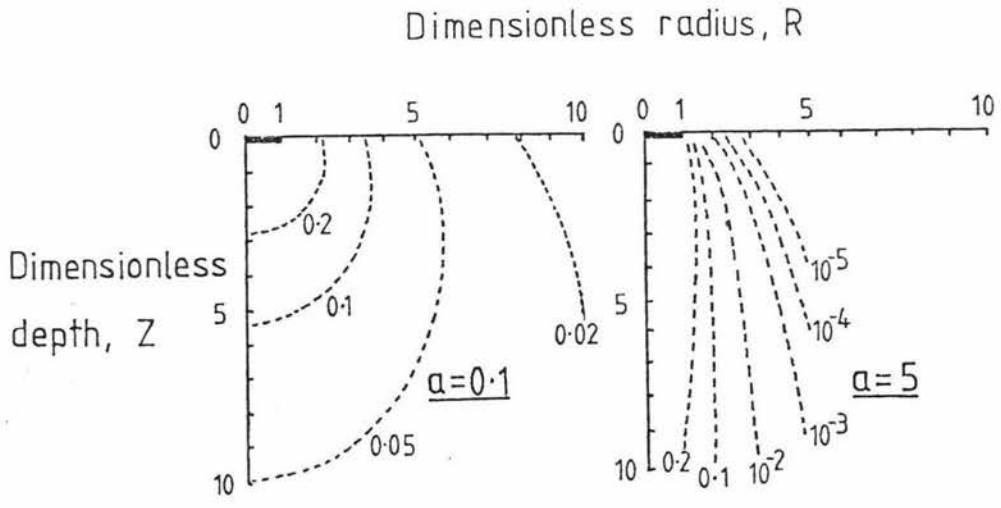

Fig. 1.3 Dimensionless matric flux potential (ϕ/ϕ_s) for two values of a plotted with dimensionless radius (R) and depth (Z). Increasing a indicates a more rapidly decreasing hydraulic conductivity (i.e. coarser soil texture). Ponded zones are shown by the dark areas from R = 0 to R = 1. After Wooding (1968).

downwards as the soil below the source becomes progressively wetter. At the same time the soil becomes drier near the surface beyond the ponded zone. It is a simple process to convert ϕ/ϕ_s to either θ or Ψ using equation 66 of Wooding (loc. cit.). Figure 1.3 shows the total dimensionless flux from Woodings solution, F, plotted against a for various numbers of terms retained from the complete series solution. The breakdown of the series solution above a = 6.5 appears inevitable, as more than 6 terms leads to divergence. However, this solution is quite stable for $a \leqslant 5, (\alpha r_u \leqslant 10)$, even for a low number of terms. With α commonly ranging up to 30 m^{-1} (Table 1; Bresler, 1978) this means sources up to 0.33 m in radius and larger (with decreasing α) can be accommodated. This range will allow most trickle irrigation systems to be described by this theory.

However, the remarkable feature of this solution is the close correspondence to the simple expression (see Figure 1.3);

$$F = 2\pi a + 4. \qquad (1.13)$$

Equation (1.13) can be written in terms of the actual discharge, Q, as;

$$Q = \pi r_u^2 \phi_s + 4\phi_s r_u \qquad (1.14)$$

or equivalently by using equation (1.8b);

$$Q = \pi r_u^2 k_s + 4k_s r_u/\alpha . \qquad (1.15)$$

In equations (1.13) through (1.15) the first term on the right hand side represents the flow under the pond from gravity alone, and will vary with the size of the source area, (i.e. the ponded radius squared). The second term is the flow due to capillarity, so that the contribution of this term varies as the radius or circumference, indicating a dominance in the edge regions. This second term corresponds to the steady-state solution for absorption alone from a shallow circular pond (Philip, 1969). Equation (1.15) in effect then says Q can be found simply by adding together these one- and three-dimensional

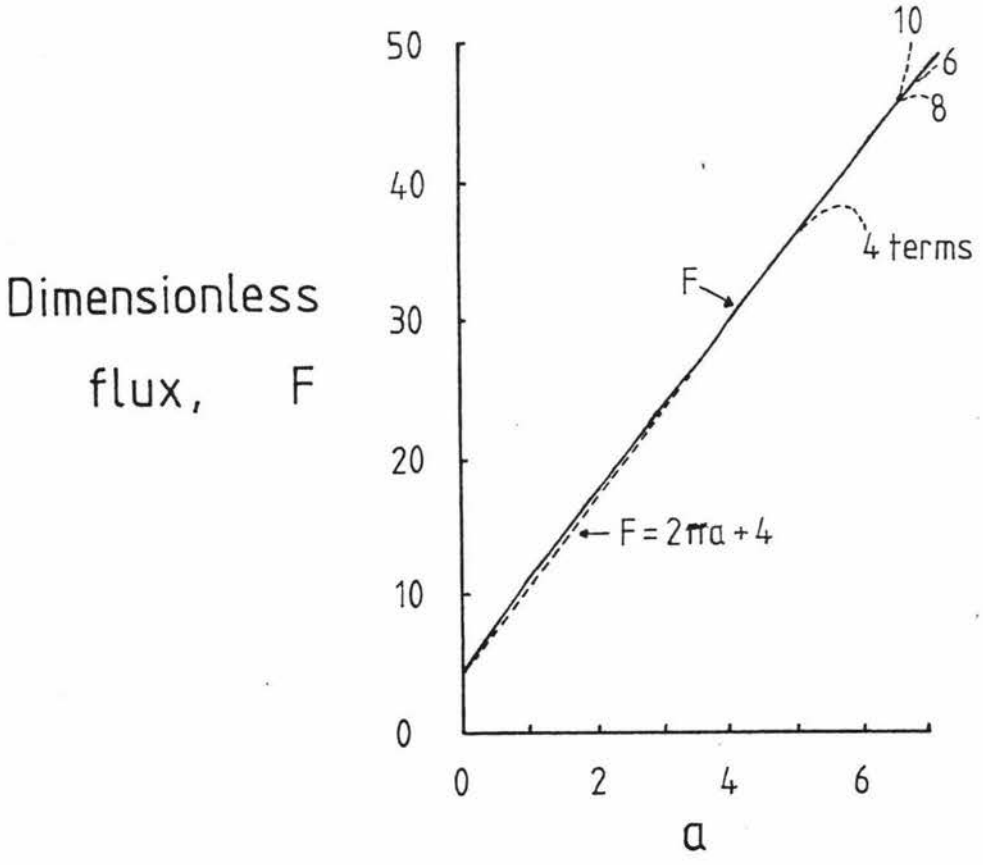

Fig 1.4 Total dimensionless flux (F) versus a. Calculated line is shown along with the approximation $F = 2\pi a + 4$. Divergence of the solution series with various numbers of terms retained in calculations is also shown. After Wooding (1968).

solutions. It is likely that equation (1.15) will still be approximately true, even if an exponential k function is not strictly valid.

Linearized infiltration solutions with time dependence have also been found for line, point, strip and disc sources (Lomen and Warrick, 1974: Warrick, 1974; and Warrick and Lomen, 1976). When taking time into consideration it is also necessary to assume that $dk/d\theta$ is constant. As Ben-Asher *et al.* (1978) note, this implies a constant diffusivity with respect to θ, an unreal assumption in most soils. This however may be of little concern when θ varies over a small range. These solutions, valid for all times reduce to analogous steady-state solutions at long times, at least in terms of the matrix flux potential. However, to preserve continuity with a constant diffusivity, D_*,θ from equation (1.10) must be given by:

$$\theta = \theta_n + \phi/D_* \quad . \qquad (1.16)$$

This restriction leads to a sharp drop in θ near the source, and very flat θ distributions at distance. This contrasts with the more gradual decline in θ found in experimental data. It is also important to note that while a time dependence is included in ϕ profiles, the flux through the disc source is set constant. Fluxes are also assumed constant across the source. In this respect Wooding's (1968) solution is more realistic with fluxes being greater in the edge regions where matric potential gradients are larger.

(e) Discussion:

Although three dimensional infiltration can be modelled numerically for any D or k function, analytical solutions are useful to permit a grasp of the fundamental nature of the physical processes involved (Philip, 1969; Parlange, 1971). Analytical and quasi-analytical solutions in general are faster and less expensive to use. They are also exact, containing no roundoff errors or instability

of calculation once input parameters have been determined. They are however, often limited to specific soil parameters and/or geometries and boundary conditions which may be unrealistic.

While numerical schemes have in general been validated with experimental data, comparison between experimental data and analytical solutions is meagre. Laboratory tests have been carried out and the results compared to point source solutions for steady infiltration by Clothier and Scotter (1982) for homogeneous soil, and for heterogeneous soil by Merrill et al. (1978). Both comparisons were reasonable. This provides a measure of reassurance when using other steady-state linearized solutions. Time dependent linearized infiltration solutions have been less rigorously tested. Ben-Asher et al. (1978) have compared the point source solution (Warrick, 1974) to numerical results and simple field results. Both solutions give similar ϕ distributions for cyclic irrigation, and compare reasonably with field data. Reservations are held concerning the assumption of constant $dk/d\theta$. Comparison of the point source solution of Raats (1971) and laboratory results (Clothier and Scotter, 1982) clearly shows the deficiency in this assumption. While ϕ distributions were similar, water content profiles from the Warrick (1974) solution were totally unrelated to experimental data. This is a direct consequence of the assumption encompassed in equation (1.16) resulting in a constant diffusivity. It is reasonable to assume that other time-dependent linearized solutions will exhibit similar deficiencies.

No direct comparison of Wooding's (1968) solution with experimental date exists. However, numerical schemes compare well with the Wooding solution at long times (Bresler et al. 1971), as do other linearized steady-state infiltration solutions especially at large distances from the source. As these solutions have been experimentally verified, Wooding's solution appears to be a realistic

representation of steady-state infiltration from a ponded source.

Equations (1.14) and (1.15) may also be written in terms of the sorptivity, $S(\theta_s,\theta_n)$, a parameter which depends on both the final and antecedent water contents. $S(\theta_s,\theta_n)$ can be found from ϕ_s given the diffusivity function. This relationship can be examined using the two extreme D functions, the linear diffusivity and the delta-function diffusivity. For a delta-function diffusivity, $S(\theta_s,\theta_n)$ is given by Philip (1973);

$$S(\theta_s,\theta_n) = [\,2\phi_s(\theta_s-\theta_n)\,]^{\frac{1}{2}}. \qquad (1.17)$$

For a soil with a constant diffusivity, Philip (1969) shows;

$$S(\theta_s,\theta_n) = [\,4\phi_s(\theta_s-\theta_n)/\pi\,]^{\frac{1}{2}}. \qquad (1.18)$$

Equations (1.17) and (1.18) provide an envelope for the possible relationships between ϕ_s and the sorptivity, and differ only by a factor of $(2/\pi)^{\frac{1}{2}}$ or 20%. As D in most soils is more akin to a delta-function diffusivity, the error in using equation (1.17) to estimate ϕ_s from the sorptivity will be less than 20%. Use of the sorptivity in equation (1.14) is preferred for two reasons. First α is an arbitary constant which may not necessarily relate well to the soil if k is not exponential, (e.g. Table 1 of Bresler, 1978). However, the sorptivity is a parameter which essentially integrates the matric properties of the soil. Secondly sorptivities are commonly measured in the field using a variety of techniques (e.g. Talsma, 1969; 1970; Clothier and White, 1981).

Field measured properties are essential if soil physics theory is to be applied in trickle irrigation system design and operation. Considering the simplicity of equation (1.14), the possibility of using sorptivities rather than α, and the boundary conditions appropriate to trickle irrigation, Wooding's solution appears to be most suited to field application. The design and operation of trickle irrigation systems is discussed briefly in the

following section.

1.4 DESIGN AND OPERATION OF TRICKLE IRRIGATION SYSTEMS

To design and operate trickle irrigation systems effectively, a knowledge of crop water requirements and soil properties is essential. Discharge rates, number and spacing of emitters and the length of application can all be varied. Although the hydraulic aspects of irrigation system design are well understood (e.g. Jobling, 1974; Bresler, 1977; 1978; Howell et al. 1980) less emphasis has been placed on soil water distribution patterns. It is this latter aspect which ultimately determines crop yield.

Design procedures in use at present are mainly empirical in nature. The simplest of these techniques is to rely on empirical equations, and tabled values for 3 to 5 ideal soils (e.g. Keller, 1974; Keller and Karmeli, 1974) to estimate Q and emitter spacing. Water content distributions are frequently estimated without recourse to available soil physics theory. Hachum et al. (1976), for example, assume elliptical wetted volumes. Even where soil physics theory is used to describe ponded zones and water content distributions, appropriate measurements are sometimes not used. Bresler (1977; 1978) while advocating the use of Wooding's solution to estimate emitter spacings for given discharges, presents tables of k_s and α, mainly for laboratory repacked soils, as a basis for design. Ironically field measurement of k_s and α is not envisaged. In this study not only is the field use of Wooding's solution carried out, but also the field measurement of appropriate parameters is attempted. This should assist in the design and operation of trickle irrigation systems in the future.

1.5 CONCLUSIONS

Although the benefits of trickle irrigation have been extensively examined in the literature, and often verified in the field, amazingly little work on the

applicability of soil physics theory to trickle irrigation has been carried out. The most useful solution in this context is considered to be that of Wooding (1968). This solution can be reduced to a simple form containing two frequently measured soil parameters, yet it still best describes steady infiltration from a trickle source.

In Chapter 2 of this thesis, methods of measuring the required parameters in the field are assessed, including a new method based on Wooding's solution.

Field verification of these parameters and Wooding's solution is attempted (Chapter 3). The utility of this theory in a commercial orchard situation is briefly investigated in Chapter 4.

CHAPTER 2

MEASUREMENT OF THE SATURATED HYDRAULIC CONDUCTIVITY, SATIATED MATRIC FLUX POTENTIAL AND SORPTIVITY

2.1 INTRODUCTION

In Chapter 1 the need for field measurements of hydraulic conductivity and the satiated matric flux potential (ϕ_s) was shown. The interdependence of ϕ_s and the slope of the exponential conductivity function (α) for soils in which equation (1.7) is valid allows the use of field measured ϕ_s values in other linearized infiltration theory apart from that of Wooding (1968). The relationship between ϕ_s and the sorptivity, $S(\theta_s, \theta_n)$, was also demonstrated (equations 1.17 and 1.18). Field and laboratory determinations of sorptivity are frequently carried out, sorptivity and k_s being the main parameters used to analyse infiltration from ponded sources into soils (Philip, 1969). While measurements of k_s and sorptivity are useful in the application of previously mentioned multi-dimensional infiltration solutions, they are also useful for hydrologic modelling and irrigation planning in general.

In later sections of this chapter, existing methods of measuring k_s are compared to a new method developed from Wooding's solution. This new technique measures sorptivity concurrently with k_s and has a number of advantages over existing methods. Methods presently in use, and problems associated with them are briefly examined in the following section.

2.2 EXISTING METHODS OF K_s, ϕ_s AND SORPTIVITY MEASUREMENT

Existing field methods of measuring k_s are discussed by Bouwer and Jackson (1974), and field and laboratory techniques to measure the unsaturated hydraulic conductivity function by Klute (1972). Many laboratory techniques which measure soil-water diffusivities can also give the unsaturated hydraulic conductivity function (e.g. Jaynes and Tyler, 1980), and hence ϕ_s. Methods to estimate the unsaturated hydraulic conductivity function from soil-water retentivity data also exist (e.g. Marshall, 1958; Mualem, 1976). A method to measure k_s from micromorphometric data has also been proposed (Bouma *et al.* 1979).

Sorptivities have been measured in the field from both one-dimensional (Talsma, 1969; Clothier and White, 1981) and three-dimensional (Talsma, 1970) infiltration data. Laboratory techniques utilizing one-dimensional absorption are also frequently used. Recent theories (Philip and Knight, 1974; Parlange, 1971; 1975; Dirksen, 1975; 1979) also provide estimates of sorptivities. A comparison of many of these estimates is given by Elrick and Robin (1981).

Many problems exist when using techniques detailed in the above references. These are summarized below.

(a) Spatial variability: Complex and time consuming field methods like the instantaneous profile method (e.g. Rose et al. 1965) and detailed laboratory studies (e.g. Passioura, 1976) only provide information for relatively small soil volumes. Previous studies have indicated order of magnitude differences in k_s (Nielsen et al. 1973; Talsma and Hallam, 1980) and sorptivities (Sharma et al. 1980 a and b) over small areas. For field use, either many measurements or measurement over a large area is necessary to give meaningful average values.

(b) Soil disturbance: k_s and sorptivities are sensitive to any soil disturbance, as shown by recent work on preferential flow in macropores (Bouma, 1981). As field measurement of k_s or sorptivity frequently involves driving a ring or corer into the soil, or augering out a cavity, some compaction, fracturing or smearing almost inevitably occurs (Bouma and Dekker, 1981). Sampling for laboratory analysis also almost always results in disturbance (Loveday, 1974).

(c) Time for infiltration rates to reach steady-state: While measurement of sorptivities usually utilizes transient infiltration data, the measurement of k_s frequently relies on steady flow being attained. Theoretically one-dimensional infiltration can only attain

a quasi-steady-state in deep soils (Philip, 1968a). Practical studies, however, indicate varying lengths of time to steady-state. Detailed laboratory studies of one-dimensional infiltration by Bond and Collis-George (1981) show transient responses at times greater than 7 hours. Other data (e.g. Aronovici, 1955; Swartzendruber and Olsen, 196la; Ahuja et al. 1976) indicates steady-state is attained between 30 minutes and 7 hours depending on source size and soil texture. Generally in field situations, flows which could be called steady, within the accuracy of the measurement technique, are obtained within a few hours, especially in coarser soils (e.g. Parr and Bertrand, 1960) where gravity quickly dominates flow. Also three-dimensional infiltration, which occurs in methods where the source is small, attains steady-state more rapidly, both theoretically (Philip, 1968a; 1969) and in practice (Talsma, 1970). Soil inhomogeneities and dynamic processes such as soil biological activity, soil swelling and pore blocking may of course lead to fluctuations in infiltration rates (Fleming and Smiles, 1975), and prevent true steady flows being found.

(d) Theoretical considerations: Many methods to measure k_s and sorptivities result from solutions of the flow equation (equation 1.2) assuming simple flow geometrics and boundary conditions. On occasion these geometrics and conditions may not be a good representation of the infiltration process. Possibly the most important case where this occurs is in small infiltrometers, where one-dimensional flow is necessary to measure k_s and sorptivity. Lateral flow must either be eliminated or corrected for. Prevention of lateral flow is accomplished by driving rings into the soil, or by removing cores, both resulting in soil disturbance, or by buffering (i.e. ponding large areas around the infiltrometer). The effectiveness of buffering appears suspect (Marshall and Stirk, 1955; Swartzendruber and Olsen, 196l a and b). Methods to correct for lateral flow exist, using gravimetric sampling (Marshall and Stirk, 1955) and tensiometry

(Ahuja et al. 1976), but these methods are time consuming and are not suited to general use

2.3 MATERIALS AND METHODS

2.3.1 INTRODUCTION

Three commonly used methods of measuring k_s were used on four soils. These techniques and sites are briefly discussed below, and a new method which measures k_s and sorptivities concurrently, is introduced.

2.3.2 SITES

Three sites were located on different phases of the Manawatu series, a naturally layered alluvial soil (Dystric Fluventic Eutrocrept: Soil Survey Staff, 1975) previously described by Clothier et al. (1978). Two sites on this series, the Manawatu sandy loam and the Manawatu fine sandy loam I sites, were under mixed pasture subject to periodic grazing. The third site, the Manawatu fine sandy loam II was located in a trickle irrigated orchard. Herbicide application had kept the surface largely vegetation free. The fourth site, the Tokomaru silt loam (Aeric Fragiaqualf: Soil Survey Staff, 1975), was also under grazed pasture. Full morphological and physical descriptions of this soil are given by Pollock (1975) and Scotter et al. (1979). Brief profile descriptions of all four soils are given in Appendix A.1.

2.3.3 MEASURING K_s USING EXISTING METHODS

The three methods used are described below;

(a) Field core permeameters: This method, subsequently referred to as the core k_s method, was carried out by driving steel infiltration rings (0.102 m radius; area ratio 0.06, Loveday, 1974) about 0.1 m into the soil. After digging the cores out and leveling the base by chipping away the soil, the cores were placed on a metal grid and water ponded on the soil in them. Infiltration rates were monitored until steady flow ensued. Sloping scales were found to be most effective for measuring flow rates. K_s was calculated using either falling- or constant-

head forms of Darcy's Law, depending on the method of measurement. On occasion Rhodamine BN dye was used to identify preferential flow paths through the cores. Frequently cores were taken from locations where three-dimensional steady-flow rates had earlier been determined (see section 2.3.4).

(b) Well permeameter: The well method was developed by Glover (in Zangar, 1953), and used here in the form described by Talsma and Hallam (1981). Steady infiltration from a 0.013 m radius auger hole with a constant head of water was measured. K_s was calculated using:

$$k_s = Q.\,[\sinh^{-1}(H/r) - 1].\,(\pi H^2)^{-1} \qquad (2.1)$$

Here Q is the steady flow rate ($m^3 s^{-1}$), measured using a mariotte device, H the ponding depth, and r the auger hole radius. Auger holes were kept within the topsoil, while retaining the preferred (H/r) ratio of about 10, through the use of a small auger.

(c) Buffered infiltrometers: Buffering, by ponding in larger infiltration rings placed round smaller rings driven about 10 mm into the soil, was used to estimate steady one-dimensional flow rates (Q_B). As only small heads of water were used k_s was calculated as the one-dimensional flux density. In all trials the inner ring radius was never greater than half the buffer ring radius. In most cases steady unbuffered infiltration rates were also determined before buffer rings were used. Re-arrangement of equation (1.14), noting that the first term on the RHS is Q_B, then allows solution for ϕ_s:

$$\phi_s = (Q - Q_B)\,(4r)^{-1} \qquad (2.2)$$

Q is the unbuffered infiltration rate, and r the inner ring radius.

2.3.4 TWIN RING METHOD OF MEASURING K_s, ϕ_s AND SORPTIVITY

If two rings of different radii, r_1 and r_2, are used different unbuffered steady-state flux densities, q_1 and q_2, are measured. Solution of simultaneous equations for k_s from equation (1.14) in a flux density form gives:

$$k_s = (q_1 \cdot r_1 - q_2 \cdot r_2) \cdot (r_1 - r_2)^{-1} . \qquad (2.3)$$

Similarly the satiated matric flux potential is found from:

$$\phi_s = (\pi/4) \cdot (q_1 - q_2) \cdot (1/r_1 - 1/r_2)^{-1} . \qquad (2.4)$$

Hence data from two unbuffered infiltrometers with different radii can give both k_s and ϕ_s. Simple expressions which provide an envelope for the relationship between ϕ_s and the sorptivity have already been given in Chapter 1. Using the above equations and measured unbuffered infiltration rates can then also give sorptivities if antecedent and satiated volumetric water contents are known. The methods used in this study using this technique, termed the twin ring method, are outlined below.

(a) Experimental technique: Sharpened rings ranging between 25 mm and 0.204 m in radius were pushed about 10 mm into the soil, just far enough to prevent lateral leakage of ponded water. At the three Manawatu series sites the top 10 - 20 mm of soil was removed before experimentation. The surface at the Tokomaru site was left intact, but it was found useful to cut through the vegetation with a knife before inserting the ring. Ponding depths of about 10 mm were used. Infiltration rates as a function of time were found using either a calibrated mariotte device, or more commonly the rings were refilled to a fixed level from a measuring cylinder at suitable time intervals. Usually measurement was continued for approximately an hour after steady-state first appeared to have been reached.

After unbuffered infiltration rates had been determined, buffering, by placing larger infiltrometer rings around, allowed one-dimensional infiltration rates to be measured

at the same location. K_s and the satiated matric flux potential were then determined independently by the use of equations (2.3) and (2.4), as previously mentioned. In all cases antecedent and satiated volumetric water contents were determined (see Appendix A.3) for sorptivity calculation.

(b) Statistical methods: While standard statistical analysis can be used for methods which directly measure k_s or sorptivity, these methods cannot be used for the twin ring method. Here means values of q are found using statistical methods, outlined in Appendix A.2. Methods of estimating the reliability of parameters gained from equations (2.3) and (2.4) are given below.

Saturated hydraulic conductivity: To obtain reasonable sensitivity it is desirable that $r_1 > 2r_2$, and r_1 be large enough for:

$$C_k = (q_1 r_1 - q_2 r_2)\ (q_1 r_1)^{-1} \qquad (2.5)$$

where C_k is a dimensionless parameter defined by the above equation. C_k equals 0.3 if $r_1 = 2r_2$, and the radius at which the two terms of Wooding's equation are equal, r_e, is set equal to $(r_1 + r_2)/2$. If the observed frequency distribution of q is approximately normal, an estimate of the standard error (s_e) of k_s is given by (Barford, 1967):

$$s_e(k) = [(r_1 s_1)^2/n_1 + (r_2 s_2)^2/n_2]^{\frac{1}{2}} \cdot (r_1 - r_2)^{-1}. \qquad (2.6)$$

Here s_1 and s_2 are the standard deviations of q_1 and q_2 respectively, and n_1 and n_2 the number of replicate measurements.

Satiated matric flux potential: To obtain reasonable sensitivity from equation (2.4), it is again desirable that $r_1 > 2r_2$ and also that r_2 be small enough for:

$$C_\phi = (q_2 - q_1)/q_2. \qquad (2.7)$$

C_ϕ is a dimensionless parameter defined by the above equation. C_ϕ equals 0.3 if $r_1 = 2r_2$ and $r_e = (r_1 + r_2)/2$. An estimate of the standard error of ϕ_s is given by:

$$s_e(\phi) = (\pi/4).\ (1/r_1 - 1/r_2)^{-1}$$
$$(s_1^2/n_1 + s_2^2/n_2)^{\frac{1}{2}}. \qquad (2.8)$$

Sorptivity: As real soils are often better described by delta function diffusivities than constant diffusivities (Philip, 1969), equation 1.17 is used to estimate the sorptivity. Errors induced by assuming a delta function diffusivity are demonstrably less than 20%. However, ignoring these errors, an estimate of the standard error of the sorptivity is given by:

$$s_e(S) = [(\theta_s - \theta_n)/2\phi_s]^{\frac{1}{2}}.\ s_e(\phi). \qquad (2.9)$$

Here errors in θ_s and θ_n are also neglected, their magnitude being small in comparison to the uncertainty in ϕ_s.

In addition to the use of equations (2.3) and (2.4) to calculate k_s and ϕ_s, a (computer) statistical regression package was used to fit the Q versus radius data to a parabola. Regression through the origin was assumed. This method provided a check on calculated parameters, and the validity of Wooding's equation.

(c) Time to reach steady-state: For the twin ring method to be useful, q must approach steady-state within a reasonable time. No analytical solutions (for transient infiltration from circular ponds) which could provide an estimate of the time to steady-state exist. While numerical schemes (e.g. Brandt et al. 1971) could be used, they are complex and expensive to run and thus not suitable for routine use. However, depending on whether the first or second term on the RHS of Wooding's equation is larger, estimates of the time to steady-state can be gained from solutions for simple flow problems. For this purpose the delta function solutions of Philip and Knight (1974) suffice.

When rings are large, or matric potential gradients small, the one-dimensional infiltration solution given below should provide a reasonable estimate of the time to reach steady-state.

$$t = (S^2/2k_s) \cdot [(k_s/(q - k_s)) - \ln(q/(q - k_s))]. \quad (2.10)$$

Here t is time, and S signifies the sorptivity, $S(\theta_s, \theta_n)$. From equation (2.10) we find $q/q_\infty = 1.2$ when $t = t_* = 1.6(S/k_s)^2$, t_* being a characteristic time when q is 20% higher than the steady-state value q_∞.

For small rings the transient three-dimensional absorption solution may be more applicable. This solution applies to flow from a spherical cavity of radius r_o, rather than a shallow circular pond. However, comparison of steady-state solutions for these two geometries shows the flux density for a given radius only differs by a factor of $\pi/4$ (Philip, 1969). Times to reach steady flow are also likely to be similar, particularly for small radii. The delta function solution for absorption from a spherical cavity is:

$$\begin{aligned} t = \; & 1 + 2(1 - S^2.(2qr_o(\theta_s - \theta_n))^{-1})^{-3} \\ & - 3(1 - S^2(2qr_o(\theta_s - \theta_n))^{-1})^{-2} \\ & (r_o^2(\theta_s - \theta_n)^2).(3S^2)^{-1}. \end{aligned} \quad (2.11)$$

It follows that when $t = t_* = (10r_o(\theta_s - \theta_n)S^{-1})^2$, equation (2.11) predicts $q/q_\infty = 1.2$.

2.4 RESULTS AND DISCUSSION

2.4.1 WELL, CORE AND INFILTROMETER K_s MEASUREMENTS

Mean saturated hydraulic conductivities, k_s, from the three techniques are shown in Table 2.1. Also sample numbers, standard errors and estimated sample numbers required for k_s to be within 10% of the true mean at a 0.05 confidence level, N, are given. Full statistics for these distributions are given in Appendix A.2.

Table 2.1 Saturated Hydraulic Conductivity from Well, Core and Buffered Infiltrometer Methods

Method		Manawatu Sandy Loam	Manawatu Fine Sandy Loam I	Manawatu Fine Sandy Loam II	Tokomaru Silt Loam
Well :	K_s ($\times 10^{-6} ms^{-1}$)	2.1	2.0	1.2	0.34
	s_e ($\times 10^{-6} ms^{-1}$)	0.2	0.4	0.2	0.05
	n	18	27	20	12
	N	30	210	110	50
Core :	K_s ($\times 10^{-6} ms^{-1}$)	8.3	54	77	31
	s_e ($\times 10^{-6} ms^{-1}$)	2	20	30	7
	n	20	22	13	23
	N	230	590	390	230
Buffered Infiltrometer :	K_s ($\times 10^{-6} ms^{-1}$)	13	-	-	6.4
	s_e ($\times 10^{-6} ms^{-1}$)	4	-	-	1
	n	6	-	-	14
	N	110	-	-	70

In all cases the well method gives the lowest estimate of k_s, the distributions of k_s from the well measurements being slightly closer to log-normal than normal for all but the Tokomaru data. Piezometer and tube k_s values for the lower A horizon on this site (Scotter et al. 1979) are also normally distributed. The mean tube and piezometer k_s value of $3.7 \times 10^{-7} ms^{-1}$ is similar to the well k_s, although several years elapsed between determinations. At all four sites well k_s was appreciably lower than core k_s, and also lower than the buffered infiltrometer values. It is likely that smearing of the auger hole walls, especially in the Tokomaru, introduces systematic error into this method.

Core k_s distributions at all four sites are well described by log-normal distributions, but only poorly by normal distributions. As mentioned above core k_s are significantly higher than well values, differences ranging up to two orders of magnitude. While smearing in the well method may partly account for these differences, other causes probably contribute. The core method gives a saturated (draining) conductivity, which is commonly about twice that of a near saturated wetting conductivity (Bouwer, 1966) as found by the well method. However, the main reason, and the cause of the markedly asymetric core k_s distributions, is probably a result of preferential flow through vertical channels or cracks in cores. Evidence for macropores influencing core k_s values is found in a comparison of unbuffered steady fluxes and core k_s measurements for identical locations. For all four sites (see Figures 2.1 a - d) some core k_s values are greater than measured steady q values (i.e. in the region below the line $q = k_s$). This is theoretically impossible. Examples of preferential flow through cores are shown in Figure 2.2, where rhodamine dye has stained earthworm channels in the Tokomaru silt loam. The extent to which macropores in cores are natural features, or are induced by ring insertion is not known. In either case they probably induce systematic error, as in situ macropores

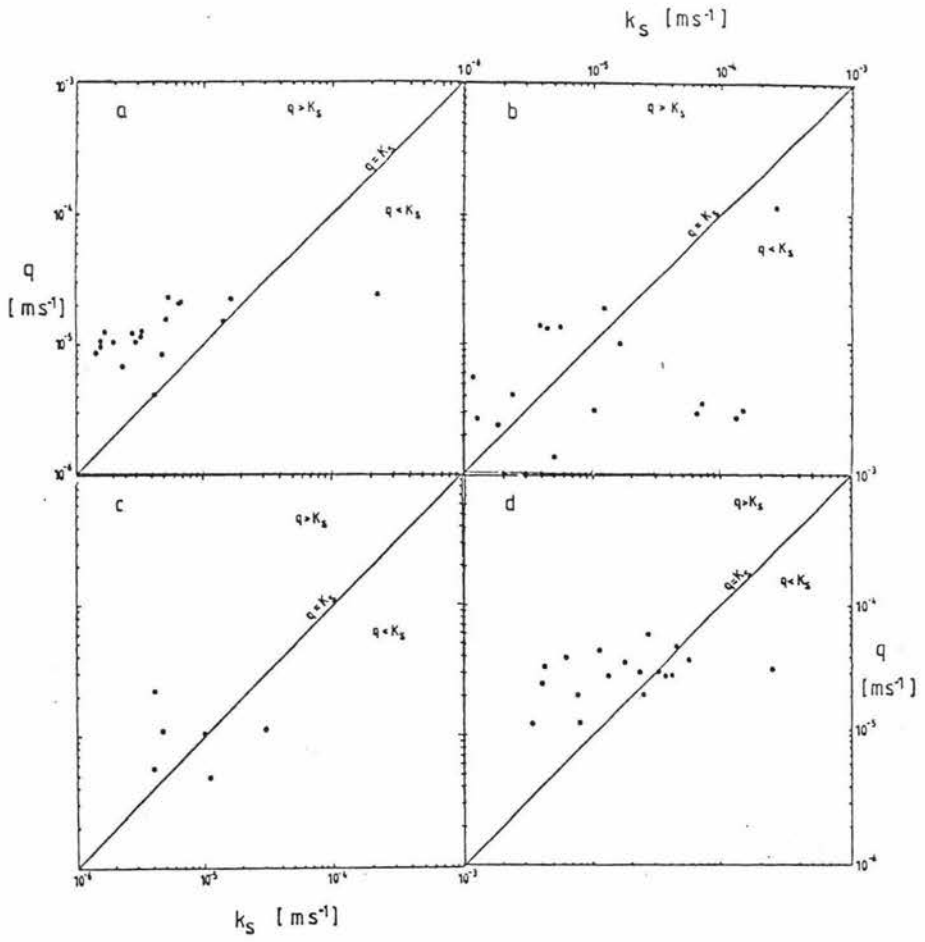

Fig. 2.1 Unbuffered infiltration fluxes from 0.102m radius rings (q) versus core k_s values for the same location. Data points below the line $q = k_s$ are theoretically impossible.

(a) Manawatu sandy loam

(b) Manawatu fine sandy loam I

(c) Manawatu fine sandy loam II

(d) Tokomaru silt loam

Fig. 2.2 Field core permeameters from the Tokomaru silt loam site. Rhodamine dye stained areas indicate preferential flow down channels. These channels may be of limited continuity *in situ*, and preferential flow may not occur to the same extent.

would tend to have restricted continuity compared to the same macropores in a core.

Infiltrometer k_s means were calculated assuming a normal distribution. In the Tokomaru site the infiltrometer k_s is intermediate to well and core values, possibly due to systematic errors present in the other methods. However, the infiltrometer k_s on the Manawatu sandy loam site is larger than the core value. This may be due to spatial variability. Comparison of the infiltrometer k_s between the two sites shows the Manawatu k_s is twice that of the Tokomaru, in contrast to core k_s values, whereas the Tokomaru was found to be 4 times as permeable as the Manawatu. Macropores are probably the source of this difference as previously noted, the Tokomaru soil being more biologically active than the Manawatu. Macropore continuity is more restricted when using infiltrometers.

2.4.2 UNBUFFERED INFILTRATION RATES

Mean values of q and standard deviations, s(q), are shown in Table 2.2, along with sample sizes (n), sample sizes required to be within 10% of the true mean at a 0.05 confidence level (N), and the range of times (T) before steady flow was achieved. Apart from the Tokomaru soil, fractile analysis showed frequency distributions to be marginally better described by log-normal than normal distributions. The marked asymetry found for core k_s measurements was not found for q (see Appendix A.2). This may again be due to macropore continuity being restricted. Average coefficients of variation (C.V.) in q are in the range of 50 to 70%, apart from the high antecedent water content Tokomaru sample, where they are somewhat lower. Sample numbers are small here, and may not reflect the true variation.

Noticeable at all sites, with the exception of the Manawatu sandy loam I, is a decrease in q with increasing radius. This is due to three dimensional components of

Table 2.2 Unbuffered infiltration data for four sites

		radius :	0.025m	0.037m	0.049m	0.075m	0.102m	0.18m	0.204m
Manawatu sandy loam	q	($x10^{-5}$ ms^{-1})	-	1.8	1.1	1.4	1.4	1.2	-
	s(q)	($x10^{-5}$ ms^{-1})	-	1	1	0.7	0.5	0.5	-
	n		-	13	10	12	20	10	-
	N		-	120	320	100	50	70	-
	T	(min.)	-	5.20	15-30	20-40	25-50	30-70	-
Manawatu fine sandy loam I	q	($x10^{-5}$ ms^{-1})	1.1	1.2	-	1.4	1.3	-	-
	s(q)	($x10^{-5}$ ms^{-1})	0.7	0.8	-	1	1	-	-
	n		12	12	-	18	41	-	-
	N		160	170	-	200	230	-	-
	T	(min.)	10-40	20-40	-	20-70	20-100	-	-
Manawatu fine sandy loam II	q	($x10^{-5}$ ms^{-1})	3.7	3.0	-	1.7	1.3	-	-
	s(q)	($x10^{-5}$ ms^{-1})	3	3	-	1	0.5	-	-
	n		13	14	-	20	23	-	-
	N		250	380	-	130	60	-	-
	T	(min.)	5-30	30-50	-	40-80	60-100	-	-
Tokomaru silt loam									
a) $\theta n = 0.30$	q	($x10^{-5}$ ms^{-1})	10	8.2	-	4.0	3.2	-	1.7
	s(q)	($x10^{-5}$ ms^{-1})	5	4	-	3	1	-	0.5
	n		12	12	-	12	25	-	4
	N		100	90	-	220	40	-	30
	T	(min.)	5-30	10-30	-	10-50	20-50	-	40-80
b) $\theta n = 0.39$	q	($x10^{-5}$ ms^{-1})	-	-	1.1	-	1.0	-	0.7
	s(q)	($x10^{-5}$ ms^{-1})	-	-	0.3	-	0.1	-	0.2
	n		-	-	3	-	4	-	4
	N		-	-	30	-	4	-	28
	T	(min.)	-	-	2-10	-	20-60	-	20-60

the total flux becoming less important with increasing radius. This effect is most noticeable on the Tokomaru site, and least in the coarser textured Manawatu sandy loam. A large decrease in q with increasing θ_n is also apparent in the two Tokomaru data sets.

2.4.3 CALCULATION OF K_s, ϕ_s AND SORPTIVITY USING THE TWIN RING METHOD

(a) K_s Calculation

Four ring radii were chosen for each site and treated as two pairs (designated A and B), allowing two independent calculations of k_s and ϕ_s. Ring pairings were selected so $r_1 > 2r_2$. Calculated k_s values and standard errors are shown in Table 2.3, along with C_k values. The low θ_n sample of the Tokomaru has the lowest C_k (less than 0.3). Here $s_e(k)$ is of a similar magnitude to k_s, indicating a large uncertainty in k_s. This is due to q being determined largely by ϕ_s rather than k_s. In this case larger rings would be required to accurately determine k_s. The high θ_n Tokomaru sample, in contrast, has a high C_k value, ϕ_s being of less importance. Consequently $s_e(k)$ is relatively small. C_k is also large in the Manawatu sandy loam and fine sandy loam I samples, $s_e(k)$ being relatively small. The two ring pairs give virtually identical estimates of k_s here.

On the Manawatu fine sandy loam II site $C_k \approx 0.3$. This, coupled with the high variability of q at this site results in $s_e(k)$ being approximately the same magnitude as k_s. Larger rings and/or more measurements are necessary to obtain a more accurate estimate of k_s.

Comparison between sites shows that where C_k is highest, k_s is also larger. C_k and k_s are highest in the coarser textured soils, which could be expected to be more permeable. It is also interesting to note the two Tokomaru samples give similar estimates of k_s.

Table 2.3 Saturated Hydraulic Conductivity data from Twin Ring Analysis

		Ks ($x10^{-6}$ ms^{-1})	$s_e(K)$ ($x10^{-6}$ ms^{-1})	C_k
Manawatu sandy loam :	A	11	3	0.5
	B	12	2	0.5
Manawatu fine sandy loam I :	A	14	3	0.7
	B	16	4	0.7
Manawatu fine sandy loam II :	A	3.3	5	0.2
	B	7.0	5	0.3
Tokomaru silt loam :				
a) $\theta n = 0.30$	A	4.0	4	0.2
	B	4.6	6	0.1
b) $\theta n = 0.39$	A	6.3	2	0.6

(b) Sorptivity and ϕ_s Calculation

Sorptivity and ϕ_s data obtained from the twin ring method are given in Table 2.4. Sites where good estimates of k_s were found have low values of C_ϕ, lateral sorption being of lesser significance. In these cases $s_e(\phi)$ is of similar magnitude to ϕ_s. Of particular interest is the Manawatu fine sandy loam I data, where ϕ_s and C_ϕ are negative. These anomalous results are probably due to a combination of the large variability in q, and a low ϕ_s value. A visual inspection of this site shows surface properties to be highly variable, compaction appearing to exist in some localities and not in others. The use of smaller rings may not help at this site, but would in the Manawatu sandy loam where $C_\phi < 0.3$.

Both the Tokomaru and Manawatu fine sandy loam II sites have $C_\phi > 0.3$. Good agreement between the two calculated ϕ_s values is found for the Tokomaru, and $s_e(\phi)$ is small in comparison to ϕ_s. High variability in q for the Manawatu leads to $s_e(\phi)$ being about half ϕ_s. However, the two ϕ_s values are similar. The Tokomaru data contains both the highest and lowest ϕ_s values. The low θ_n sample has a calculated ϕ_s less than a quarter that of the high θ_n sample. While this may be partly due to an increased antecedent water content, changes in soil properties between the two determinations and spatial variability could also be envisaged as causes. The expected trend of increasing sorptivity (or ϕ_s) with finer texture is clearly seen in the data. Sorptivities show less variability than ϕ_s, sorptivity varying as $\phi_s^{\frac{1}{2}}$.

(c) Regression Analysis and Buffered Infiltrometer Measurement of ϕ_s

K_s and ϕ_s values calculated by computer regression (onto a parabola) of all unbuffered infiltration data are shown in Table 2.5. Associated standard errors, and correlation coefficients (r_{xy}) are also given. Comparison of the results in Table 2.5 with those from the twin ring analysis (i.e. Tables 2.3 and 2.4) shows that the two

Table 2.4 Sorptivity and Satiated Matric Flux Potential Data from Twin Ring Analysis

		ϕ_s ($\times 10^{-7} m^2 s^{-1}$)	$s_e(\phi)$ ($\times 10^{-7} m^2 s^{-1}$)	C_ϕ	$S(\theta_s, \theta_n)$ ($\times 10^{-4} ms^{-\frac{1}{2}}$)	$s_e(S)$ ($\times 10^{-4} ms^{-\frac{1}{2}}$)	θ_s	θ_n	r_e (m)
Manawatu sandy loam	A	2.0	3	0.1	3.5	3	0.43	0.12	0.02
	B	1.8	3	0.2	3.3	3	0.43	0.12	0.02
Manawatu fine sandy loam I	A	-0.5	1	-0.1	-	-	0.44	0.15	-
	B	-0.9	0.9	-0.3	-	-	0.44	0.15	-
Manawatu fine sandy loam II	A	7.8	4	0.6	6.0	2	0.43	0.20	0.3
	B	5.9	3	0.5	5.2	1	0.43	0.20	0.1
Tokomaru silt loam :									
a) $\theta_n = 0.30$	A	21	2	0.6	8.2	0.4	0.46	0.30	0.7
	B	22	5	0.6	8.4	1	0.46	0.30	0.6
b) $\theta_n = 0.39$	A	1.8	1	0.3	1.6	0.4	0.46	0.39	0.04

Table 2.5 Saturated hydraulic conductivity and satiated matric flux potential from regression of all ring data

	K_s ($\times 10^{-6}$ ms^{-1})	$s_e(K)$ ($\times 10^{-6}$ ms^{-1})	ϕ_s ($\times 10^{-7}$ m^2 s^{-1})	$s_e(\phi)$ ($\times 10^{-7}$ m^2 s^{-1})	r_{xy}
Manawatu sandy loam	9.9	2	2.7	2	0.997
Manawatu fine sandy loam I	15	10	-1.2	8	0.999
Manawatu fine sandy loam II	3.2	4	14	3	0.998
Tokomaru silt loam					
a) $\theta n = 0.30$	3.1	3	23	3	0.998
b) $\theta n = 0.39$	5.5	3	3.1	1	0.999

methods give values of k_s and ϕ_s which are not significantly different ($P < 0.01$ by t-test) in general. Only slight differences are found: ϕ_s only differs for the Manawatu fine sandy loam II, where high variability in q occured. K_s only differs slightly where sorption is more prevalent, on the Tokomaru and Manawatu fine sandy loam II sites.

This agreement between methods validates the data analysis technique used in the twin ring method to an extent. Wooding's equation, used to describe the relationship between q (or Q) and r, is also validated by these results. Correlation coefficients in Table 2.5 are all near 1, showing a parabola to describe Q versus r data very well. Also supporting this conclusion is the close correspondence between the two independent calculations of k_s for the Manawatu sandy loam and fine sandy loam I sites, and for ϕ_s on the Tokomaru. Both the above factors also suggest Q values obtained are close to steady-state. Otherwise different transient responses with separate ring radii would probably result in inconsistent k_s and ϕ_s values, and non-parabolic regressions. Transient behaviour is discussed further in the next section.

Sample numbers for the calculation of ϕ_s from buffered and unbuffered infiltration data using equation (2.2) are small. Results are unreliable as a consequence. The ϕ_s value for the Tokomaru site with $\theta_n = 0.30$ [$\phi_s = (18 \pm 6) \times 10^{-7} m^2 s^{-1}$] is not significantly different from those values calculated by the twin ring analysis or computer regression methods. Values for the Manawatu sandy loam [$(0.13 \pm 0.04) \times 10^{-7} m^2 s^{-1}$] and Tokomaru with $\theta_n = 0.39$ [$(0.2 \pm 0.6) \times 10^{-7} m^2 s^{-1}$] however are both about one tenth those of previous analysis. While practical problems such as maintaining similar ponding heights between buffer and inner rings, and spatial variability will play a role in these results, the above results do not provide a conclusive test of this method. Comparison of k_s values from buffered infiltrometers and

the twin ring analysis is presented later.

(d) Transient behaviour

The general range of times before q appeared steady (T) for each radius at the four sites is given in Table 2.2. Sites where ϕ_s is low show more rapid attainment of steady-flow, sorption effects being less important (c.f. gravity). Smaller ring size data also tend to show a faster approach to steady-state, three-dimensional geometry effects being more apparent. Use of equations (2.10) and (2.11) to calculate times to steady-state for one-dimensional infiltration and three-dimensional absorption respectively show reasonable agreement with measured T values. Smaller ring radii are better described by three-dimensional sorption. Two illustrative examples are now presented.

Transient infiltration for two 0.18 m radius rings on the Manawatu sandy loam is shown in Figure 2.3. After 10 minutes the change in q is small relative to measurement resolution, and very small compared to differences between replicate ring q values. Comparison of measured data with predicted transient behaviour (equations 2.10 and 2.11, using average k_s and sorptivities from Tables 2.3 and 2.4) shows the one-dimensional infiltration solution to give The better indication of transient behaviour. Also t_* for one-dimensional infiltration is 21 minutes. This compares well with a measured T of 30 to 70 minutes. Also illustrated in Figure 2.3 is the effect of higher θ_n in hastening the approach to steady-state. Despite the smaller contribution to q, the three-dimensional absorption solution (equation 2.11) shown in Figure 2.3 has a greater absolute transient error after 100 minutes than equation 2.10. (For three-dimensional absorption t_* = 31 days). But this is an over-estimate of the error, the two solutions interacting during the early transient phase, gravity wetting the soil below the source much more quickly than would absorption alone.

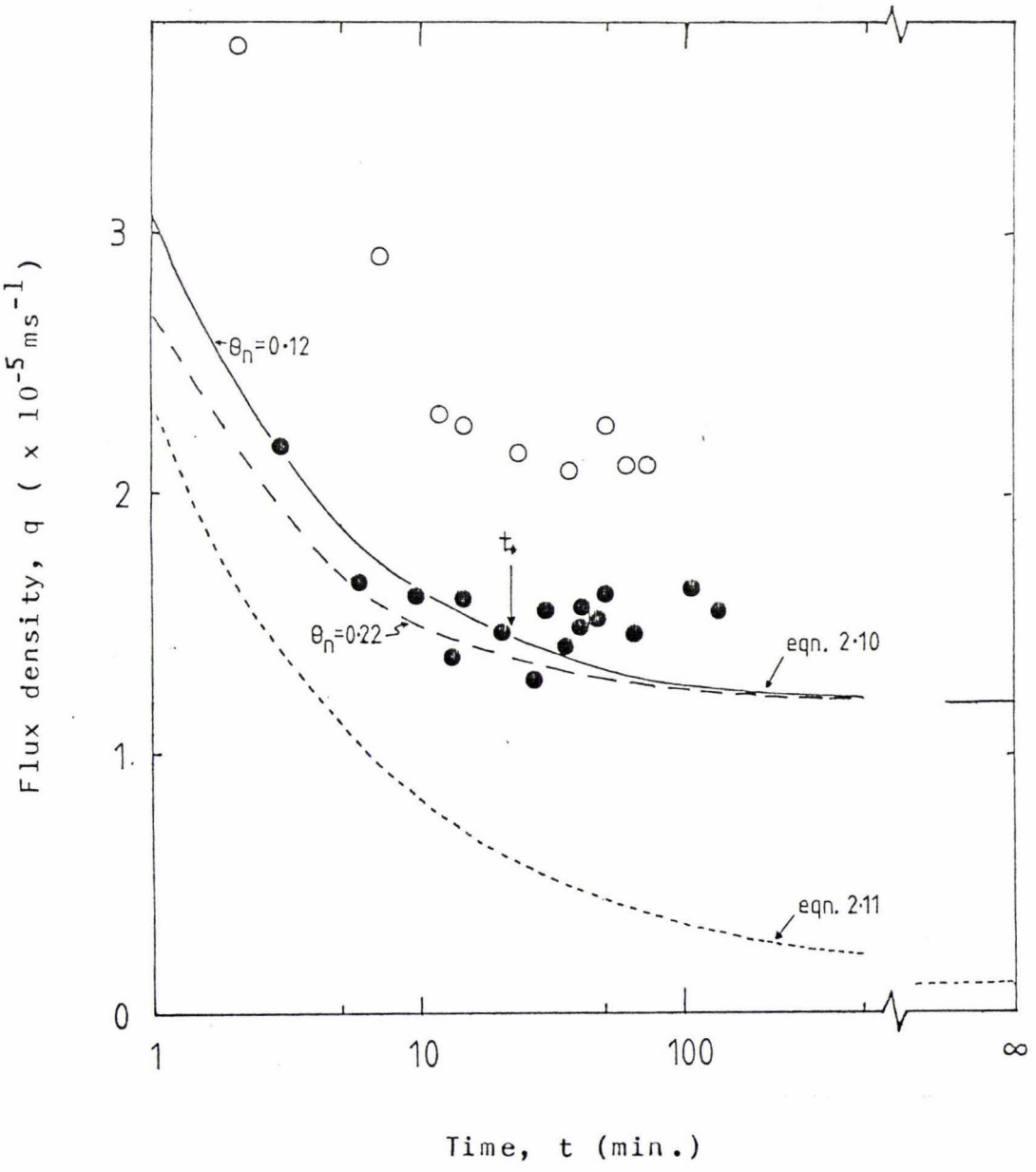

Fig. 2.3 Observed changes in q with time for two 0.18m radius rings at the Manawatu sandy loam site (● and ○). Also shown are calculated curves from equations (2.10) and (2.11), and values of t_* and q_∞. Average values of k_s and sorptivity from the twin ring analysis were used. The expected variation in q with θ_n is also illustrated by the second curve from equation (2.10) with θ_n = 0.22.

Calculated and measured transient behaviour for two 0.037 m radius rings on the Manawatu fine sandy loam II are shown in Figure 2.4. In this case the second term on the RHS of Wooding's equation dominates flow. Equation (2.11) predicts $t_* = 390$ minutes, but due to the interaction with gravity this is again probably an overestimate. Higher θ_n hastens the approach to steady-state again. T values in Table 2.2 indicate q to be steady after 30 to 50 minutes (i.e. systematic change in q during the subsequent hour was not detectable). This does not mean a true steady-state has been reached, but compared to other uncertainties affecting measurement of q, non-steady behaviour should not be a serious problem in many soils. Measured transient behaviour shown in Figure 2.4 is in general agreement with calculated responses, except that after 120 minutes when q in one ring suddenly doubled. This is thought to be due to an earthworm venting it's burrow at the surface, ponding tending to encourage such behaviour. Other examples of rapid, theoretically unexplainable responses also exist in the ring data. At this site the presence of a sandy horizon below 0.3 m probably tends to enhance the effect of such macropores on infiltration. Effects such as this may explain the high variability in q at this site. While exceptional, sudden increases in q such as this are a dramatic illustration of temporal variation in soil physical properties.

2.4.4 DISCUSSION

Comparison of twin ring k_s values to well and core k_s data shows large differences. Well k_s values (Table 2.1) are considerably lower than twin ring values, significantly so ($P < 0.01$ by t-test) in the Manawatu sandy loam II and sandy loam sites. These differences are near an order of magnitude in all cases. In contrast core k_s values, with the exception of the Manawatu sandy loam value, are greater than twin ring values. An order of magnitude difference was found for the Manawatu fine

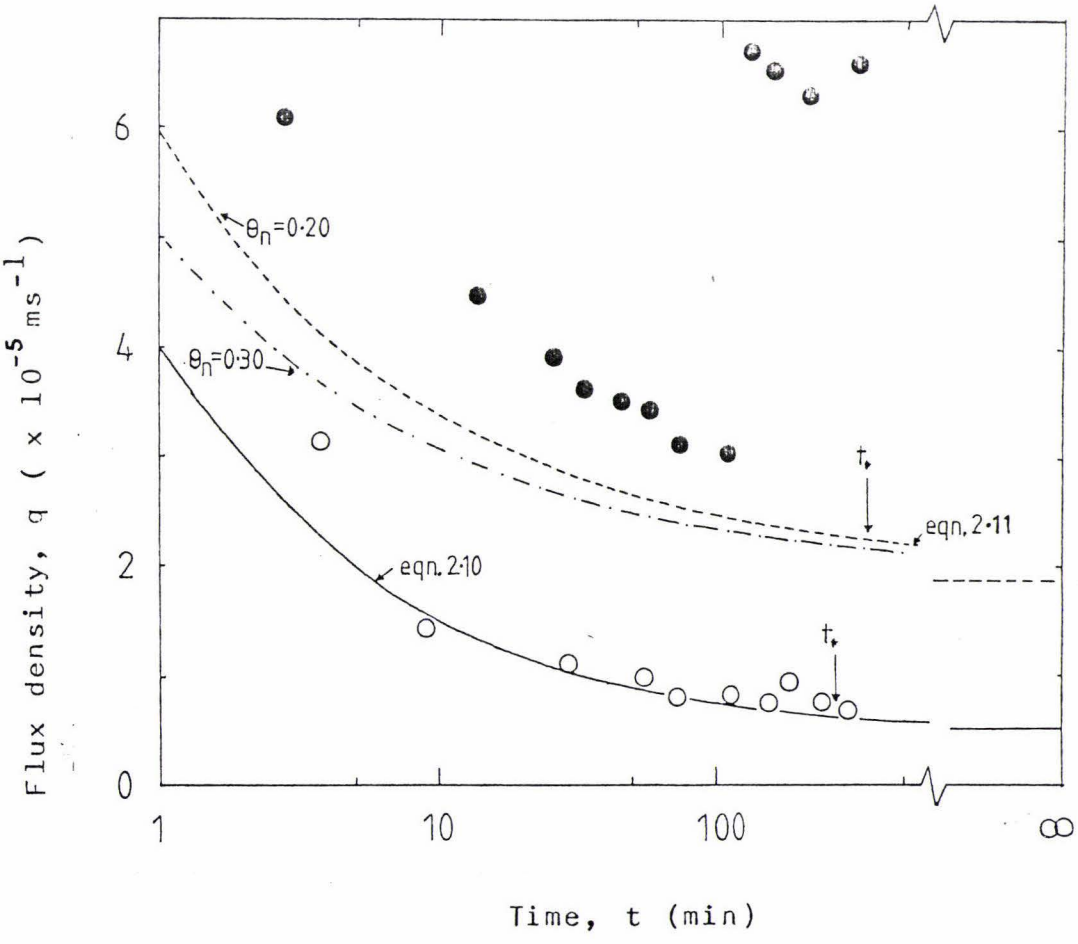

Fig. 2.4 Observed changes in q with time for two 0.037m radius rings at the Manawatu fine sandy loam II site (● and O). Also shown are calculated curves from equations (2.10) and (2.11), and values of t_* and q_∞. Average values of k_s and sorptivity from the twin ring analysis were used. The expected variation in q with θ_n is also illustrated by the second curve from equation (2.11) with θ_n = 0.30.

sandy loam II site, where many continuous macropores were observed in cores. Buffered infiltrometer values, for the two sites on which this method was used, show close correspondence to twin ring values. It should be noted that ϕ_s is lower in both these cases, so lateral sorption will be of lesser significance, and buffering efficiency higher.

Sample numbers required to be within 10% of the true mean at the 0.05 confidence level (N) for well, core and buffered infiltrometer methods (see Table 2.1) are all large. This is in accord with other authors observations (e.g. Gumma, reported by Warrick and Nielsen, 1980). N is greatest for the core method. K_s distributions are, in general, better described by log-normal than normal distributions. This is also in agreement with other authors observations (Rogowski, 1972; Nielsen *et al.* 1973; Warrick *et al.* 1977). Core k_s values are more strongly log-normally distributed than k_s measured with the other methods. This difference and the lower magnitude of the well k_s values (c.f. core k_s values) are presumably due to systematic errors inherent in these methods. These errors, as previously mentioned, are probably caused by disturbance and the creation of continuous macropores in cores, and the smearing of auger hole walls in the well method. Large differences between core k_s values and Piezometer k_s values (this method being similar to the well method) are also found by Watts *et al.* (1982) for a variety of soil textures. Core k_s values are consistently found to be higher, ranging from 2 to 700 times that of piezometer k_s values, the later method being thought to give more realistic values. These results are in contrast with those of Talsma and Hallam (1981), who find close correspondence between well and core k_s values for some Australian subsoils. The New Zealand topsoils studied here would probably be more biologically active, and wetter when sampled. The effects of smearing and macropore short circuiting are thus liable to be more pronounced.

These effects are minimal in the twin ring method, and the buffered infiltrometer method as used here, and should explain the intermediate values of k_s gained in most cases. The twin ring method appears to be a viable field technique for measuring k_s on the basis of these results. While values of r_e (Table 2.4) range from 0.04 to 0.7 m, different ring radii being optimal for different soils, values of r_1 = 0.5 m and r_2 = 0.025 would be satisfactory for many soils. However, to get meaningful average q values, the number of replicate measurements required is just as large as for other methods, as demonstrated by the N values in Table 2.2.

2.5 CONCLUSIONS

The results of this chapter demonstrate the validity of Wooding's equation in a field situation, and also shows that the twin ring method is a viable means of measuring k_s and sorptivity. Comparison of the twin ring method with the core and well methods suggests shortcomings in these methods. Buffered infiltrometers appear to give similar experimental results. However, a more rigorous comparison between these two methods is required. Similarly comparison of the twin ring method and other techniques to measure sorptivity in the field is desirable.

The main advantages of the twin ring method, apart from concurrent measurement of k_s and sorptivity, are;

i) A minimum of equipment and effort is required, allowing adequate replication. This is a necessity for a field method. Sophisticated data analysis, such as Kriging (Journel and Huijbregts, 1978) to interpolate spatial changes in k_s and sorptivity is then possible.

ii) Measurement of <u>in situ</u> soil properties, with a minimum of disturbance and smearing.

This method does have disadvantages. Unless large pits are dug, only soil surface properties can be measured. Where surface crusts or other marked anisotropy exists other techniques will have to be used. In many drainage

applications horizontal conductivities are required, and methods such as the well technique are of more use. Also steady flow may not be attained in some cases. Initially dry, poorly structured or swelling soils in particular may take long times to attain steady flow. In this study however, while none of the soils are uniform with depth, q usually approached steady-state within $\frac{1}{2}$ to 2 hours.

CHAPTER 3

THREE-DIMENSIONAL INFILTRATION FROM POINT SOURCES

3.1 INTRODUCTION

Trickle experiments were carried out on three sites previously studied; the Manawatu sandy loam, fine sandy loam I and II sites. These experiments were used to test the usefulness of the soil parameters determined in the previous chapter, and also to investigate water movement from point sources discharging onto the soil surface. In contrast to experiments using rings, where source radii are fixed and flow rates are variable, here constant flow rates are imposed. The wetted radius is then free to expand with time, with the ponded area increasing as the soil's ability to accomodate the imposed flux decreases with time. Eventually steady ponded zone sizes should be attained, but these may not necessarily correspond to steady-state water content distributions in the soil under the emitter. This disparity in times to reach steady-state is clearly illustrated by numerical simulations (e.g. Brandt et al. 1971), with steady ponded radii being relatively rapidly attained, but wetted volumes still expanding at long times. Figures 1.1 and 1.2, given earlier, demonstrate this.

3.2 MATERIALS AND METHODS

3.2.1 EXPERIMENTAL TECHNIQUE

Prior to applying water to the soil, the surface vegetation was removed, and the surface levelled with a sharp knife to smooth the microtopography. Constant water application rates were achieved by using either a constant head water supply and small internal diameter emitter tubing (a so called Torricelli tube) or a peristaltic pump. Flow rates below $7.5 \times 10^{-7} m^3 s^{-1}$ (approx. 2.7 l/hr) were used, as levelling of the larger areas required for higher flow rates was difficult. On several occasions Rhodamine BN dye was added to the water to identify flow paths of the soil-water away from the ponded zone.

3.2.2 WATER CONTENT DISTRIBUTIONS

Soil water content profile distributions were determined at the completion of irrigation by gravimetric sampling with a tube corer. The water contents are given in the form of the increment above the antecedent water content i.e. $(\theta - \theta_n)$. Limitations of equipment and time (redistribution beginning immediately at cessation of irrigation) prevented a large scale systematic sampling that would be required to adequately describe θ distributions under trickle sources (Ben-Asher, 1979). Also the effect of variability may make it impossible to effectively describe water distributions (Cassel and Nelson, 1980). Only 3 to 4 samples were taken radially from the emitter to provide the general pattern of water movement from the emitter.

The total water content increment at each radius ($\Delta\theta$) was estimated by:

$$\Delta\theta = \sum_{\Delta z_i=1}^{n} (\theta_{(i)} - \theta_{n(i)})\,\Delta z_i \qquad (3.1)$$

with n the number of samples of length Δz in the profile. The increase in water content from irrigation, $W(m^3)$, in the sampled soil volume is estimated as:

$$W = \pi r_w^2\, \overline{\Delta\theta} \qquad (3.2)$$

where r_w is the wet front radius, and $\overline{\Delta\theta}$ the mean profile water content from (3.1). This simple method assumes a uniform radial distribution.

3.2.3 PONDED AND WET FRONT RADII

Photographs were taken directly above the source for different elapsed times, and the average ponded (r_p) and wetted (r_w) radii estimated by graphical integration off the prints. An upper limit on k_s can be found from the steady-state ponded radius by assuming horizontal sorption to be negligible, and so $k_s \leq Q.(\pi r_p^2)^{-1}$.

Occasionally more than one flow rate was used on the same site, with the higher flow rate following lower rate.

In this case the effects of spatial variability in soil properties are minimized, and k_s and ϕ_s can be found from methods used for buffered infiltrometers in Chapter 2.

3.2.4 PREDICTED WET FRONT DEPTH

Wet front penetration depths were estimated using conservation of mass and the simple wetted profile of Green and Ampt (1911). This assumes that the water penetrates the soil with a sharp wet front, behind which the soil is satiated (i.e. $\theta = \theta_s$). Wet front penetration is calculated simply from:

$$z_w = Qt[\, r_w^2 \pi(\theta_s - \theta_n)\,] \qquad (3.3)$$

where z_w is the wet front penetration, and t the length of time of application. Although r_p can be estimated using Wooding's equation and suitable values of k_s and ϕ_s, no simple analytical theory with field utility allows prediction of r_w. To estimate wet front penetration then field observations of r_w were used.

3.3 RESULTS

3.3.1 PONDED AND WETTED RADII

(a) Field observations during trickle experiments

Plan outlines of ponded zones for experiments on the three soils, and wetted zones at the completion of irrigation are shown in Figures 3.1a, 3.2a and 3.3a. While care was taken in levelling the soil surface, the effects of microtopography, coupled with spatial variability in soil properties are still quite evident. These exert a dominant control over the shape of ponded zones, and hence wetted zones. Estimation of r_p is hindered by this variability, and also by a lack of definition of the ponded zone edge. Ponded and wetted radii with time for these experiments are plotted in Figures 3.1b, 3.2b and 3.3b.

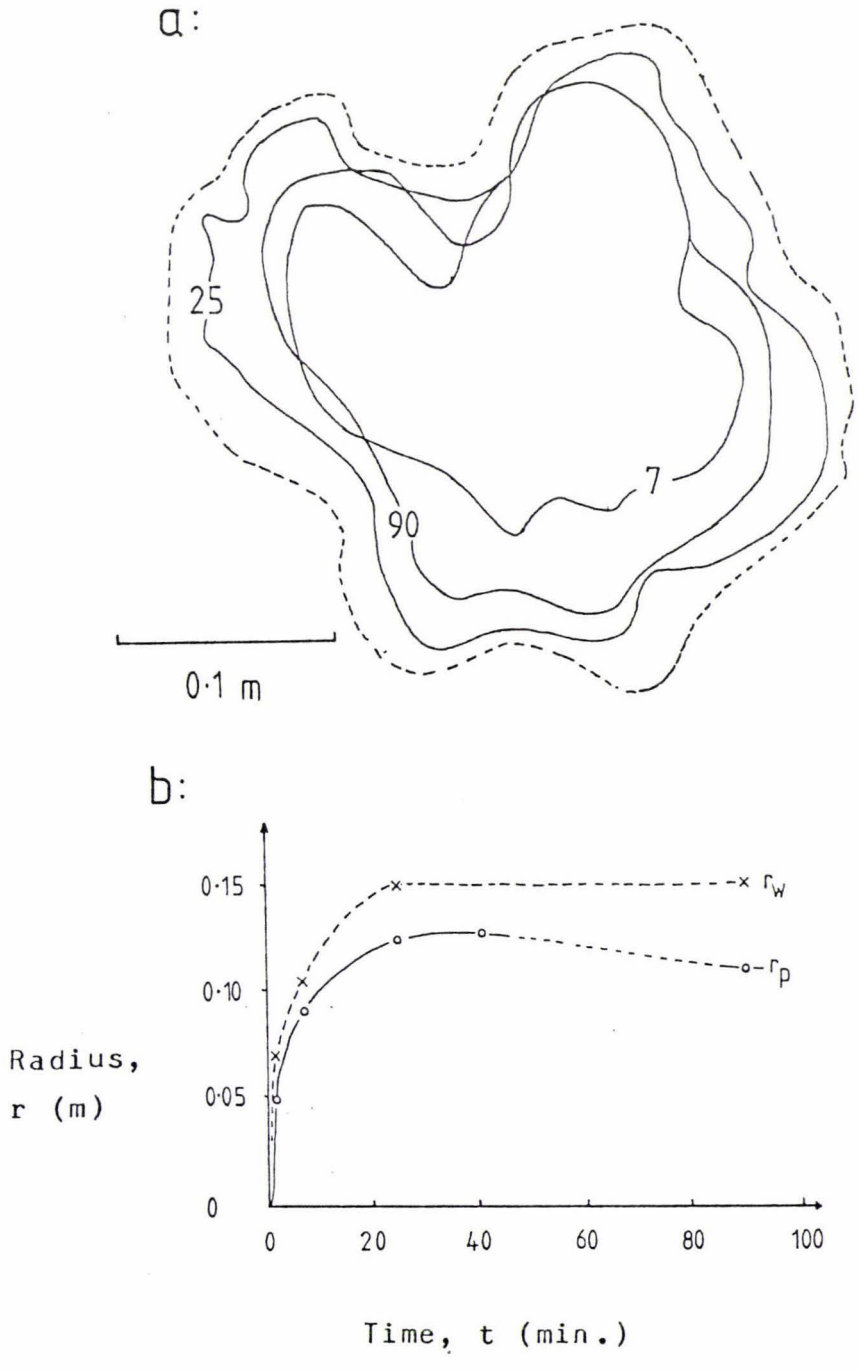

Fig. 3.1 Trickle experiment on the Manawatu sandy loam, with $Q = 2.6 \times 10^{-7} m^3 s^{-1}$.

(a) Plan outline of ponded zone with time.
— Ponded zone. Numbers on lines identify time in minutes.
--- Wetted zone at completion of experiment (t = 90 min.).

(b) Ponded (O) and wetted (X) radii with time, estimated from graphical integration off photographs.

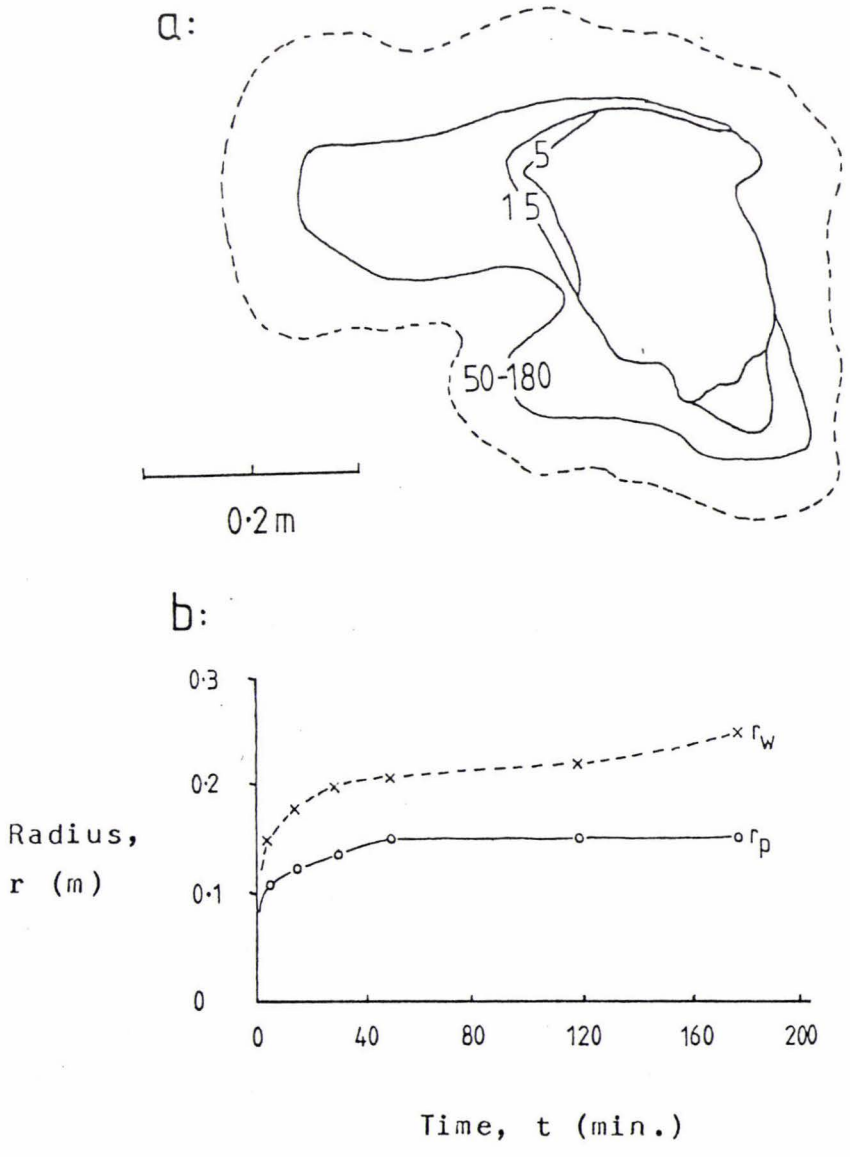

Fig. 3.2 Trickle experiment on the Manawatu fine sandy loam I, with $Q = 6.8 \times 10^{-7} m^3 s^{-1}$.

(a) Plan outline of ponded zone with time.
— Ponded zone. Numbers on lines identify time in minutes.
--- Wetted zone at completion of experiment (t = 180 min.).

(b) Ponded (o) and wetted (x) radii with time, estimated from graphical integration off photographs.

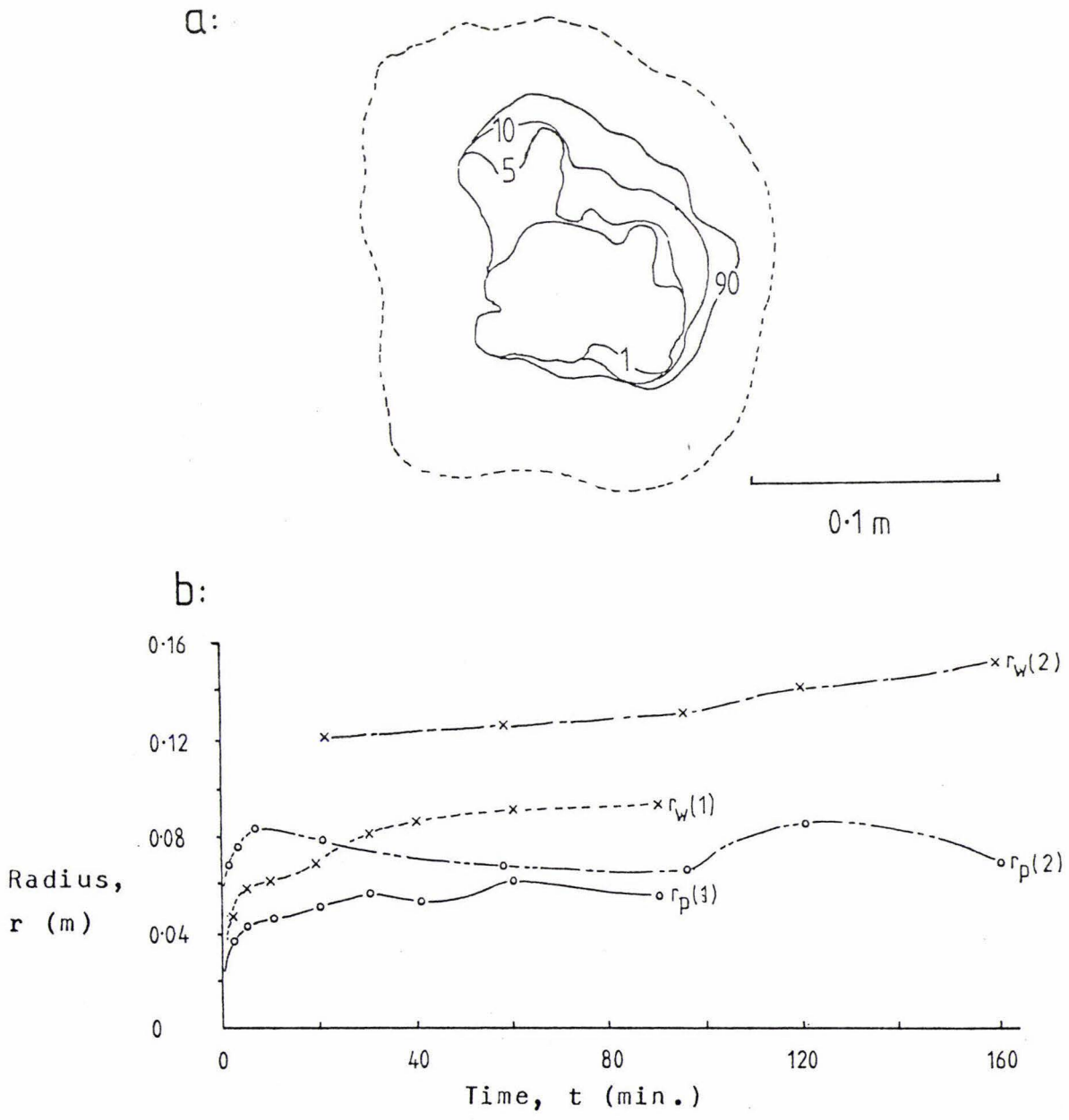

Fig. 3.3 Trickle experiment on the Manawatu fine sandy loam II. Two flow rates were used. First $Q = 1.5 \times 10^{-7} m^3 s^{-1}$, followed by $Q = 4.6 \times 10^{-7} m^3 s^{-1}$.

(a) Plan outline of ponded zone for $Q = 1.5 \times 10^{-7} m^3 s^{-1}$.

—Ponded zone. Numbers on lines identify time in minutes.

---Wetted zone at completion of experiment (t = 90 min.).

(b) Ponded (O) and wet front (×) radii with time. Figures identify whether radii are for first (1) or second (2) flow rate.

In all experiments the ponded zone size increased rapidly initially, and then slowly approached a steady size. However, in only one case (Figure 3.2) was a constant radius maintained for any length of time. In the other two experiments described here (and many others) large variations in radii with time were seen. This is attributed to soil detachment and the blocking of pores by soil particles, pore wall erosion, and earthworm activity in at least one case. In an experiment on the Manawatu fine sandy loam I site, with $Q = 7.2 \times 10^{-7} m^3 s^{-1}$, a steady r_p of 0.13 m was found after about 65 minutes (Figure 3.4a). The next morning, some 1100 minutes after the start of irrigation r_p had decreased drastically to 0.02 m (Figure 3.4b). Earthworms had vented their burrows directly under the emitter. Assuming only one-dimensional flow, this would represent a 400% increase in k_s in less than 17 hours.

(b) Calculated saturated hydraulic conductivities

Mean k_s and ϕ_s values calculated from trickle experiments where two or more flow rates were used are given in Table 3.1, along with estimated upper limits to k_s from all trickle experiments. The k_s and ϕ_s values for both Manawatu fine sandy loams show little resemblance to those derived from the twin ring method (Tables 2.3 and 2.4). An order of magnitude difference exists between the k_s values, and similarly the ϕ_s values exhibit little correspondence. Spatial variability and the differing nature of ponding between the two experiments may account for some of this difference. Large macropores are often only partially filled in trickle experiments, whereas they can represent a major flow path when a ponded zone is maintained above them. Related to this is also the variability of r_p with time. For some experiments large increases in Q resulted in only small increases in r_p, suggesting temporal variations in k_s. In one example on the Manawatu fine sandy loam II the higher Q was found to have a smaller r_p compared to the earlier, lower Q. This results in a negative k_s value, which is physically

a

b

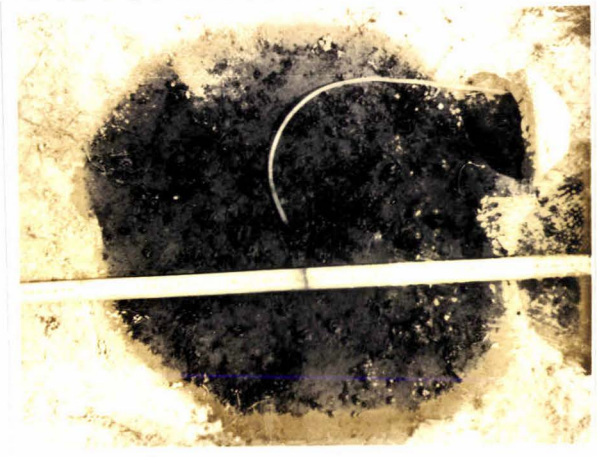

Fig 3.4 Trickle experiment on the Manawatu fine sandy loam I, with $Q = 7.2 \times 10^{-7} m^3 s^{-1}$.

(a) 65 minutes after the beginning of irrigation. The ponded radius is approximately 0.13m. Scale is in centimetres.

(b) 1100 minutes after the beginning of irrigation. The ponded radius is now approximately 0.02m. Many worm castes are apparent. Scale is in centimetres.

Table 3.1 Comparison of Twin Ring and Trickle Experiment methods of measuring k_s and ϕ_s, and the Upper Limit to k_s from Trickle Experiments.

Method:			Manawatu sandy loam	Manawatu fine sandy loam I	Manawatu fine sandy loam II
Trickle experiments with two flow rates	k_s	($\times 10^{-6} ms^{-1}$)	-	1.7 ± 0.8	30 ± 5
	ϕ_s	($\times 10^{-7} m^2 s^{-1}$)	-	0.03 ± 0.08	-7.7 ± 6
Upper limit to k_s from trickle experiments	k_s	($\times 10^{-6} ms^{-1}$)	19 ± 29	11 ± 7	0.2 ± 0.2
Twin Ring method (Chapter 2)	k_s	($\times 10^{-6} ms^{-1}$)	12 ± 3	15 ± 4	5.2 ± 5
	ϕ_s	($\times 10^{-7} m^2 s^{-1}$)	1.9 ± 3	-0.7 ± 1.3	6.9 ± 7

impossible. Problems such as flux tend to indicate that this method is of little use in estimating k_s and ϕ_s.

The measured upper limit to k_s, calculated assuming only one-dimensional flow, also varies temporally. With the exception of the Manawatu fine sandy loam II site, mean upper limits to k_s (calculated from final ponded zone sizes) are similar in magnitude to k_s values from the twin ring method. The near order of magnitude difference between the two methods for the Manawatu fine sandy loam II site, will be due to both the assumption of only one-dimensional flow occuring being untrue (ϕ_s is high in this site as shown in Chapter 2), and to the high level of biological activity resulting in many surface venting macropores. These surface vented pores, as previously mentioned, may not fill completely during trickle experiments, but may be major flow paths when a head of about 10 mm is present. These results suggest that using trickle experiments to estimate the upper limit to k_s is only a reliable method where ϕ_s and biological activity are low. Temporal variation in k_s, which can be quite marked, could easily be examined though.

(c) Comparison of trickle experiments with the results of the twin ring method

Experimental trickle r_p data for various flow rates are plotted for the three sites in Figures 3.5, 3.6 and 3.7. Also shown are parabolas from Wooding's equation, calculated using the mean k_s and ϕ_s values from the twin ring experiments. These values are reiterated in Table 3.1. The shaded areas in Figures 3.5 to 3.7 enclose the 95% confidence intervals calculated from differential-error analysis (Fritschen and Gay, 1979).

A reasonable degree of scatter is found in the trickle experiment points due to both spatial and temporal variability in soil properties. However, most experimental

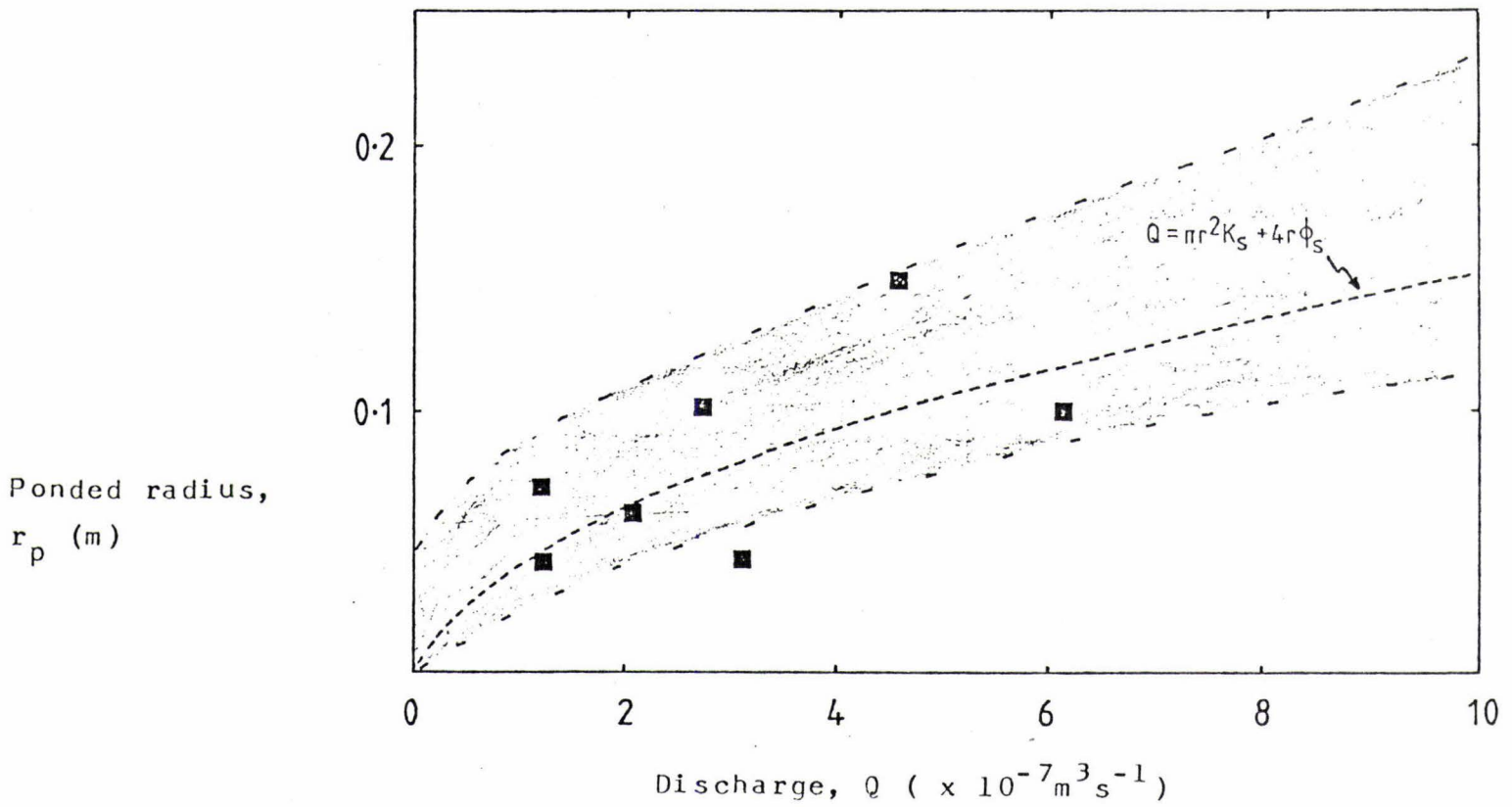

Fig. 3.5 Trickle experiments (■) in relation to predicted ponded radii from Wooding's equation (equation 1.14) for the Manawatu sandy loam. Average values of k_s and ϕ_s from the twin ring analysis are used. Shaded area indicates the 95% confidence interval.

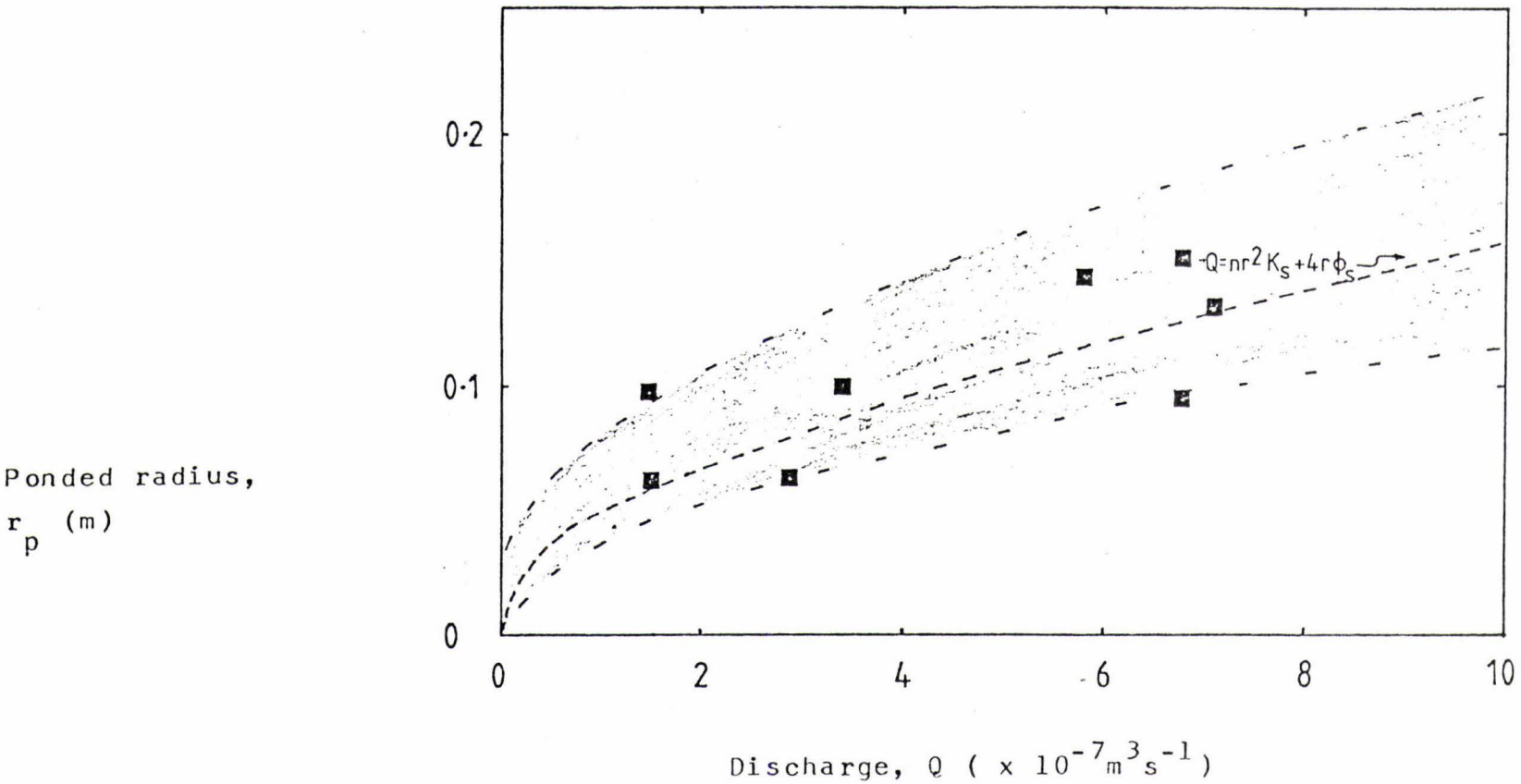

Fig. 3.6 Trickle experiments (■) in relation to predicted ponded radii from Wooding's equation (equation 1.14) for the Manawatu fine sandy loam I. Average values of k_s and ϕ_s from the twin ring analysis are used. Shaded area indicates the 95% confidence interval.

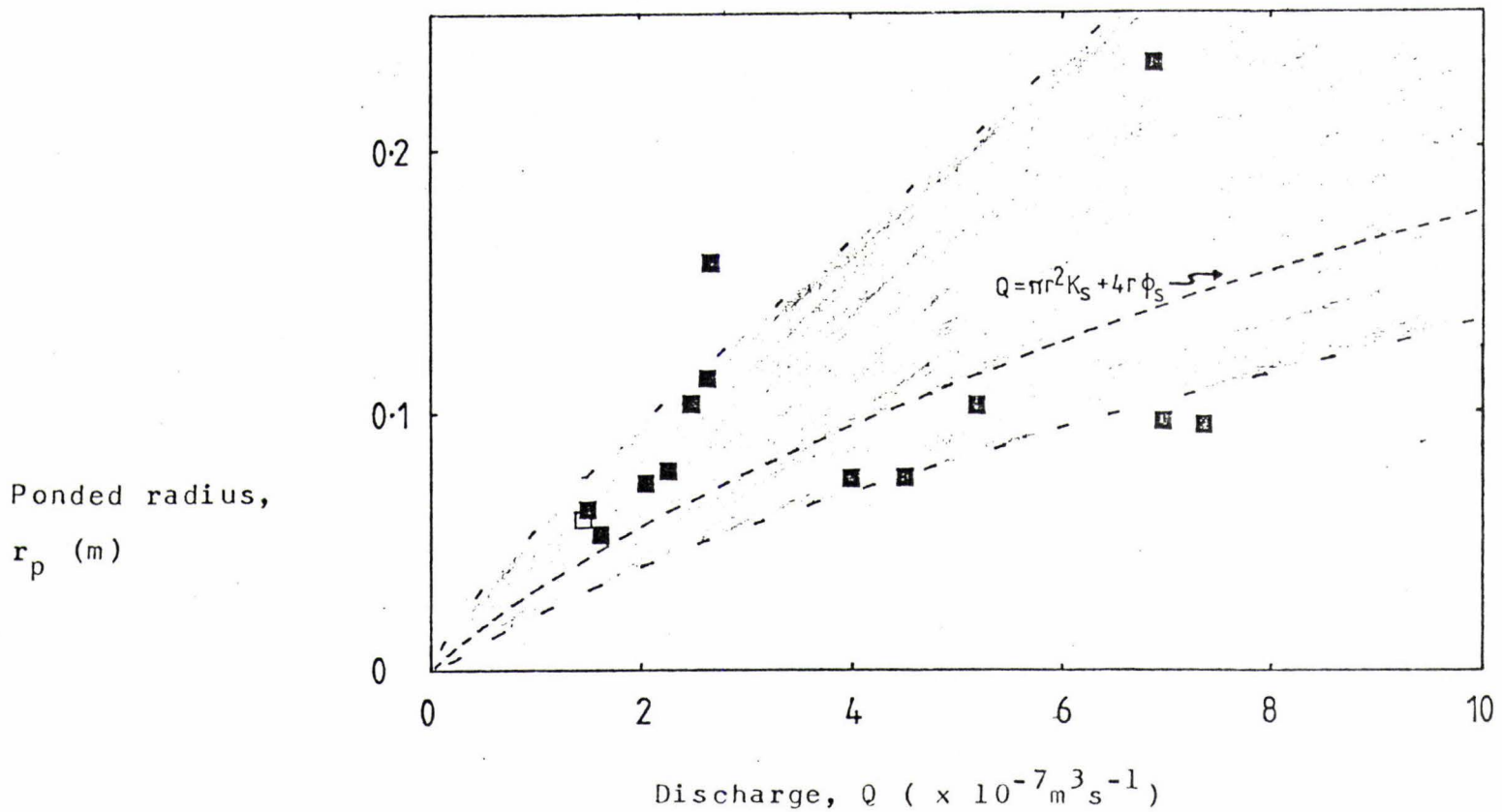

Fig. 3.7 Trickle experiments (■) in relation to predicted ponded radii from Wooding's equation (equation 1.14) for the Manawatu fine sandy loam II. Average values of k_s and ϕ_s from the twin ring analysis are used. Shaded area indicates the 95% confidence interval.

points are contained within the 95% confidence interval about the predicted curve. Of particular mote is the better correspondence in the Manawatu sandy loam and fine sandy loam I sites, where more reliable values of k_s were found (see errors in Table 2.1). In the Manawatu fine sandy loam II site the k_s data is less reliable, so a much wider confidence interval is found. The effect of this is especially pronounced at high flow rates where k_s is of greater importance. The contribution of k_s increases with r^2. The actual variability in k_s in the field also results in a larger degree of scatter at these high flow rates. In the other two sites the large uncertainty in ϕ_s is of little concern, due to the low value of ϕ_s. Also it is only important at very low flow rates.

All three sites have similar predicted r_p values (circa. 0.05 to 0.15 m) for similar flow rates despite k_s varying by a factor of 2. This is due to an interaction between ϕ_s and k_s. The parameters found by the twin ring analysis predict the experimental trickle ponded radii moderatly well, especially when taking into account variability in soil properties and the differing nature of ponding between rings and trickle emitters. That this simple theory could be of use in predicting r_p under trickle emitters is of practical interest in design of trickle irrigation systems.

3.3.2 WATER CONTENT DISTRIBUTIONS

Long times are required for water content distributions to attain steady-state under emitters. At steady-state large volumes of additional water are required to cause even small θ increments far from the source. In the trickle experiments described here elapsed times are far too short for steady water contents to be reached even near the emitter, and so no examination of solutions which give water content distribution at steady-state (e.g. Wooding, 1968) was undertaken. Water content distributions after the completion of trickle experiments were examined however, to examine the qualitative pattern of water

movement. Water content profiles, which are generally representative of all trickle experiments, for the three experiments given as examples in the previous section are shown in Figures 3.8 to 3.10.

In all experiments the depth of wet front penetration was quite variable with radius from the emitter. Wet fronts were found at greater depths where the like of earthworm castes or old root channels obviously acted as preferential flow paths. On the Manawatu fine sandy loam II Rhodamine dye, when used, was found almost exclusively in large channels, many of which were found to penetrate to great depths, (see Figure 3.11). In some cases these macropore pathways may result in water by-passing the effective root zone especially if there is a permeable underlying stratum. This variability in water content distribution is seen clearly in Figure 3.9, where the wet front at 0.1 m from the emitter is only 30 mm deep, while at the edge of the ponded zone (r_p = 0.15m) the wet front is found at z = 0.11 m. Similar irregularities in ($\theta - \theta_n$) with depth can also be seen in Figures 3.8 and 3.10. These are also likely to reflect preferential flow down macropores.

Wet front depths predicted by equation (3.3), which assumes uniform wetting of the soil over the whole wetted area, are also seen in Figures 3.8 to 3.10. This simple model adequately predicts z_w in two cases here (Figures 3.8 and 3.9), although actual ($\theta - \theta_n$) profiles are considerably more variable, and do not correspond well with ideal Green and Ampt (1911) wetted profiles. These predicted wet front depths are integrally correct since they are calculated from the total volume of water applied. In the Manawatu fine sandy loam II example this model does not adequately predict z_w. Such a discrepancy is surmised to be due to large macropores conducting a large portion of the applied water to depths below those sampled.

While radially symetric θ distributions were not found

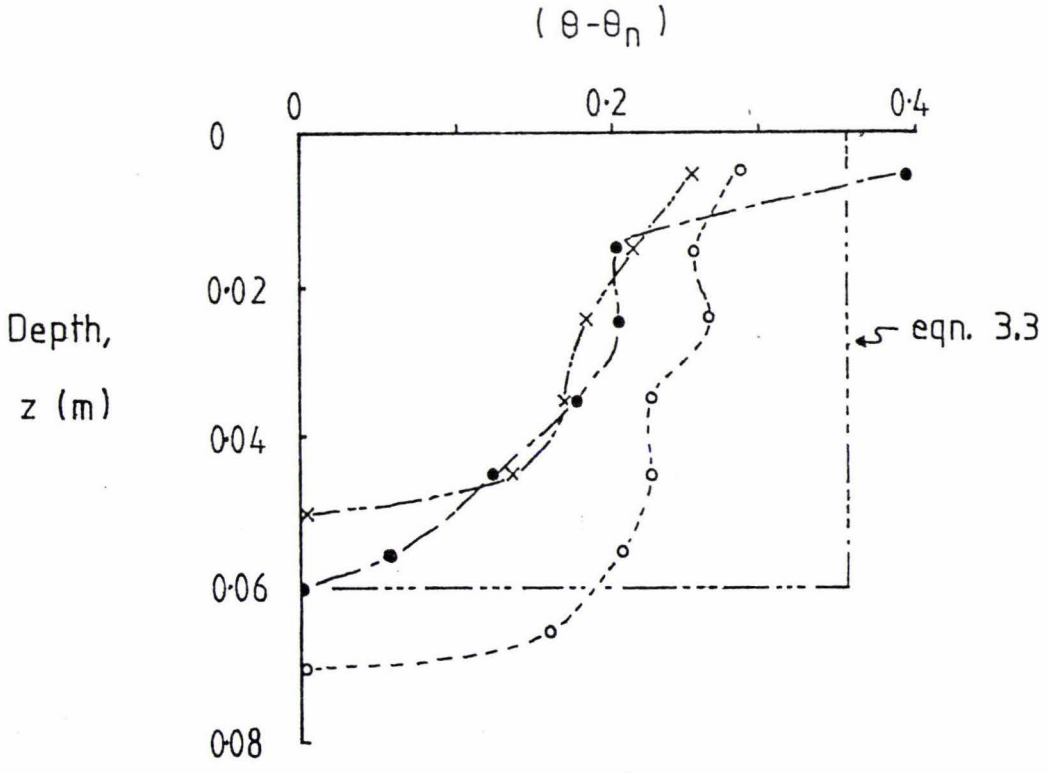

Fig. 3.8 Water content distribution for a trickle experiment on the Manawatu sandy loam with $Q = 7.2 \times 10^{-7} m^3 s^{-1}$. Shown are measured $(\theta - \theta_n)$ profiles under the emitter (O), 5cm from the emitter (X) and at the edge of the ponded zone 10cm from the emitter (●). The predicted wet front from equation (3.3) is also shown. This experiment corresponds with that shown in Figure 3.1.

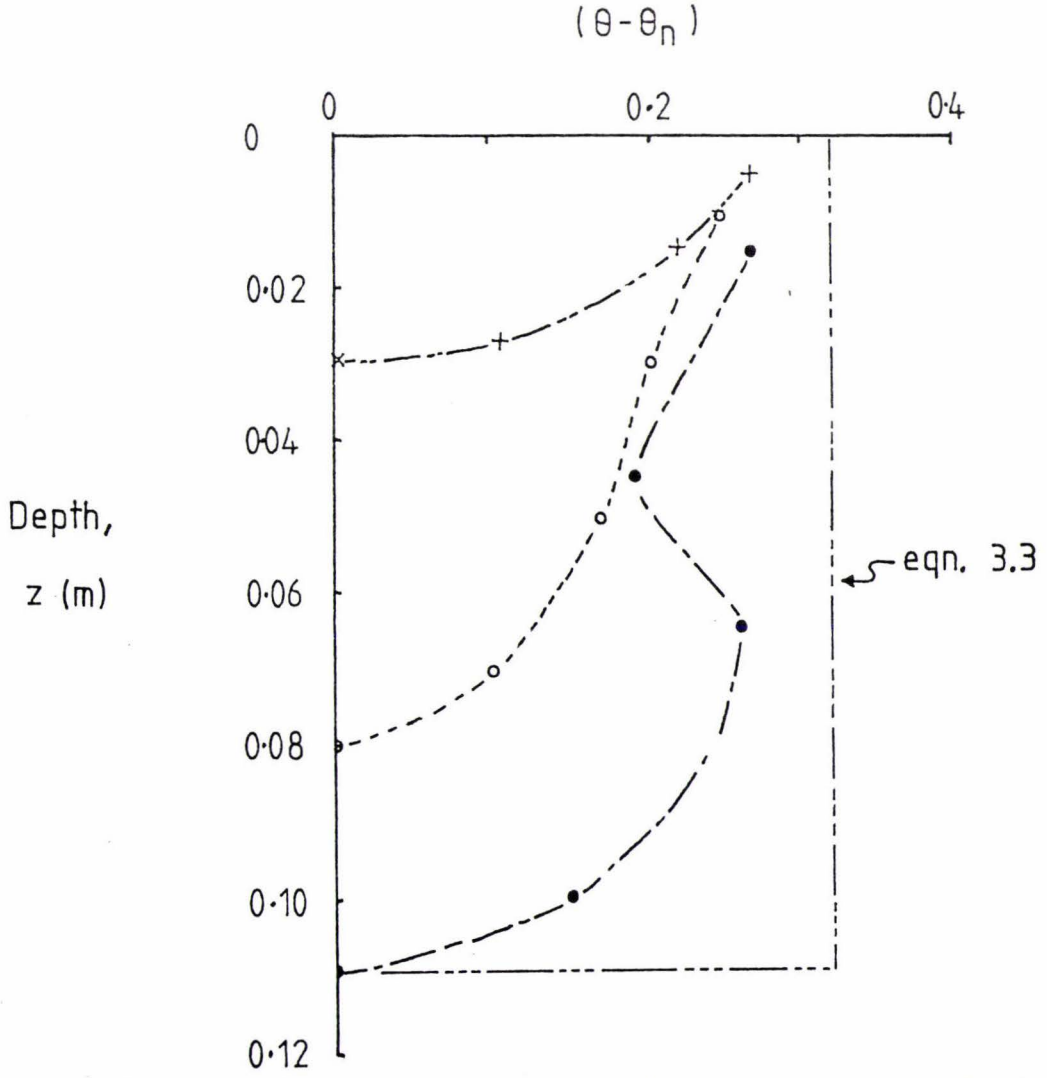

Fig. 3.9 Water content distribution for a trickle experiment on the Manawatu fine sandy loam I with $Q = 6.8 \times 10^{-7} m^3 s^{-1}$. Shown are measured $(\theta-\theta_n)$ profiles under the emitter (o), 10 cm from the emitter (×) and at the edge of the ponded zone 15 cm from the emitter (●). The predicted wet front from equation (3.3) is also shown. This experiment corresponds with that shown in Figure 3.2.

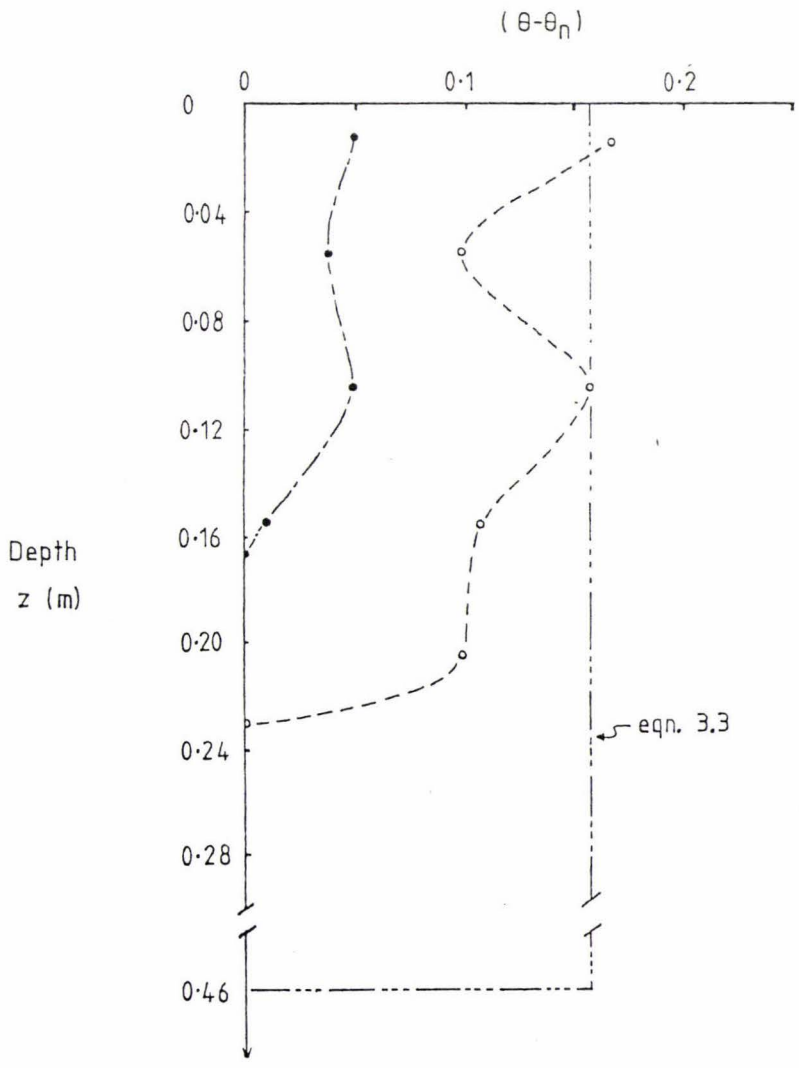

Fig. 3.10 Water content distribution for a trickle experiment on the Manawatu fine sandy loam II. Two flow rates were used, first $Q = 1.5 \times 10^{-7} m^3 s^{-1}$, followed by $Q = 4.6 \times 10^{-7} m^3 s^{-1}$. Shown are measured $(\theta - \theta_n)$ profiles under the emitter (O) and at the edge of the wetted zone 15cm from the emitter (●). The predicted wet front from equation (3.3) is also shown. This experiment corresponds with that shown in Figure 3.3.

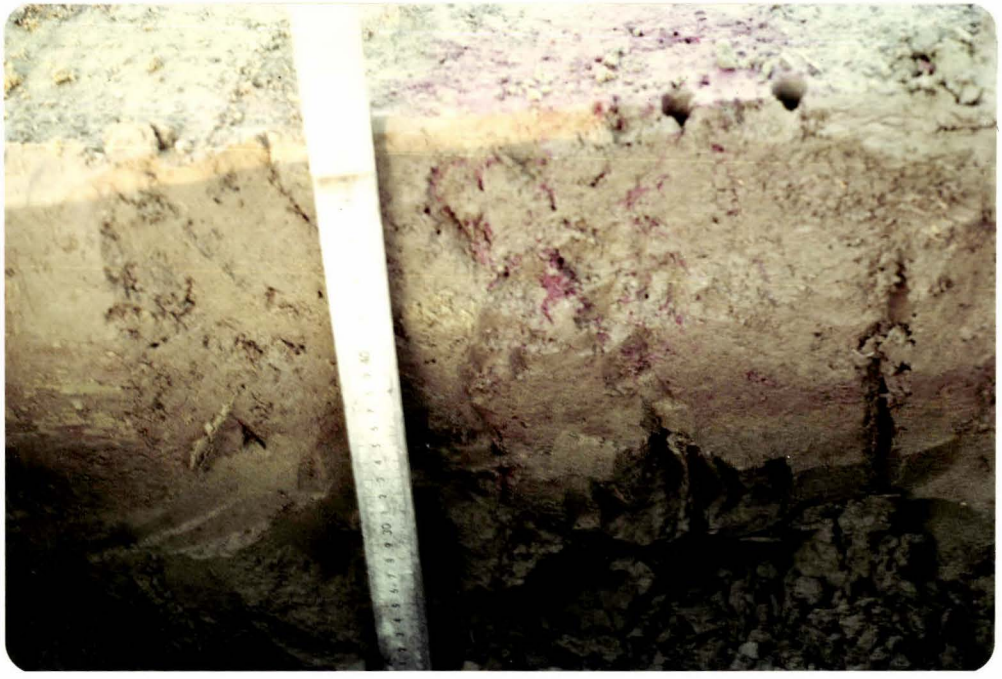

Fig. 3.11 Trickle experiment on the Manawatu fine sandy loam II site. Rhodamine dye was used in the irrigation water to identify preferential flow paths.

Table 3.2 Total Irrigation Input and Measured Water Content Increase

	Input Q.t ($\times 10^{-3} m^3$)	Measured Increase W ($\times 10^{-3} m^3$)	Percent Recovered W/Q.t (%)
Manawatu sandy loam	1.4	0.72	51 (65)[1]
Manawatu fine sandy loam I	7.4	4.9	67 (59)[1]
Manawatu fine sandy loam II	5.2	1.9	37 (42)[1]

1. Average percentage of Q.t recovered by sampling.

in any experiments, such distributions were assumed to estimate the total water content increase that should result from irrigation. This estimated water content increase, for the three examples above, is shown in Table 3.2, along with the total irrigation input (Q.t). In each case significant proportions of the applied water remain unaccounted for, especially in the Manawatu sandy loam II example. Average water content increases for all trickle experiments similarly show deficits over applied water. These figures are also given in Table 3.2. Measured water content increases are much closer for the two soils where macropores were found to be less prevalent. Along with sampling errors, macropores conducting water away from areas where core samples were taken, are probably the main causes of these discrepancies.

3.4 CONCLUSIONS

While infiltration theory is comparatively well developed, it is used little in field situations (Philip, 1980). In this chapter it has been demonstrated that the linearized steady-state infiltration solution of Wooding (1968), in conjunction with field measured physical parameters, can adequately predict the ponded radii that form on the soil surface under trickle emitters. This could be of use in designing trickle irrigation systems, as discussed in Chapter 1. While steady-state water content distributions were unlikely to be found in these experiments, due to their short duration, the pattern of water content distribution following irrigation was briefly examined. It was found that macropores exert a large degree of control over water content distributions, as well as ponded zone shapes and sizes. Micro-relief compounds this even further. Such heterogeneity may have important consequences in orchard soils. These consequences are discussed in the following chapter, where a commercial trickle irrigation system is examined.

CHAPTER 4

TRICKLE IRRIGATION OF THE MASSEY UNIVERSITY ORCHARD

4.1 INTRODUCTION

A trickle irrigation system operated by Massey University in an apple orchard was studied with two main aims:

- To examine the efficiency of the trickle irrigation system and to determine optimum rates of irrigation

- To examine the utility of the previously determined soil physical parameters in the design and operation of a commercial irrigation system, and to further examine Wooding's (1968) solution in the field.

4.2 MATERIALS AND METHODS

4.2.1 MASSEY ORCHARD

The Massey Orchard is located on the edge of an alluvial terrace, on the Manawatu fine sandy loam II soil. Several varieties of apples are grown (Splendour, Granny Smith, Coxes Orange and Fuji) at 3.7 m spacings in rows 4.5 m apart. Trickle irrigation has been in operation since orchard establishment in 1978.

An automated trickle irrigation system is used, with water drawn from domestic mains. The system is composed of:
(a) a pressure regulator, time clock and control valve assembly,
(b) an in-line water-filter,
(c) and 0.05 m (2 inch) polythene mains feeding to 0.012m ($\frac{1}{2}$ inch) laterals,
(d) and two multi-chambered pressure regulating emitters, spaced 0.75 m each side of the tree (see Figure 4.1).

In the Manawatu region irrigation often only fills a role of being supplementary to rainfall. Automatic irrigation control is used so as to lower labour requirements. At the beginning of the orchard production

Fig. 4.1 A multi-chambered pressure regulating emitter of the type used in the Massey Orchard. Note the numerous worm castes.

season irrigation was carried out for four hours (8 a.m. to 12 p.m.) every second day. This was later increased to daily irrigation during late summer (February to March). Herbicide application down a 2 m strip along laterals is used to control weed growth to a certain extent.

4.2.2 TENSIOMETRY

In 1980/81 several tensiometers were used to monitor root zone soil-water potentials (Ψ) during normal operation of the system. Tensiometers were installed along one lateral around a tree (as shown in Figure 4.2) to measure soil water potentials, and also to allow calculation of instantaneous drainage fluxes. The six Bourdon gauge type tensiometers used (Irrometer Co.) were calibrated before installation using a pressure transducer and vacuum source. Thirteen mercury manometer tensiometers were also used. Soil water potential for these manometer tensiometers was calculated using the equation in Figure 4.2(b). All tensiometers were installed on the 23rd December 1980, during rain. Initially a hole was augered, and prior to the insertion of the tensiometer a slurry of fine sandy loam poured down to ensure good contact between the soil and ceramic cup, and also to prevent preferential water flow down the tube side. Figure 4.3 illustrates the good contact between the tensiometer cup and soil that was achieved. Also noticeable in Figure 4.3 are apple-tree roots, at a distance of 0.5 m from the tree. While no roots were seen at the 0.8 m depth, the shallower tensiometers should have provided a measure of Ψ within the tree root zone.

Drainage fluxes were calculated from (average) soil-water potentials using Darcy's Law:

$$J = - k(\Psi) . d\Psi_t/dz \qquad (4.1)$$

Here J is the (one-dimensional) vertical drainage flux, and Ψ_t the total soil water potential (i.e. the sum of gravitational and matric potentials). An exponential conductivity function (equation 1.7) was assumed with the

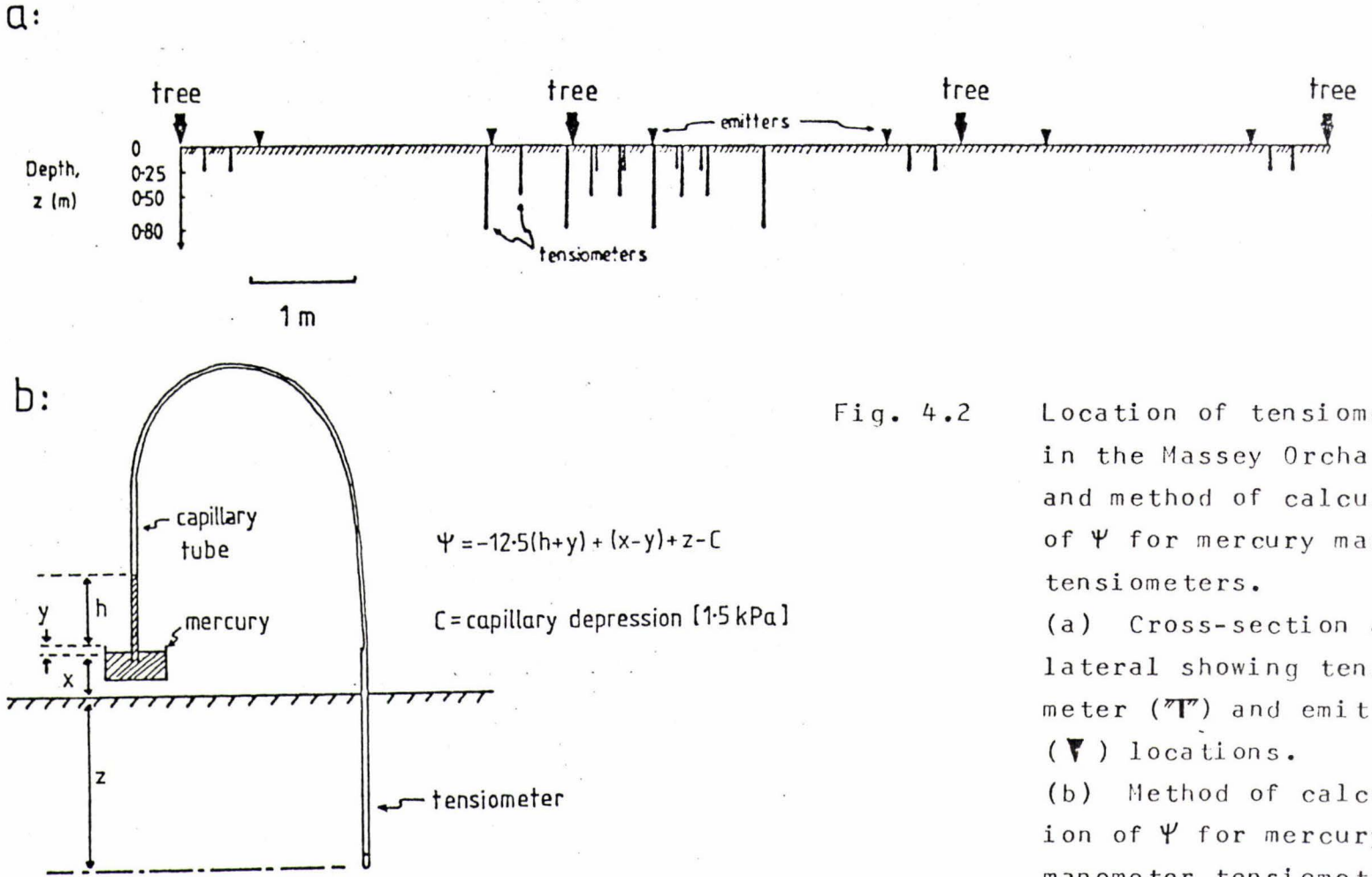

Fig. 4.2 Location of tensiometers in the Massey Orchard, and method of calculation of Ψ for mercury manometer tensiometers.
(a) Cross-section along lateral showing tensiometer ("T") and emitter (▼) locations.
(b) Method of calculation of Ψ for mercury manometer tensiometers.

Fig. 4.3 Installed tensiometer cup. Note the close contact with the soil and large apple tree roots. This tensiometer was located 0.5m from the tree at a depth of 0.25m.

required values of k_s and α derived from the twin ring analysis (Chapter 2). An arithmetic average value of Ψ from the tensiometer data was used to estimate $k(\Psi)$ at the mid-point between the two tensiometers. These drainage fluxes should at least indicate the direction of water movement under trickle emitters, although their magnitude will be subject to error especially near saturation.

Water balance drainage fluxes (see section 4.2.3) are assumed constant over the whole wetted area, and are calculated on a whole day basis. Drainage fluxes calculated from tensiometer data are only instantaneous rates for midday when readings were taken (at the completion of irrigation, if it occured, when the soil is wettest). These fluxes also only apply to a particular distance and depth from the emitter.

4.2.3 WATER BALANCE FOR THE MASSEY ORCHARD

(a) Introduction

To examine the usefulness of irrigation in this orchard a simple water balance was developed. A schematic representation of this is shown in figure 4.4. While trickle irrigation only wets isolated volumes of soil, this balance is applied uniformly and therefore could, if required, also be used for orchard spray irrigation for example, where water is applied to a large proportion of the orchard. For practical use water balances should be simple, and use readily available information. While more complex models exist than presented here (e.g. Baier and Robertson,1968; Hewett, 1976), the extra information and calculation required may not be feasible in this complex situation.

Basic to the construction of any water balance is the statement of the balance of mass. Here this takes the form of:

$$\Delta St = RF + I - ET - d \qquad (4.2)$$

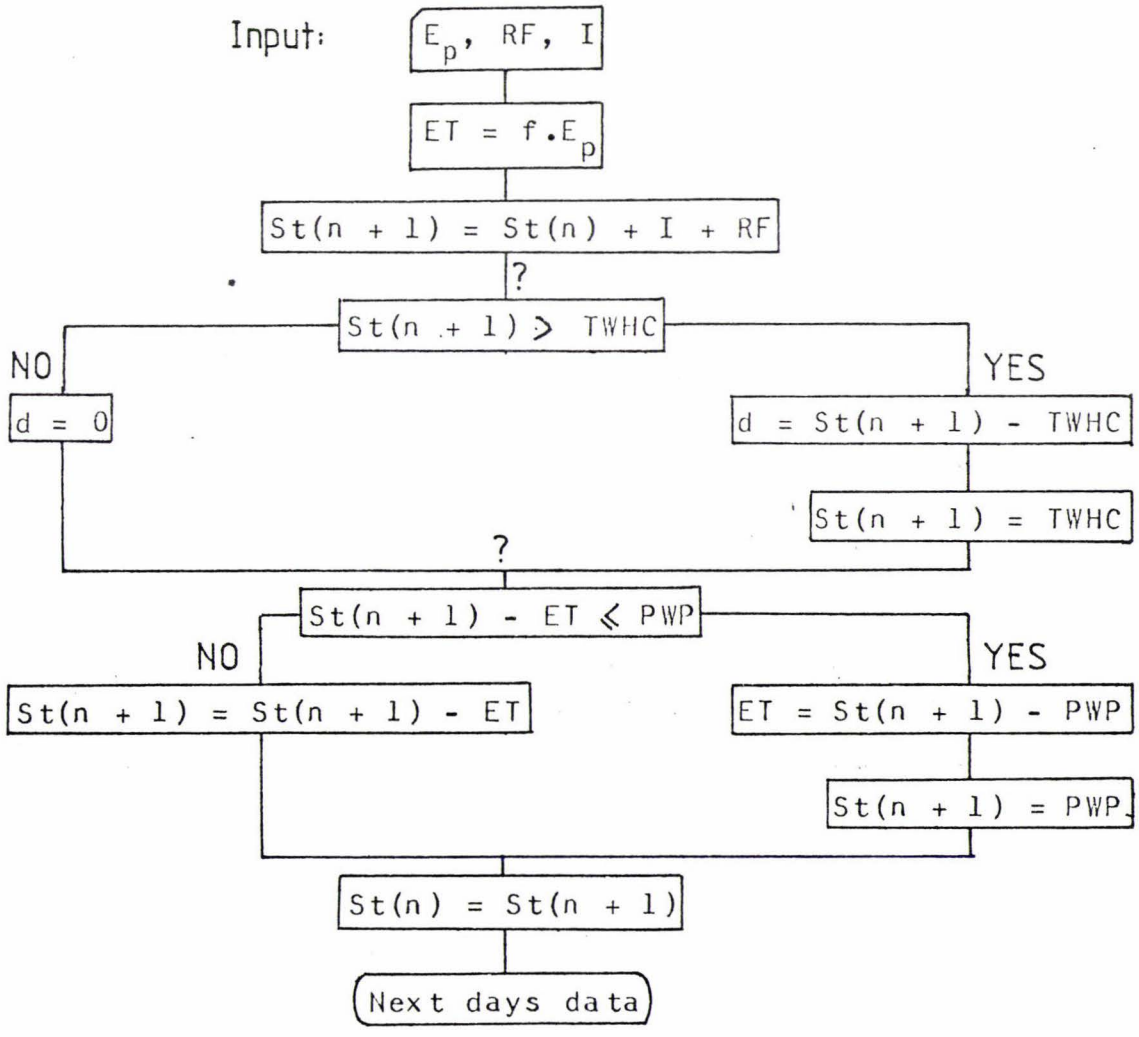

Fig. 4.4 Schematic representation of the water balance (Section 4.2.3). Symbols, defined in the text, are as follows: E_p pan evaporation, RF rainfall, I irrigation, ET evapotranspiration, f crop factor, St(n) soil-water storage on day n, TWHC total water holding capacity, d drainage, PWP Permanent wilting point capacity.

where the change in soil-water storage over a day (ΔSt) is a response to inputs (rainfall RF, and irrigation I), minus losses (evapotranspiration ET, and drainage d). All terms in equation (4.2) have units of length (i.e. volume per unit surface area). Surface runoff, which is often a major component in the water balance of slopes and impermeable soils (Rubin, 1966) is in this case assumed negligible. As this site is level, and k_s is high compared to likely instantaneous rainfall rates, this assumption appears reasonable.

For water balances it is usual to assume that soil profile characteristics are uniform with depth over a given area, and also that balance components are similarly constant over this area. The first assumption may be untenable where vertical differentiation or macropores alter soil-water flow patterns. The second assumption of spatial uniformity in the individual balance components obviously does not hold over the whole orchard area in this case. In the orchard irrigation inputs and crop cover are confined to small areas, so that other balance components will differ spatially as a consequence. The water balance is used only over a small proportion of the orchard (the estimated wetted area) as a result.

(b) Water balance

The principles involved in the construction of the water balance (Figure 4.4) are listed below.

(1) All daily inputs are assumed to be instantaneous, and to occur before ET losses. With irrigation being carried out in the morning, and since ET is most likely greatest during early and mid-afternoon, this appears reasonable. For rainfall this assumption would also be inconsequental. Irrigation inputs in mm day^{-1} are calculated from the total water application (in litres) divided by the assumed wetted area.

(2) Drainage is assumed to occur instantaneously when the soil-water storage is greater than "field capacity". Field capacity is taken here as the water content at -10kPa. While profile drainage is commonly a slow process, rapid percolation of water in macropores under near saturated conditions commonly occurs (Thomas and Phillips, 1979), and this may be important at this site as shown in Chapter 3. A pressure potential of -10kPa is then a reasonable value for field capacity. Furthermore, drainage in soils underlain by a coarse-textured layer, such as at this site (see Appendix A.1), tends to occur only over a narrow range of relatively high potentials (Eagleman and Jamieson, 1962; Clothier et al. 1977). This soil has been found to be well represented by such a simple drainage model (Clothier et al. 1977).

(3) Total profile soil-water storage is the integral of water content with respect to depth:

$$St = \int_0^z \theta dz. \qquad (4.3)$$

Thus the total water holding capacity at the field capacity already defined (TWHC) is:

$$TWHC = \int_0^z \theta_{FC} dz. \qquad (4.4)$$

where θ_{FC} is the volumetric water content at field capacity. For simplicity θ_{FC} is set equal to that of the topsoil and assumed constant with depth.

(4) Plant water uptake is assumed to occur equally from all depths within the root-zone, and also to continue unimpaired until the "permanent wilting point" is reached. This is the concept of Veihmeyer and Hendrickson (1928), which is now generally discredited as discussed in Chapter 1. While many other more realistic models exist (e.g. see McNaughton et al. 1979) their use may not offer any significant benefit considering other assumptions made. The small number of days where there was less than 50% of available water left are given in the results later, indicating days when crops may possibly be affected by water stress. Available water is

the TWHC minus that stored in the profile at the permanent wilting (PWP). PWP is estimated from the water content at $\Psi = -1.5 \times 10^3$ kPa.

(5) Central to the operation of water balances, and the prediction of crop water use in general, is the measurement or estimation of ET. Measurement techniques such as lysimetry or the Bowen ratio energy balance approach (Tanner, 1960) require sophisticated and expensive equipment unsuitable for routine use. Furthermore, their operation is difficult in this non-uniform surface of bare soil (both wetted and dry) with isolated, aerodynamically rough, well-watered apple trees, and with interstitial areas of grass in various stages of water stress.

Several approaches to ET estimation exist. Physically based models such as the Penman - Monteith equation (Penman, 1948; Monteith, 1965) are developed considering a uniform canopy of transpiring leaves, and tend to be the most realistic. While detailed studies of physiological responses of apple trees exist (e.g. Landsberg et al. 1975), the lack of reliable data on necessary factors such as stomatal resistances, and net radiation interception by the canopy preclude the routine use of these physical models. These models can however be simplified (e.g. Priestly and Taylor, 1972). In general models such as this are developed for surfaces which bear little resemblance to an orchard. They can however be used as a basis for ET estimation by using simple reduction factors to account for the unique facets of orchard trees. Bearing in mind the above reservations, it is easiest to use empirical means to estimate ET. In view of the other uncertaintities in the water balance, errors in ET estimation are unlikely to be a limitation.

For simplicity pan evaporation (E_p) is multiplied by a reduction factor (f) to give ET. ET has often been shown to be closely correlated with E_p when crops

are well watered (Goldberg et al. 1976). In this balance ET is given by:

$$ET = f.E_p. \qquad (4.5)$$

The reduction factor, f, is affected by crop type and age, as well as climate, and also varies seasonally (Penman, 1948). For mature apple trees f = 0.8 was found adequate for trickle irrigated orchards in Israel (Shalhevet et al. 1976), while f = 0.6 has been used in Australia (Black, 1970, as reported by Jobling, 1974). A value of f = 0.8 was used here. Considering the age of the trees in this orchard, and New Zealand's temperate climate, this is likely to be an overestimate. Actual drainage was probably thus greater than calculated. Seasonal variability effects on f are neglected.

4.3 RESULTS AND DISCUSSION

Engineering aspects of the irrigation system are presented first and followed by the water balance results for the 1980-81 summer. The relationship of these results to tensiometer data, and resulting drainage calculations are also discussed. Theoretically predicted Ψ distributions and ponded zones are compared with measurements.

4.3.1 TRICKLE IRRIGATION SYSTEM

During normal operation, flow rates from randomly sampled emitters were determined to assess irrigation rates. Flow from these emitters, nominally rated at 4 l/hr were found to have a normal distribution with a mean of 4.1 l/hr and standard deviation of 0.3 l/hr. The range of flow rates, from 3.6 to 4.9 l/hr is reasonable. Six out of 22 emitters were found to spray water in jets up to heights of 0.3 m (see Figure 4.5). This frequently resulted in a small ponded zone, but an accompanying large unsaturated but spray wetted zone.

Assuming the orchard to be irrigated at 4.1 l/hr per

Fig. 4.5 Emitter during irrigation. Note the spray from the emitter and the basin like ponded zone.

emitter, with two emitters per tree on a grid spacing of 3.7 x 4.5 m results in an application rate of 2 mm per 4 hour irrigation. This figure is on a whole orchard basis. However, because of the limited area covered by ponded zones (see section 4.3.4), far higher effective application rates to the apple tree root zone occur. The average ponded radius for these flow rates is approximately 0.2 m. Here a wetted radius of 0.85 m around each emitter was chosen for water balance calculations. This may give an overestimate of the wetted area considering the size of ponded zones, and the important effect macropores play on this site (Chapter 3). With two emitters per tree a wetted radius of 0.85 m results in the fraction of the total orchard wetted to be 0.26. If only the ponded zone area was considered to be the wetted area, this fraction would be 0.015 and the irrigation rate a phenomenal 131 mm per four hour irrigation. This demonstrates the need to understand the spatial distribution of applied water when designing and operating trickle irrigation systems. A wetted proportion of 0.26 is considered adequate for a temperate climate (Keller, 1974; Keller and Karmeli, 1974). Assuming uniform flux across the whole wetted area gives an application rate of 7.3 mm per four hour irrigation.

4.3.2 WATER BALANCE CALCULATIONS

(a) General: Irrigation is generally only required to supplement rainfall in Palmerston North. Average annual rainfall from 1975-80 was 1030 mm, while average pan evaporation was 1060 mm. Annual average ET will then be less than RF, although crop requirements may exceed soil-water storage on a monthly or seasonal basis. This water balance is used to identify periods where irrigation is necessary to maximize crop yield.

(b) Model Operation: The water balance was used to estimate soil-water storage, drainage and ET for the period 1 November, 1980 to 31 March, 1981. Inputs of RF and E_p were measured at Grasslands Division, DSIR, Palmerston

North at 9 a.m. Water balance parameters and their assumed values are given in Table 4.1. Two water balance simulations are given in the following section. The first is for the irrigation regime is used in the Massey Orchard, that is irrigation every second day initially and then daily irrigation from 19 February to 22 March 1981. Irrigation was then reduced to every second day again. A second simulation using the same climate data, but with no irrigation input was also carried out. This simulation indicates if irrigation was in fact necessary during the 1980/81 season.

It is pertinent to reiterate that calculations are applied only to 26% of the orchard area, trickle irrigation wetting isolated volumes of soil.

(c) Results: Monthly summaries of the water balance components are given in Table 4.2. For the simulation with irrigation it is apparent that the sharp decline in drainage in January (i.e. St < TWHC) is due to a decrease in rainfall. November 1980 was unusually wet. With the increase in irrigation frequency in late February, drainage again becomes a significant component of the balance. Also ET declined through February to April, while rainfall remained relatively constant.

Under the irrigation schedule used this water balance suggests that only three days in this period of high ET demand had soil-water storage below 50% of the available soil-water storage. Consequently the assumption of there being no decline in ET rates until PWP is reached was of little relevance in this case. Use of the water balance with no irrigation results in drainage only in November, when rainfall exceeds ET. In the following months however soil-water storage became so depleted that ET was predicted to have dropped below the potential rate from January through to March. The high number of days where ET is predicted to be limited by soil-water storage (stress days) in January illustrates this. While this

Table 4.1 Parameters used in the water balance

Symbol	Parameter and assigned value
f	Crop factor ; 0.8
St(1)	Initial soil water storage ; 140mm on 31 Oct. 1980
I	Irrigation rate ; 7.3mm per irrigation
TWHC	Total water holding capacity ; 140mm for top 0.5m soil
PWP	Permanent wilting point ; 65mm for top 0.5m soil
z	Rooting and storage profile depth ; 0.5m

Table 4.2 Monthly table of Water Balance Components for period November 1980 to March 1981

a) Irrigation as used in the Massey Orchard

Month	Rain[1] (mm)	Irrigation[2] (mm)	Drainage[2] (mm)	ET (mm)	Stress Days[3]	Days[4] <0.5AWC	Drainage/ Irrigation (%)
November	146 (79)	110	166	93	-	-	151
December	55 (99)	110	72	103	-	-	66
January	17 (85)	120	0.3	159	-	1	0.3
February	67 (74)	130	59	116	-	2	45
March	58 (67)	200	162	93	-	-	82
Totals	343 (404)	670	459.3	564			

b) Simulation with no irrigation

Month	Rain[1] (mm)	Irrigation[2] (mm)	Drainage[2] (mm)	ET (mm)	Stress days[3]	Days[4] <0.5AWC	Drainage/ Irrigation (%)
November	146 (79)	-	53	93	-	-	-
December	55 (99)	-	-	103	-	17	-
January	17 (85)	-	-	40	24	31	-
February	67 (74)	-	-	57	12	31	-
March	58 (67)	-	-	29	18	29	-
Totals	343 (404)	-	53	322			

(1) Climatological norm (1928-1969) monthly rainfall in brackets
(2) Water depth equivalents apply to 26% of orchard area
(3) Days on which ET is less than 0.8 Ep due to soil storage being limited
(4) Days on which less than 50% of available soil-water storage exists (i.e. S<103mm)

simple balance suggests that irrigation was advantageous in the 1980-81 season, it appears as if the scheduling adopted was in excess of plant requirements and soil-water storage capacity. Drainage as a proportion of irrigation (in Table 4.2) shows this; January alone has an insignificant proportion of I leaving the profile as drainage. Also by choosing a crop factor of 0.8, ET is liable to be overestimated, and hence drainage losses underestimated.

4.3.3 ROOT-ZONE SOIL-WATER POTENTIAL DISTRIBUTIONS

A comparison of water balance components and soil-water potential data was carried out over two periods, one an eight day period in January (irrigation every second day), and one an eight day period in February (daily irrigation). Daily ET, rainfall and drainage predicted from the water balance for these two periods are shown in Figure 4.6. During this January period no drainage is predicted. However, during the February period it appears that daily irrigation has resulted in a large proportion of the irrigation water leaving as drainage. ET is variable in both periods.

Tensiometer data for three different radii from the emitter and at various depths for these two periods are presented in Figures 4.7 to 4.9. Apparent in the trace of Ψ at a depth of 0.25 m (Figure 4.7) is a marked response to irrigation every second day. Just after irrigation Ψ is high, in the region of - 2 to - 6 kPa (readings were taken just after the completion of irrigation), while on non-irrigation days Ψ is commonly around - 10 to - 15 kPa. This response to surface applied water is dampened with depth, becoming non-existent at z = 0.8 m (see Figures 4.8 and 4.9). There is also dampening of this fluctuation with increasing distance from the emitter, and Ψ is lower toward the trees. These fluctuations and dampening effects are in accord with both theory and the observations of other authors (e.g. Earl and Jury,

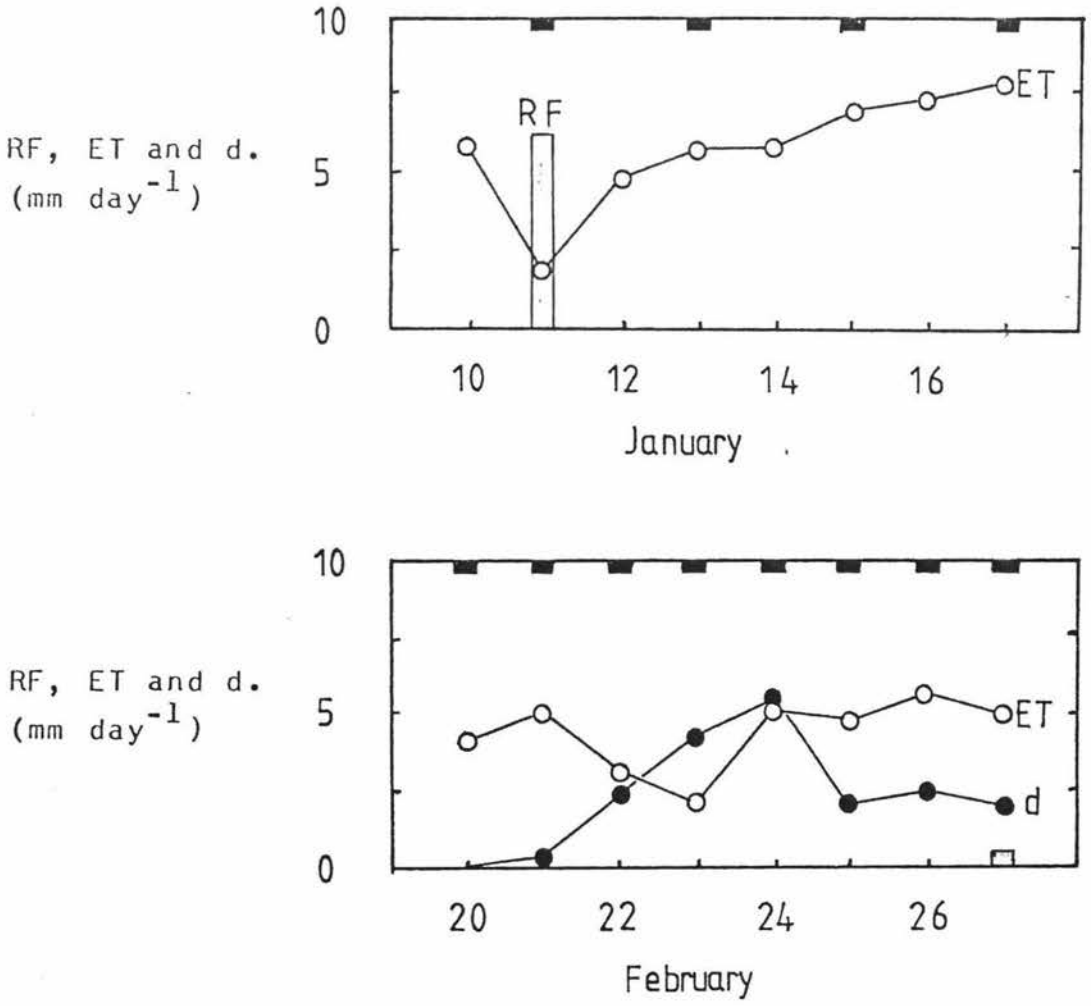

Fig. 4.6 Calculated drainage (d), evapotranspiration (ET) and rainfall (histogram) for two periods from the water balance. Irrigation events are denoted by dark histogram along the top scale.
(a) Period from 10 to 17 January. Irrigation every second day. No drainage is predicted.
(b) Period from 20 to 27 February. Daily irrigation.

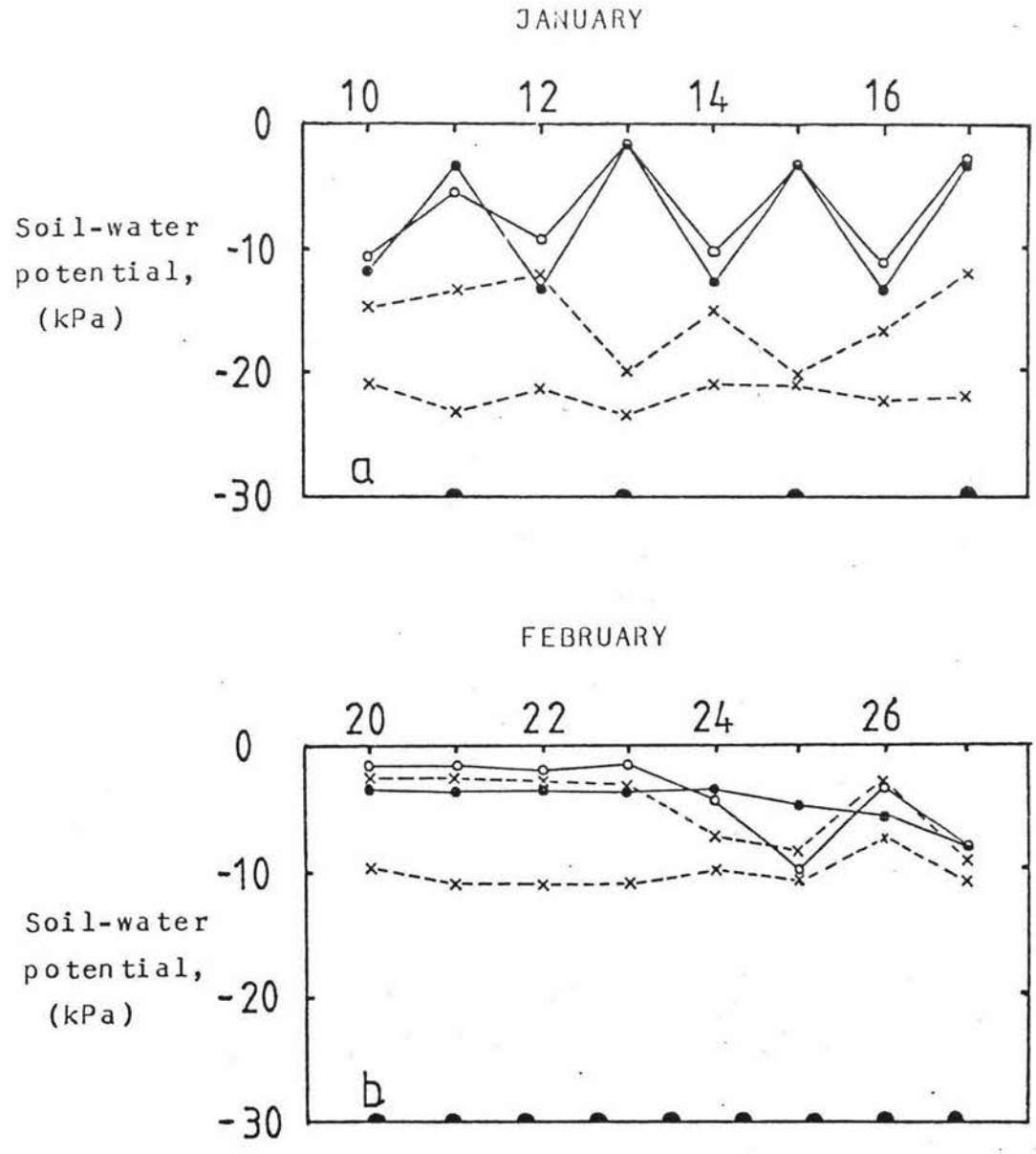

Fig. 4.7 Tensiometer response at 0.25m depth for two periods. Tensiometers are located 0.25m from the emitter (——) toward the tree, and 0.5 from the emitter (----) toward the tree. Irrigation events are denoted by ▲.

(a) Period from 10 to 17 January. Irrigation every second day.

(b) Period from 20 to 27 February. Daily irrigation.

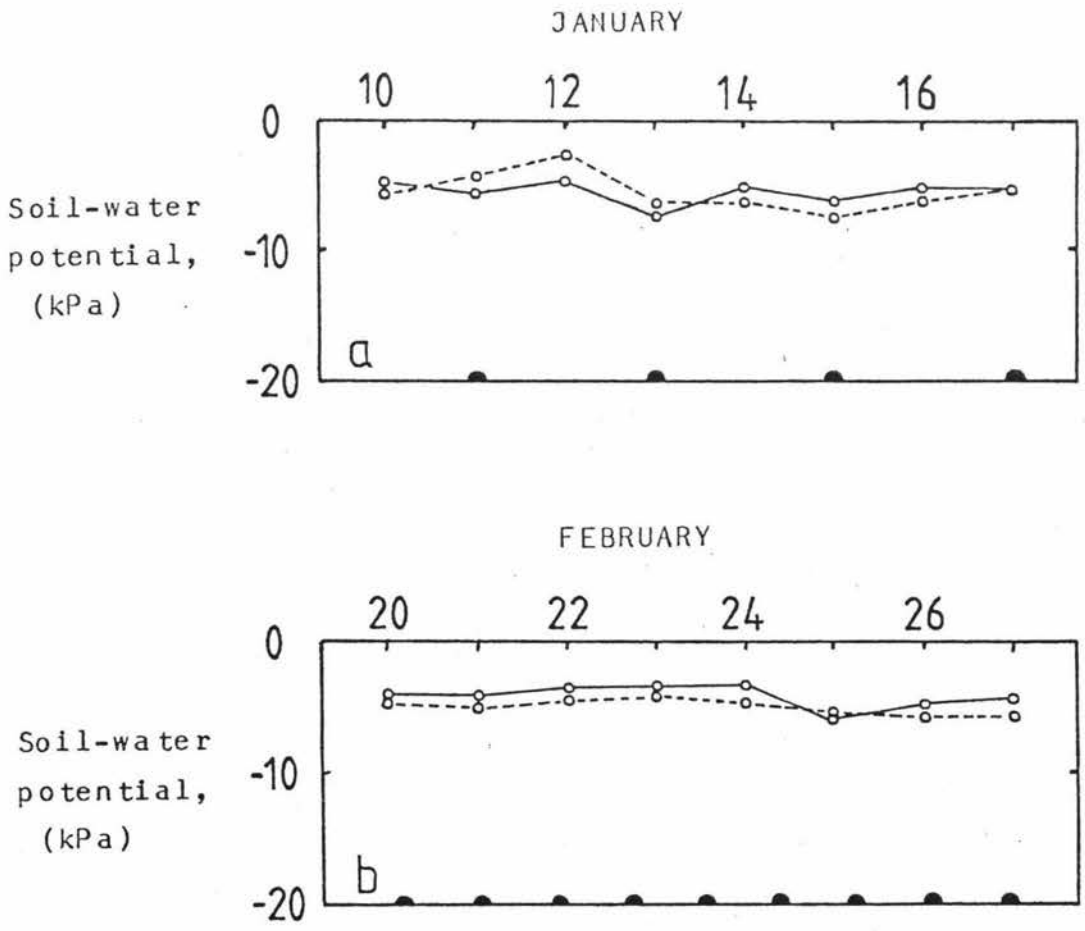

Fig. 4.8 Tensiometer response at 0.5m depth for two periods. Tensiometers are located 0.25m from the emitter (——) toward the tree, and 0.5m from the emitter (----) toward the tree. Irrigation events are denoted by ▲.

(a) Period from 10 to 17 January. Irrigation every second day.

(b) Period from 20 to 27 February. Daily irrigation.

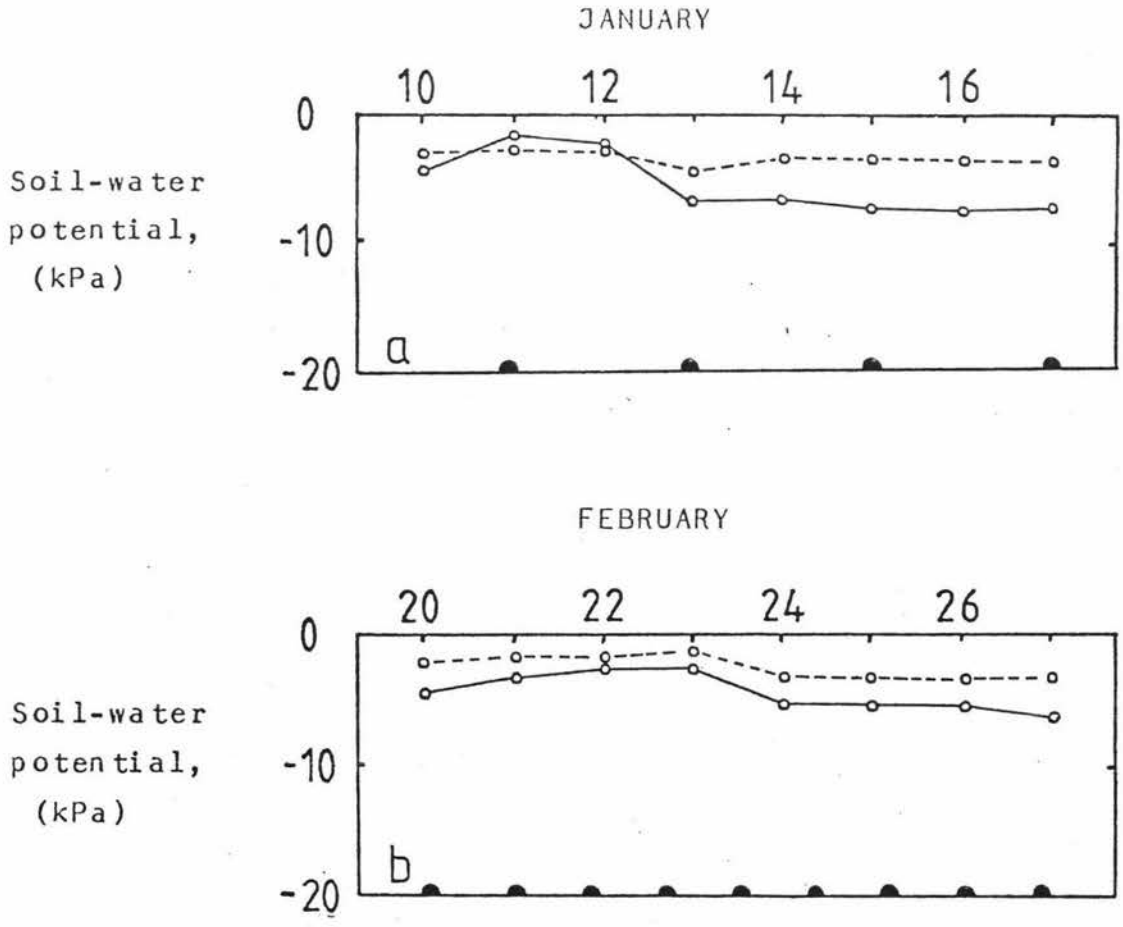

Fig. 4.9 Tensiometer response at 0.8m depth for two periods. Tensiometers are located under the emitter (——) and under the tree (----). Irrigation events are denoted by ▲.

(a) Period from 10 to 17 January. Irrigation every second day.

(b) Period from 20 to 27 January. Daily irrigation.

1977; Tsipori and Shimshi, 1979).

With the commencement of daily irrigation Ψ at all depths and distances from the emitter rose to become higher than when irrigating every second day. No consistent relationship between Ψ and ET in either period can be seen. Obviously soil-water storage (especially after irrigation) is sufficiently well buffered against such small scale changes. The increase in drainage, predicted by the water balance, with increasing irrigation frequency is reflected in increased Ψ values. Soil-water conductivity will be large at these Ψ values.

Potentials at 0.5 and 0.8 m depths in both periods are high, and tend to indicate the movement of some water to wet these lower portions of the profile. The root zone Ψ distribution for 24 February illustrates this (see Figure 4.12), Ψ at 0.8 m being in the region of - 6 kPa. On several occasions potentials wetter than - 2 kPa were recorded at 0.8 m, both under trees and emitters.

Instantaneous drainage fluxes at midday calculated from measured tensiometer data for 0.38 m in depth (Figures 4.10a and b) show large drainage fluxes. These fluxes only apply to the time at the end of irrigation (if it occured), and are calculated assuming $k_s = 5.2 \times 10^{-6} ms^{-1}$ and $\alpha = k_s/\phi_s = 7.9m^{-1}$ (from Chapter 2). In both periods it is apparent that drainage fluxes are much higher closer to the emitter. In fact at 0.5 m from the eimtter (0.25 m from the tree) drainage is negligible, slight upward fluxes being predicted in general. The magnitude of these fluxes is so small they may be due to errors in measurement of Ψ or in the conductivity values assumed. That drainage fluxes are higher closer to the emitter is predicted by many solutions (e.g. Wooding, 1968; Brandt et al. 1971). During the January period the Darcy drainage flux is only significant on irrigation days, being close to zero on non-irrigation

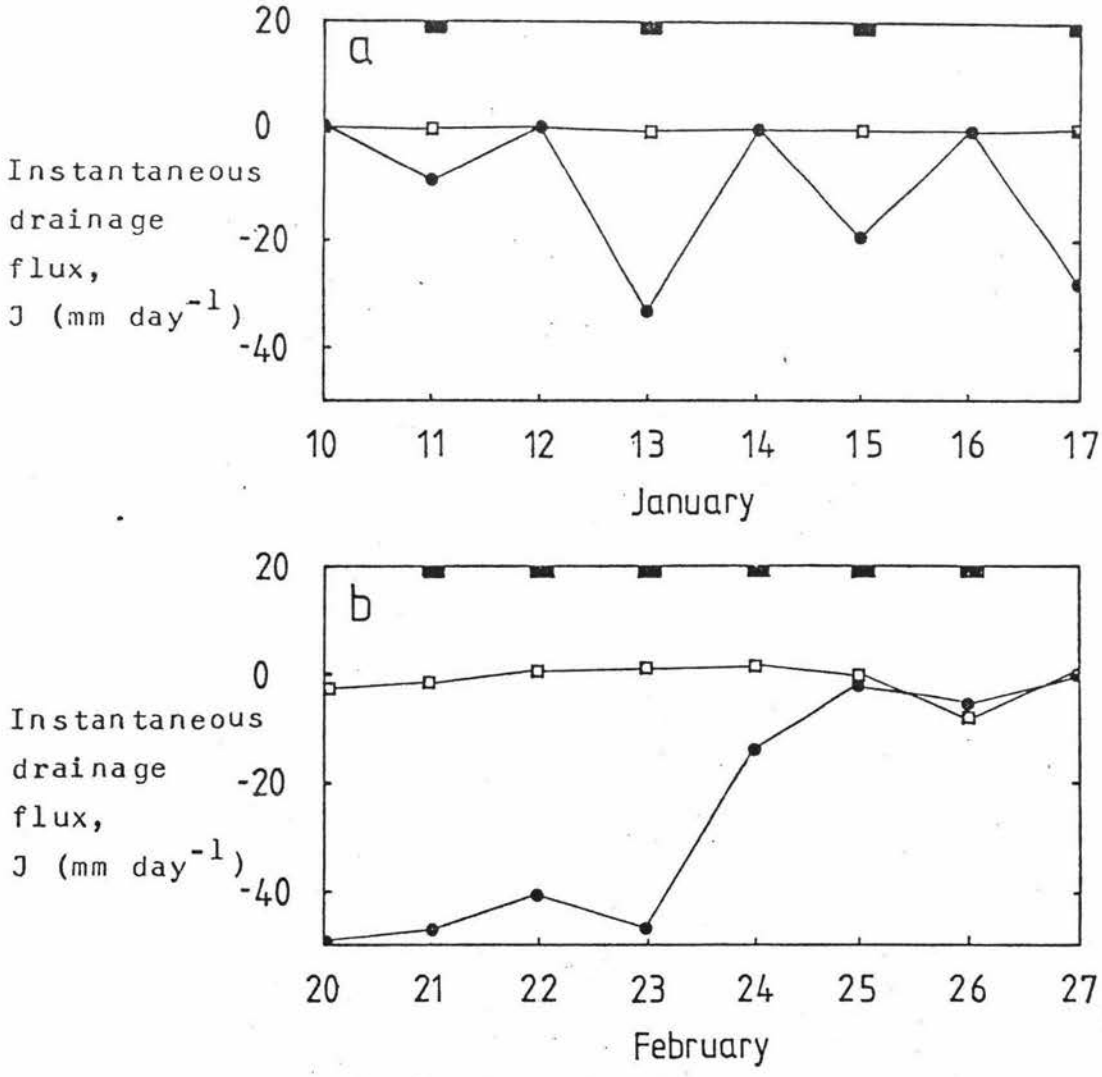

Fig. 4.10 Instantaneous drainage fluxes at 0.38m depth 0.25m from the emitter (●) and 0.5m from the emitter (□) at midday. Irrigation events are denoted by dark histogram on top scale.

(a) Period from 10 to 17 January. Irrigation every second day.

(b) Period from 20 to 27 February. Daily irrigation.

days. This is not predicted by the water balance. The water balance however, assumes both irrigation and drainage to occur evenly over a wetted area 0.85 m in radius around each emitter. It is not possible to integrate the spot measurements of the Darcy flux to form a representative estimate of total drainage. Suffice it to say that both are of the same order of magnitude and the relativity between January and February is similar. Also the water balance cannot account for flow down macropores or the high flux under the ponded zone. Both these factors may affect the tensiometer readings. Drainage is then likely to be different from that predicted by the water balance.

4.3.4 PRACTICAL USE OF INFILTRATION THEORY

In this section Wooding's (1968) steady-state linearized infiltration theory is used to predict ponded radii and Ψ distributions under trickle irrigation. These predicted values are compared with field measurements.

(a) Ponded Radii: Predicted and measured ponded radii are presented in Figure 4.11. Values of k_s and ϕ_s from the twin ring analysis are used, and predict ponded radii to a reasonable degree of accuracy, only one data point not being within the 68% confidence interval. Much of this agreement is due to the ponded radius being largely controlled by k_s.

The large degree of scatter in data points is due to spatial variation in both macropore density and surface crusting. These greatly influence the infiltration of surface applied water. In most cases the ponded zones were not circular, with micro-relief playing an important role in pond shape. Often ponded zones were more akin to basins or furrows. To a lesser extent, the irrigation system characteristics may also obstruct the use of infiltration theory. For example emitters which spray water over large surface areas consequently have ponded

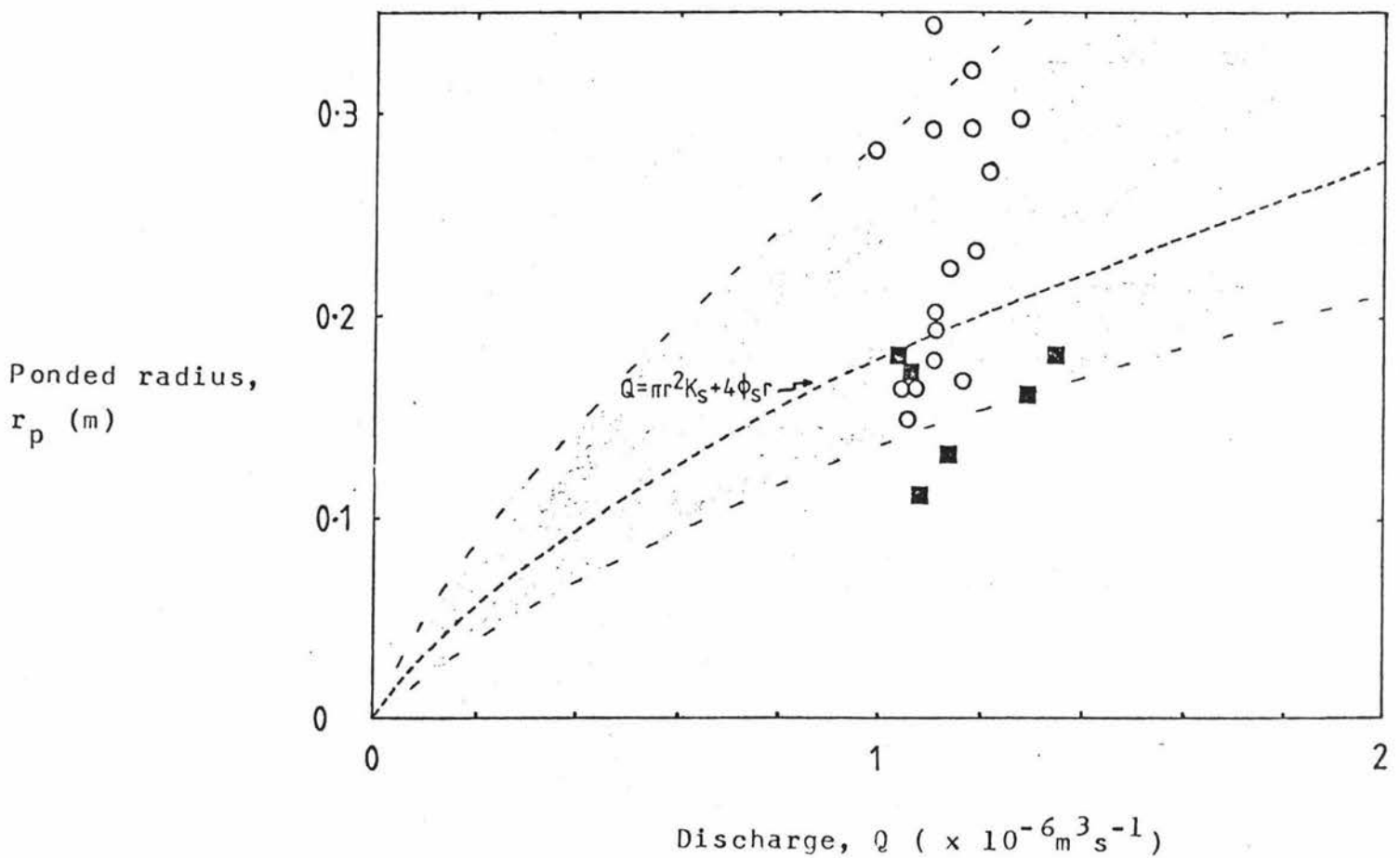

Fig. 4.11 Ponded radii from trickle emitters in the Massey Orchard in relation to predicted radii from Wooding's equation (equation 1.14) using average values of k_s and ϕ_s from the twin ring analysis. Data points are for emitters which spray water (■) and only trickle (O) water. Shaded area is the 68% confidence interval.

areas smaller than predicted.

(b) Soil-water potential distribution: Soil-water potential distributions can be deduced from Figures 6 a-g of Wooding (1968), and reproduced in part previously as Figure 1.3. Plots of the dimensionless matric flux potential (ϕ/ϕ_s) are found for various values of the non-dimensional radius $a = \alpha r_p/2$. Using the above values of k_s and α, the mean steady-state ponded radius for Q = 4.1 l/hr is found to be 0.2 m, so that $a \approx 1$. Replotting of Figure 6e of Wooding (1968) for a = 1 gives curves of constant Ψ easily, by noting that:

$$\Psi = \ln(\phi/\phi_s)\alpha^{-1}. \qquad (4.5)$$

The predicted Ψ distribution for steady-state conditions is given in Figure 4.12, along with the measured Ψ values for February 24. Measured and predicted distributions show a similarity in the magnitude and broad pattern of Ψ, but not necessarily in the details of the distribution. While plant uptake is not accommodated for by Wooding's solution, the main source of difference is more likely to be the spatial heterogeneity of soil properties. The predicted solution, which is for homogeneous soil, shows lower potentials to much greater depths than measured, and also a symmetrical form that was not found. Infiltration in this soil has already been found to be determined by macropore density to a large extent (Chapter 3). This then tends to confine drainage to those areas virtually directly below the ponded zone (Section 4.3.3). Water is often conducted rapidly down channels, and then subsequently may be absorbed into the surrounding soil mass deeper in the profile. Considering the qualitative agreement in predicting the Ψ pattern, and especially the utility of using k_s and ϕ_s or α values to predict ponded radii, Wooding's theory then appears to be useful for field trickle irrigation as proposed by Bresler (1977; 1978).

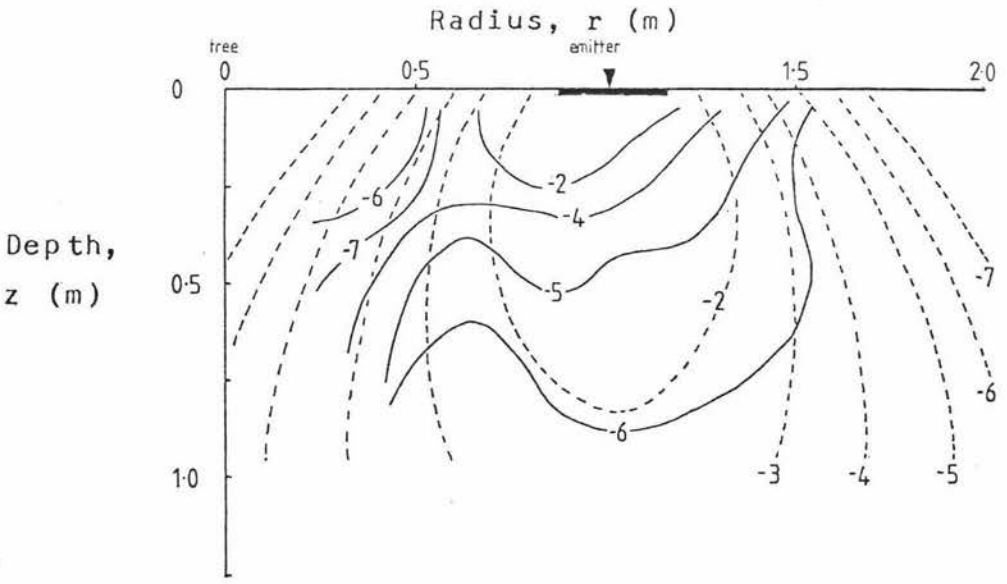

Fig. 4.12 Comparison of measured and predicted soil-water potential distributions from Wooding's (1968) solution. Solid lines are measured potentials on 24 February. Broken lines are predicted from equation (4.5) and Figure 6e of Wooding (1968) with a = 1. Figures on lines are soil-water potential values in kPa. Dark region below emitter indicates the ponded zone.

4.4 CONCLUSIONS

(1) In the 1980-81 season the Massey Orchard was probably over-irrigated. This conclusion is drawn from both the water balance predictions and measured tensiometer data. Soil-water potentials in the root-zone were never less than - 30 kPa, while root-zone Ψ would need to drop below - 50 kPa before significant water stress was encountered. In fact on many occasions potentials are near zero. With the soil this wet oxygen supply to roots may be limited, which could result in crop damage. While the simple water balance used here has it's defects, it indicates that large proportions of irrigation left the root-zone as drainage. This is in accord with the drainage estimated from the tensiometer data. Not only was an increase in irrigation frequency deemed unnecessary, but it was also instigated in a period of lower ET demand. It is suggested that water-balance irrigation schedules be developed along with monitoring of soil-water status, either by tensiometers or even neutron-probes. Irrigation scheduling should be tied to ET losses and rainfall inputs, but also should take into account the buffering offered by soil-storage.

(2) Tensiometers have been found to provide an adequate means of determining soil-water status. While some tensiometers should be installed within the root-zone, others should be installed at depth to provide an indication of drainage losses. Three tensiometers at differing depths, duplicated for two radii from the emitter should prove sufficient to measure root-zone Ψ and allow calculation of drainage fluxes.

(3) On permeable soils with high biological activity, such as this site, irrigation systems should be designed and chosen so as to minimize surface ponding. On this site surface venting macropores control infiltration to a large degree. Consequently flow down macropores leads to drainage losses into the coarse sand underlay.

While this may minimize leaching losses, application of horticultural chemicals in the irrigation water will be inefficient. Theoretical studies (e.g. Scotter, 1978) have shown that solute movement into the soil matrix from macropore flow is minimal. Groundwater pollution may also be increased. Options which may have resulted in a more suitable irrigation system for this site are now listed.

(i) The use of lower flow rates for longer times, or several low flow rate emitters for each tree. With lower flow rates the effect of gravity on vertical extension of the pattern of water distribution is lessened (Philip, 1969). More significantly the ponded radii are smaller than those obtained for higher flow rates. Thus the number of macropores liable to be intercepted is smaller, which should result in a more uniform root-zone water content distribution. Sample calculations, using Wooding's equation and values of k_s and ϕ_s for this soil from Chapter 2, in Table 4.3 illustrate this. It can be seen that an irrigation system designed to deliver one quarter the flow rate will theoretically have a ponded zone one tenth the area since capillarity effects are correspondingly greater. If a single emitter is used, the irrigation time has to be longer, and as well the chances of a mechanical malfunction or blockage are greater. Use of four emitters eliminates this, but will increase the cost of the irrigation system.

(ii) The use of irrigation systems which supply water to the soil surface at a sufficiently low rate (less than k_s) so that ponding does not occur. Low intensity sprinklers or minijets could be used for this. These come in sizes small enough to wet only the soil immediately surrounding the tree.

In both the above options more reliance is placed on the soil matrix properties, which are more spatially uniform (Clothier and White, 1981). Reliance upon the unsaturated flow of water in the soil matrix will result in a more

Table 4.3 Sample calculations for the Manawatu fine sandy loam II using Woodings equation to estimate ponded zone size.

flow rate (l/hr)	ponded zone area (m^2)	capillary contribution to flow (1) (%)
1	0.015	70
4.1	0.13	45

(1) Percentage of second term in $Q = \pi r^2 K_s + 4\phi_s r$

uniform root-zone soil-water distribution. Theory also exists which may be of use in designing and operating such irrigation systems (e.g. Philip and Knight, 1974).

(4) Wooding's (1968) theory is found to be useful in the field. Differences between predicted and measured Ψ distributions and ponded radii are in general within the range expected, considering the highly variable nature of soil properties on this site. This theory appears to be of utility in the design of trickle irrigation systems, provided that reliable field measured values of k_s and ϕ_s are available.

CHAPTER 5

CONCLUSIONS

In the preceding chapters various aspects of a simple approximation to the linearized infiltration solution of Wooding (1968) were examined. Field experiments (Chapter 3) and observation in a trickle irrigated orchard (Chapter 4) have demonstrated the utility of this theory to describe steady-state infiltration from a shallow pond of water. Ponded radii are predicted from flow rate and soil properties with a reasonable degree of success for a variety of flow rates on different soils. This success is due largely to the control the saturated hydraulic conductivity exerts over ponded zone sizes in these soils. Reasonable agreement may also be expected in soils where matric-potential gradients are significant. In view of the problems found in applying theory developed for homogeneous soil to heterogeneous soils in the field, this agreement is considered good. For example in field experiments (Chapter 3) ponded zone sizes are found to vary considerably with time, presumably from both biological activity and the blocking or eroding of pores. A two order of magnitude change in k_s was found within 12 hours during one experiment.

Water content distributions were similarly found to be affected by the dynamic nature of soil physical properties. Preferential flow down macropores was observed in both field ponding experiments, and under trickle emitters in the orchard. The effect of micro-topography in controlling ponded zone shapes was also seen to be important in this respect. Although Wooding's solution provided a reasonable estimate of soil-water potential distribution in the orchard, when steady-state conditions were approximated, no rigorous test of this solution in this respect was carried out. Soil-water potential distribution is important in maintaining plant growth, and can be manipulated by emitter discharge rate and spacing, and so may be worthy of further study.

Essential to the agreement found between experimental results and those predicted by Wooding's solution is the use of appropriate soil physical parameters measured by the twin ring method (Chapter 2). This method, which is based on Wooding's solution, was found to give realistic k_s values. When used, along with satiated matric-flux potential values, to predict ponded zone sizes, good correspondence is found as discussed above. Values of k_s measured by other techniques (i.e. well and core methods) are of less utility, and their measurement technique renders them inappropriate for trickle irrigation. Systematic errors in these methods, mainly soil disturbance and smearing, probably cause this difference. The twin ring method has the advantages of not disturbing the soil, utilizing three dimensional flow, and also concurrently measuring sorptivity or satiated matric flux potentials with k_s.

Wooding's solution and field measured parameters are of use in designing trickle irrigation systems. However, consideration should be given to the suitability of such systems. On soils such as the Manawatu fine sandy loam II, biological activity results in large surface venting macropores, which may conduct free water away from the root-zone. In cases such as this it may be best to reduce the ponded zone size by lowering application rates, or to use irrigation systems which supply water at rates less than k_s to prevent surface ponding (e.g. mini sprinklers).

Effective management is also essential to maximize the benefits of irrigation. In this study both water balance and tensiometer data indicate excess irrigation of the Massey Orchard in the 1980-81 season. As well as wasting water, this may result in leaching of soil nutrients and crop yield reductions through low soil oxygen levels. Simple techniques such as water balances and tensiometry will prove useful in scheduling irrigation.

APPENDIX I

SOIL PROFILE DESCRIPTIONS

Experimental work was carried out on four sites, three located on different phases of a naturally layered alluvial soil (the Manawatu series), and the other on the Tokomaru series, a soil developed in loess. The Manawatu series soils are similar to that described by Clothier (1977) and Clothier *et al*. (1978). The Tokomaru has previously been studied and described by Pollok (1975) and Scotter *et al*. (1979). Apart from the Manawatu sandy loam II site, which is located in the Massey University Orchard, all sites are under mixed pasture subject to periodic grazing. Brief profile descriptions are given below.

MANAWATU SANDY LOAM

Horizon (depth)	Description
Ap (0-20cm)	Dark greyish brown sandy loam; weakly developed blocky structure; many roots.
Bw (20-35cm)	Greyish brown sandy loam with a few faint mottles; very weekly developed blocky structure; some roots.
C (35-80cm)	Grey sandy loam mottled at lower boundary; few roots.
2C (80cm +)	Olive grey coarse sand; loose; single grained.

MANAWATU FINE SANDY LOAM I

Horizon (depth)	Description
Ap (0-25cm)	Dark greyish brown fine sandy loam; moderately developed medium blocky structure; many roots.
Bw (25-40cm)	Greyish brown fine sandy loam; weakly developed blocky structure; some roots.
C (40-92cm)	Olive grey fine sand with mottles at lower boundary; loose; single grained; few roots.
2C (92cm +)	Olive grey coarse sand; loose; single grained.

MANAWATU FINE SANDY LOAM II

Horizon (depth)	Description
Ap (0-18cm)	Dark greyish brown fine sandy loam; well developed medium nutty structure; many roots
Bw (18-30cm)	Dark greyish brown fine sandy loam; poorly developed blocky structure; many roots.
C (30-40cm)	Grey medium sand; loose; single grained; few roots.
2C (40-80cm +)	Grey fine sand; loose; single grained; few roots.

TOKOMARU SILT LOAM

Horizon (depth)	Description
Ap (0-25cm)	Dark greyish brown silt loam; moderately developed fine and medium crumb structure; many roots.
ABg (25-40cm)	Greyish brown light clay loam with moderate mottling; moderately developed nutty structure; many roots.
Btg (40-76cm)	Light brownish grey clay loam with many brown mottles; moderately developed blocky and prismatic structure; few roots; impeded drainage.
Cxg (76cm +)	Light olive grey and strong brown in reticulate pattern; silt loam; strongly developed coarse polygonal structure; few roots only between peds.

APPENDIX II

STATISTICAL METHODS AND SUMMARY OF EXPERIMENTAL DATA

A2.1 STATISTICAL METHODS

When a sufficiently large sample number was obtained, fractile analysis (Warrick and Nielsen, 1980) was carried out to find which frequency distribution form provided the best fit to the data. Normal, log-normal and Weibull distributions were examined. It was found that the extra calculation involved for the latter distribution was unwarranted. Regression analysis was used to give a qualitative measure of distribution fit to data.

For normal distributions, arithmetic means ($\bar{x}$) and sample standard deviations (s) are given by:

$$\bar{x} = \sum x/n, \qquad \text{(A2.1)}$$

$$s = [(\sum x - (\sum x)^2/n)/(n - 1)]. \qquad \text{(A2.2)}$$

Here x is the sample value. The probability density function (G) for a normal distribution is:

$$G(x) = (1/s.\sqrt{2\pi})\exp[-(x - \bar{x})/(2s^2)]. \qquad \text{(A2.3)}$$

For a log-normal distribution G(x) is given by;

$$G(x) = (1/x.s_{ln}.\sqrt{2\pi})\exp[-(\ln x - \bar{x}_{ln})/(2s_{ln}^2)] \qquad \text{(A2.4)}$$

where $\bar{x}_{ln}$ and s_{ln} are the arithmetic mean and standard deviation, respectively, of the log transformed data. For log-normally distributed variables a numerical value of the mean is given by;

$$\bar{x} = \exp(\bar{x}_{ln} + s^2_{ln}/2). \qquad \text{(A2.5)}$$

Error theory (Barford, 1967) suggests that the standard deviation may be approximated as;

$$s = s_{ln}\,\bar{x}. \qquad \text{(A2.6)}$$

Numerical values of the mode and median for log-normal distributions can also be found, using equations given by Warrick and Nielsen (1980).

The minimum sample size required to obtain an acceptable estimate of the mean is found from;

$$N = t_{\alpha}^2 s^2 / d^2 \qquad (A2.7)$$

where t_{α} is the Students-t with infinite degrees of freedom at the α probability level, and d is the specified acceptable error in the mean. The assumptions present in the formulation of equation A2.7 are discussed by Warrick and Nielsen (1980).

A2.2 SUMMARY OF EXPERIMENTAL RESULTS

Tables A2.1 and A2.4 give both normal and log-normal statistics for measured k_s and unbuffered flow rates from rings (Q) respectively. In both tables correlation coefficients (r_{xy}) from linear regression analysis are given for both distribution forms. The mean and standard deviation from the distribution form giving the best fit to data were used in previous calculations (i.e. Chapter 2).

Representative examples of data best described by both distribution forms are shown in Figures A2.1 and A2.2 for illustrative purposes. Figure A2.1 shows the core k_s data for the Manawatu sandy loam in both normal and log-transformed states. Here a log-normal distribution provides the best fit, as indicated by the linearity of data (and correlation coefficients). In Figure A2.2 unbuffered flow rates from rings 0.102 m in radius on the Tokomaru site are shown. Here a normal distribution provides a better description of data.

Table A2.1 Saturated Hydraulic Conductivity: Distribution Statistics

Site:	Method:	n	Normal distribution statistics			Log-normal distribution statistics		
			k_s ($\times 10^{-6} ms^{-1}$)	s ($\times 10^{-6} ms^{-1}$)	r_{xy}	k_{ln}	s_{ln}	r_{xy}
Manawatu sandy loam	Core	20	15	50	0.521	-12.4	1.2	0.895
	Well	18	2.1	0.7	0.964	-13.2	0.4	0.974
Manawatu fine sandy loam I	Core	22	42	70	0.799	-11.7	1.9	0.964
	Well	27	1.7	2	0.808	-13.6	1.0	0.991
Manawatu fine sandy loam II	Core	13	70	100	0.796	-10.9	1.7	0.948
	Well	20	1.2	1	0.864	-14.0	0.9	0.989
Tokomaru silt loam	Core	23	33	50	0.695	-10.9	1.0	0.979
	Well	12	0.34	0.2	0.909	-15.1	0.7	0.885

Table. A2.2 Unbuffered Infiltration Rates from rings (Q): Distribution Statistics

Site:	Ring radius	Normal distribution statistics			Log-normal distribution statistics		
		n	Q	s	r_{xy}	Q_{ln}	s_{ln}	r_{xy}
	(m)		(x $10^{-7}m^3s^{-1}$)	(x $10^{-7}m^3s^{-1}$)				
Manawatu sandy loam	0.037	13	0.74	0.4	0.961	-16.6	0.7	0.979
	0.049	10	0.81	0.3	0.941	-16.4	0.4	0.937
	0.075	12	2.4	1	0.945	-15.4	0.5	0.987
	0.102	20	4.7	2	0.965	-14.6	0.4	0.985
	0.18	10	12	5	0.972	-13.7	0.4	0.969
Manawatu fine sandy loam I	0.025	12	0.21	0.2	0.889	-17.9	0.7	0.947
	0.037	12	0.50	0.4	0.891	-17.0	0.7	0.989
	0.075	18	2.4	2	0.888	-15.6	0.8	0.978
	0.102	41	4.3	6	0.692	-15.1	0.9	0.979
Manawatu fine sandy loam II	0.025	13	0.77	1	0.792	-16.8	0.9	0.949
	0.037	14	1.2	0.9	0.938	-16.4	1.0	0.966
	0.075	20	3.0	2	0.947	-15.2	0.6	0.976
	0.102	23	4.1	2	0.986	-14.8	0.5	0.968
Tokomaru silt loam	0.025	12	2.0	1	0.979	-15.6	0.6	0.965
	0.037	12	3.5	2	0.990	-15.0	0.6	0.938
	0.075	12	7.0	5	0.914	-14.3	0.8	0.903
	0.102	25	11	3	0.988	-13.8	0.4	0.961
	0.204	4	22	7	-	-	-	-

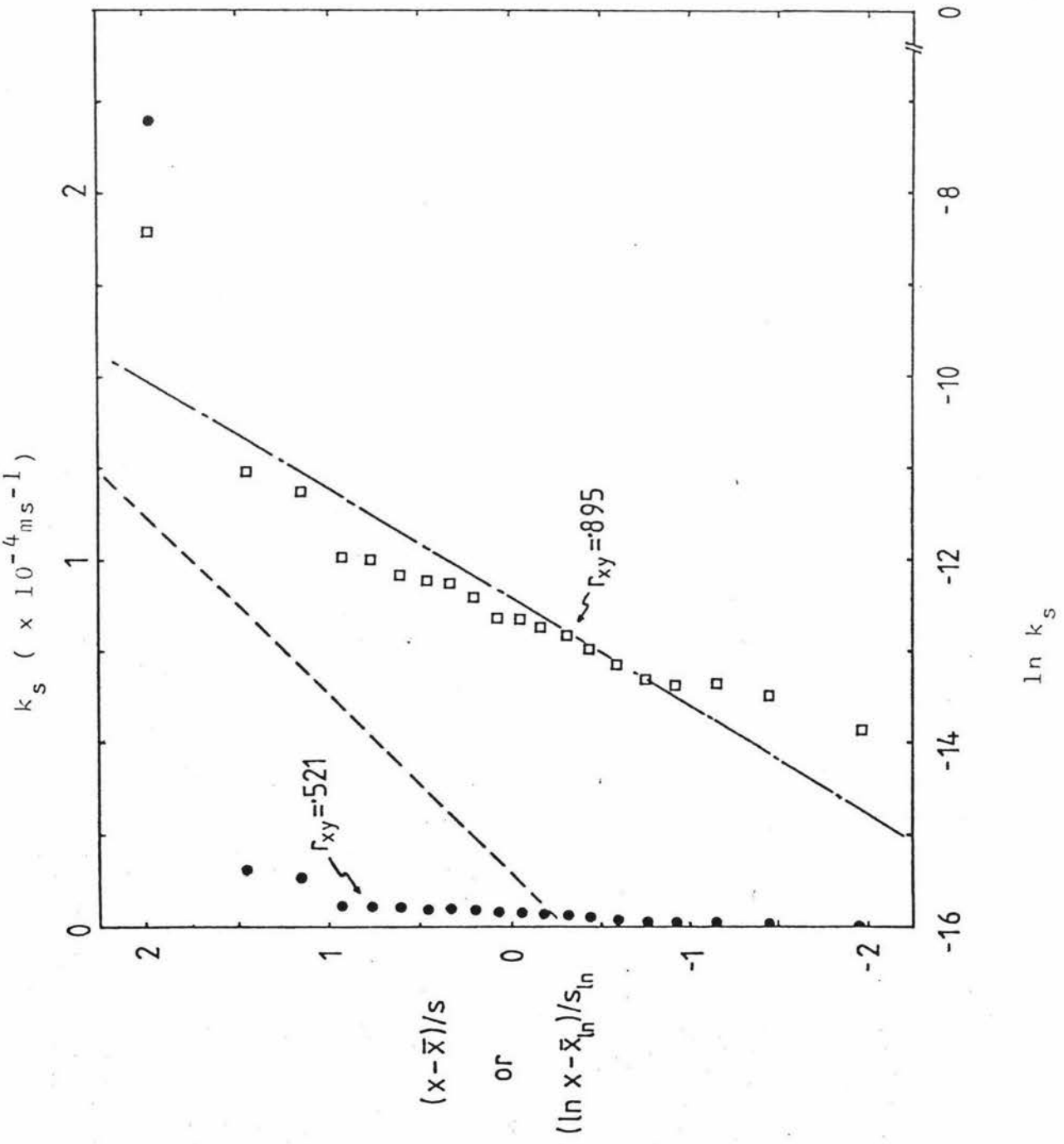

Fig. A2.1 Core permeameter k_s data from the Manawatu sandy loam. Shown are measured values (●) and log-transformed data (□). Lines shown are for ideal normal (---) and log-normal (—·—) distributions using statistics from Table A2.1. Correlation coefficients indicate a log-normal distribution to provide the best fit to data.

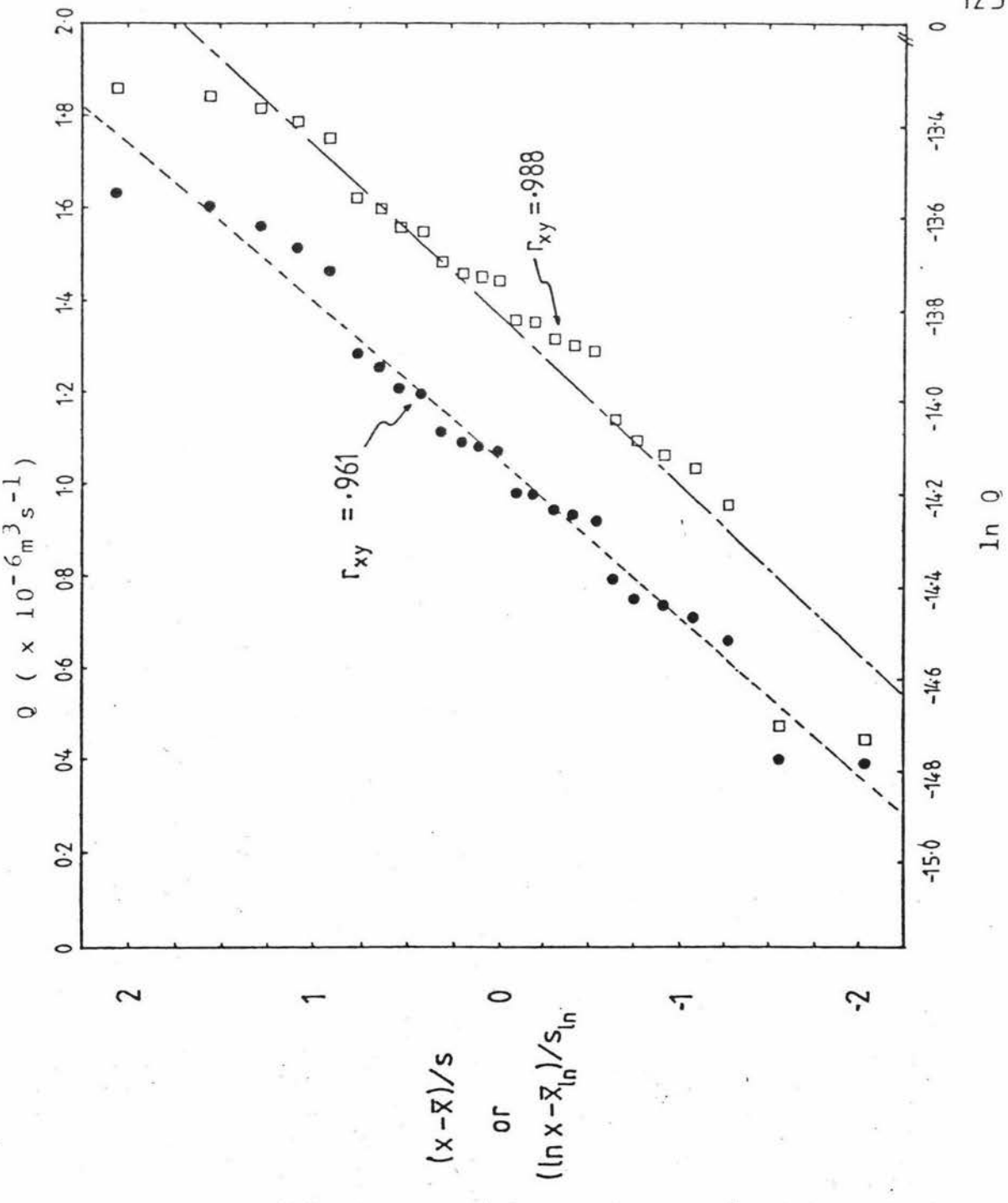

Fig. A2.2 Unbuffered infiltration rates from 0.102m radius rings on the Tokomaru silt loam. Shown are measured values (□) and log-transformed data (●). Lines shown are for ideal normal (—·—) and log-normal (----) distributions using statistics from Table A2.2. Correlation coefficients (r_{xy}) indicate a normal distribution to provide the best fit to data.

APPENDIX III

BASIC PHYSICAL PROPERTIES

A3.1 INTRODUCTION

The basic physical properties of the soil at the four sites were determined using the methods discussed below. Results are then summarized.

A3.2 METHODS

Dry bulk density, ρ_b, and particle density, ρ_s, were determined using the methods described by Gradwell and Birrell (1979). For ρ_b cylindrical aluminium cores 5 cm long and 5 cm in diameter (area ratio of 0.14: Loveday, 1974) were used. No obvious compaction of samples was observed. Cores were kept at field moisture contents by sealing in plastic bags. Antecedent water contents, for experiments in Chapters 2 and 3, were then determined by oven drying to 105°C. Porosity, p, was calculated from ρ_b and ρ_s using simple relationships given by Hillel (1980).

Water contents at -10, -100 and -1.5×10^3 kPa were found using the pressure plate apparatus. Clods approximately 1.5 cm high, trimmed smooth at the base, were used at -10 and -100 kPa. A thin layer of soil between the clod and plate was used to ensure hydraulic continuity. For the -1.5×10^3 kPa determinations disturbed soil was used, packed into rings 5 cm in diameter to a height of approximately 1 cm. The structural condition of the sample usually has a negligible effect on the -1.5×10^3 kPa retentivity (Elrick and Tanner, 1955). Samples were maintained at field moisture prior to use of the pressure plates, when they were saturated. Equilibriation times ranged from seven days for -10 kPa determinations, to two weeks for -1.5×10^3 kPa samples.

Satiated water contents, θ_s, for ponded infiltration experiments were determined by sampling the top centimetre of soil just after ponded water disappeared, and then oven drying (to 105°C) the sample. Errors in θ_s, and also retentivity data, are due to both measurement errors, and errors in ρ_b.

A3.3 RESULTS

Fractile analysis of θ_s and γ_b indicates that these parameters are normally distributed, in accord with other authors observations (e.g. Cassel and Bauer, 1975). Sample sizes for other parameters are too small to permit fractile analysis, but it is expected that normal distribution statistics provide an adequate description. Mean values, standard deviations, and minimum sample sizes required to be within 10% of the mean at a 0.05 confidence level, N, for γ_b, γ_s, θ_s and retentivity data for the four sites are shown in Table A3.1.

All these parameters show trends expected with texture change. Retentivities are highest, and γ_b and γ_s lowest in the Tokomaru, where biological activity is greatest and the texture is the finest. Sample sizes required to be within 10% of the true mean are small, as expected, all these parameters being either low or medium variation properties (Warrick and Nielsen, !980). It is worth noting that θ_s is larger than p in two sites, the Manawatu sandy loam and the Manawatu fine sandy loam I. While this may be in part due to errors in γ_b and γ_s, sampling of "oversaturated" soil is thought to be the main cause.

Table A3.1 Basic Physical Properties

Site:		Bulk density (x 10^3kg m^{-3})	Particle density (x 10^3kg m^{-3})	Porosity	Satiated water content	θ at -10 kPa	θ at -100 kPa	θ at -1.5 x 10^3 kPa
Manawatu sandy loam	mean	1.55	2.56	0.39	0.43	0.19	0.18	0.09
	s	0.07	0.09	-	0.06	0.02	0.06	0.01
	$n^{(1)}$	36	6	-	36	5	6	5
	$N^{(2)}$	1	1	-	8	9	75	10
Manawatu fine sandy loam I	mean	1.48	2.56	0.42	0.44	0.28	0.20	0.14
	s	0.09	0.1	-	0.06	0.03	0.03	0.03
	$n^{(1)}$	43	6	-	44	6	6	6
	$N^{(2)}$	2	1	-	7	8	15	31
Manawatu fine sandy loam II	mean	1.39	2.53	0.45	0.43	0.28	0.22	0.13
	s	0.06	0.06	-	0.06	0.02	0.02	0.01
	$n^{(1)}$	43	10	-	40	5	6	6
	$N^{(2)}$	1	1	-	8	4	6	4
Tokomaru silt loam	mean	1.15	2.52	0.54	0.46	0.30	0.26	0.18
	s	0.05	0.07	-	0.05	0.04	0.03	0.03
	$n^{(1)}$	25	7	-	21	6	6	6
	$N^{(2)}$	1	1	-	5	12	9	19

(1) n is sample size

(2) N is sample size required to be within 10% of the true mean at a 0.05 confidence level.

BIBLIOGRAPHY

Ahuja, L.R., S.A. El-Swaify and A. Rahman. 1976. Measuring hydrologic properties of soils with a double-ring infiltrometer and multiple-depth tensiometers. Soil Sci. Soc. Am. J. 40: 494-499.

Aronovici, V.S. 1955. Model study of ring infiltrometer performance under low intitial soil moisture. Soil Sci. Soc. Am. Proc. 19: 1-6.

Baier, G and G.W. Robertson. 1968. A new versatile soil moisture budget. Canadian J. Plant Sci. 46: 299-315.

Barford, N.C. 1967. Experimental Measurements: Precision, Error and Truth. Addison - Wesley. London.

Bar-Yosef, B. and M.R. Sheikholslami. 1976. Distribution of water and ions in soils irrigated and fertilized from a trickle source. Soil Sci. Soc. Am. J. 40: 575-582.

Batu, V. 1977. Steady infiltration from a ditch. Theory and experiment. Soil Sci. Soc. Am. J. 41: 677-682.

Batu, V. 1978. Steady infiltration from single and periodic strip sources. Soil Sci. Soc. Am. J. 42: 544-549.

Ben-Asher, J., D.O. Lomen and A.W. Warrick. 1978. Linear and non-linear models of infiltration from a point source. Soil Sci. Soc. Am. J. 42: 3-6.

Ben-Asher, J. 1979. Errors in determination of the water content of a trickle irrigated soil volume. Soil Sci. Soc. Am. J. 43: 665-668.

Bernstien, L. and L.E. Francois. 1973. Comparison of drip, furrow and sprinkler irrigation. Soil Sci. 115: 73-76.

Black, J.D.F and D.W. West. 1974. Water uptake by an apple tree with various portions of the root system supplied with water. Proc 2nd. Inter. Drip Irrig. Congr. (San Diego) 432-433.

Bond, W.J. and N. Collis-George. 1981. Ponded infiltration into simple soil systems: 3. The behaviour of infiltration rate with time. Soil Sci. 131: 327-333.

Bouma, J., A. Jongerius and D. Schoonderbeck. 1979. Calculation of saturated hydraulic conductivity of some pedal clay soils using micromorphometric data. Soil Sci. Soc. Am. J. 43:261-264.

Bouma, J. 1981. Soil morphology and preferential flow along macropores. Agric. Water Management 3: 235-250.

Bouma, J. and L.W. Dekker. 1981. A method for measuring the vertical and horizontal k_{sat} of clay soils with macropores. Soil Sci. Soc. Am. J. 45: 662-663.

Bouwer, H. 1966. Rapid field measurement of air-entry value and hydraulic conductivity of soil as significant parameters in flow system analysis. Water Resour. Res. 2: 729-738.

Bouwer, H. and R.D. Jackson. 1974 Determining soil properties. In Drainage for Agriculture. J. Van Schilfgaarde (Ed) Am. Soc. Agron. Wisconsin.

Brandt, A., E. Bresler, N. Diner, I. Ben-Asher, J. Heller and D. Goldberg. 1971. Infiltration from a trickle source: I. Mathematical models. Soil Sci. Soc. Am. Proc. 35: 675-682.

Bresler, E., J. Heller, N. Diner, I. Ben-Asher, A. Brandt and D. Goldberg. 1971. Infiltration from a trickle source: II. Experimental data and theoretical predictions. Soil Sci. Soc. Am. Proc. 35:683-689.

Bresler, E. and D. Yaron. 1972. Soil water regime in economic evaluation of salinity in irrigation. Water Resour. Res. 8: 791-800.

Bresler, E. 1975. Two-dimensional transport of solutes during non-steady infiltration from a trickle source. Soil Sci. Soc. Am. Proc. 39:604-613.

Bresler, E. and D. Russo. 1975. Two-dimensional solute transfer during non-steady infiltration: Laboratory test of mathematical model. Soil Sci. Soc. Am. Proc. 39: 585-587.

Bresler, E. 1977. Trickle-drip irrigation: Principles and application to soil-water management. Advan. Agron. 29: 343-393.

Bresler, E. 1978. Analysis of trickle irrigation with application to design problems. Irrig. Sci. 1: 3-17.

Brutsaert, W. 1979. Universal constants for scaling the exponential soil-water diffusivity. Water Resour. Res. 15: 481-483.

Bucks, D.A., L.J. Erie and O.F. French. 1974. Quantity and frequency of trickle and furrow irrigation for efficient cabbage production. Agron. J. 66: 53-57.

Bucks, D.A., F.S. Nakayama and A.W. Warrick. 1982. Principles, practices and potentialities of trickle (drip) irrigation. Advances in Irrig. 1: 219-297.

Cassel, D.K. and A. Bauer. 1975. Spatial variability in soils below depth of tillage: bulk density and fifteen atmosphere percentage. Soil Sci. Soc. Am. Proc. 39: 247-250.

Cassel, D.K., and L.A. Nelson. 1981. Selection of variables to be used in statistical analysis of field-measured soil-water content. Soil Sci. Soc. Am. J. 45: 1007-1012.

Celestre, P. 1964. Drop irrigation system. Trans. 8th. Int. Congr. Soil Sci. (Bucharest) 471-487.

Clothier, B.E. 1977. Aspects of the water balance of an oats crop grown on a layered soil. PhD thesis. Massey University, New Zealand.

Clothier, B.E., D.R. Scotter and J.P. Kerr. 1977. Drainage flux in permeable soil underlain by a coarse-textured horizon. Soil Sci. Soc. Am. J. 41: 671-676.

Clothier, B.E., J.A. Pollock and D.R. Scotter. 1978. Mottling in soil profiles containing a coarse-textured horizon. Soil Sci. Soc. Am. J. 42: 761-763.

Clothier, B.E. and I. White. 1981. Measurement of sorptivity and soil-water diffusivity in the field. Soil Sci. Soc. Am. J. 45: 241-245.

Clothier, B.E. and D.R. Scotter. 1982. Constant-flux infiltration from a hemispherical cavity. Soil Sci. Soc. Am. J. 46: 696-700.

Curtis, A.A. and K.K. Watson. 1979. Infiltration and redistribution of water from a trickle source. Irrigation Efficiency Seminar (Sydney, Australia) 425-435.

Dane, J.H. 1980. Comparison of field and laboratory determined hydraulic conductivity values. Soil Sci. Soc. Am. J. 44: 228-231.

Dirksen, C. 1975. Determination of soil-water diffusivity by sorptivity measurement. Soil Sci. Soc. Am. Proc. 39: 22-27.

Dirksen, C. 1978. Transient and steady flow from subsurface line sources at constant hydraulic head in anisotropic soil. Trans. ASAE 21: 913-919.

Dirksen, C. 1979. Flux-controlled sorptivity measurements to determine soil hydraulic property functions. Soil Sci. Soc. Am. J. 43: 827-834.

Eagleman, J.R. and V.C. Jamieson. 1962. Soil layering and compaction effects on unsaturated moisture movement. Soil Sci. Soc. Am. Proc. 26: 519-522.

Earl, K.D. and W.A. Jury. 1977. Water movement in bare and cropped soil under isolated trickle emitters. II. Analysis of cropped soil experiments. Soil Sci. Soc. Am. J. 41: 856-861.

Elrick, D.E. and C.B. Tanner. 1955. Influence of sample pre-treatment on soil moisture retention. Soil Sci. Soc. Am. Proc. 19: 279-282.

Elrick, D.E. and M.J. Robin. 1981. Estimating the sorptivity of soils. Soil Sci. 132: 127-133.

F.A.O. 1977. Water for Agriculture. Food and Agric. Organ. of the U.N. UN Water Confr., Mar del Plata.

Fleming, P.M. and D.E. Smiles. 1975. Infiltration of water into soils. Prediction in Catchment Hydrology. Aust. Acad. Sci. 83-109.

Freeburg, R.S., D.J. Cotter and N.S. Urquhart. 1974. An explaination of the growth advantage of drip irrigation. Proc. 2nd. Inter. Drip. Irrig. Congr. (San Diego) 265-270.

Freeman, B.M., J. Blackwell, and K.V. Garzoli. 1976. Irrigation frequency and total water application with trickle and furrow systems. Agric. Water Manag. 1: 21-31.

Frith, G.J.T. and D.G. Nichols. 1974. Effects of nitrogen fertilizer applications to part of a root system. Proc. 2nd. Inter. Drip Irrig. Congr. (San Diego) 434-436.

Fritschen, L.J. and L.W. Gay. 1979. Environmental Instrumentation. Springer-Verlag. N.Y.

Gardner, W.R. 1958. Some steady-state solutions of the unsaturated moisture flow equation with application to evaporation from a water table. Soil Sci. 85: 228-232.

Gardner, W.R. 1964. Water movement below the root zone. Int. Congr. Soil Sci. Trans. 8th. (Bucharest, Rumania) II: 63-68.

Gardner, W.R. and A.A. Millar. 1973. Plant response to field water balance. Soil Moisture and Irrig. Studies II: 143-147.

Gilley, J.R. and E.R. Allred. 1974. Irrigation and root extraction from subsurface irrigation laterals. Trans. ASAE 17: 927-933.

Goldberg, D. and M. Shmueli. 1970. Drip irrigation - A method used under arid and desert conditions of high water and soil salinity. Trans. Am. Soc. Ag. Eng. 33: 38-41.

Goldberg, D., B. Gornat and D. Rimon. 1976. Drip irrigation. Drip Irrig. Soc. Publication. Israel.

Gradwell, M.C. and K.S. Birrell. 1979. Methods for Physical Analysis of Soil. N.Z. Soil Bureau Report 10c.

Green, W.H. and G.A. Ampt. 1911. Studies on soil physics I: The flow of air and water through soils. J. Agric. Sci. 4: 1-24.

Gur, A., S. Dasberg, I. Schkolnik, E. Sapir and M. Peled. 1979. The influence of method and frequency of irrigation on soil aeration and some biochemical responses of apple trees. Irrig. Sci. 1: 125-134.

Hachum, A.Y., J.F. Alfaro and L.S. Willardson. 1976. Water movement in soil from trickle sources. J. Irrig. and Drainage Div. 179-192.

Hewett, E.W. 1976. Apple tree irrigation on the Moutere Hills, Nelson. Proc. Soil and Plant Water Symp. (Palmerston North, N.Z.) 118-125.

Hiler, E.A. and T.A. Howell. 1973. Grain sorghum response to trickle and subsurface irrigation. Trans. ASAE 16: 799-803.

Hillel, D. 1980. Fundamentals of Soil Physics. Academic Press. N.Y.

Howell, T.A., D.S. Stevenson, F.K. Aljubury, H.M. Gitlin, I.P. Wu, A.W. Warrick and P.A.C. Raats. 1980. Design and operation of trickle (drip) systems. In Design and Operation of Farm Irrigation Systems. M.E. Jensen. (Ed.). Am. Soc. Agric. Eng. Michigan.

Hsiao, T.C. 1973. Plant response to water stress. Ann. Rev. Plant Physiol. 24: 519-570.

Jaynes, D.B. and E.J. Tyler. 1980. Comparison of one-step outflow laboratory method to an in situ method for measuring hydraulic conductivity. Soil Sci. Soc. Am. J. 44:903-907.

Jensen, M.E. 1980. Introduction. In Design and Operation of Farm Irrigation Systems. M.E. Jensen (Ed.) Am. Soc. Agric. Eng. Michigan.

Jobling, G.A. 1974. Trickle irrigation design manual - Part 1. N.Z. Agric. Eng. Inst. Lincoln College, N.Z.

Journel, S.G. and Ch. J. Huijbregts. 1978. Mining Geostatistics. Academic Press, London.

Keller, J. 1974. Trickle irrigation design for optimal soil wetting. Proc. 2nd Int. Drip Irrig. Cong. (San Diego) 240-245.

Keller, J. and D. Karmeli. 1974. Trickle irrigation design. 1st Ed. Rain Bird Sprinkler Mfg. Co. Glendora, California.

Klute, A. 1972. The determination of hydraulic conductivity and diffusivity of unsaturated soils. Soil Sci. 113: 264-276.

Landsberg, J., C.L. Beadle, P.V. Briscoe, D.R. Butler, B. Davidson, L.D. Inull, G.B. James, P.G. Jarvis, P.J. Martin, R.E. Nielsen, D.B.B. Powell, E.M. Slack, M.R. Thorpe, N.C. Turner, B. Warrit and W.R. Watts. 1975). Diurnal water, energy and CO_2 exchanges in an apple (Malus Pumila) orchard. J. Appl. Ecol. 12: 659-684.

Levin, I., R. Assaf and B-A. Bravdo. 1974. Soil Moisture distribution and depletion in an apple orchard irrigated by tricklers. Proc. 2nd Int. Drip Irrig. Congr. (San Diego) 252-257.

Levin, J., P.C. van Rooyen and F.C. van Rooyen. 1979. The effect of discharge rate and intermittent water application by point-source irrigation on the soil moisture distribution pattern. Soil Sci. Soc. Am. J. 43: 8-16.

Lomen, D.O. and A.W. Warrick. 1974. Time dependent linearized infiltration: II. Line sources. Soil Sci. Soc. Am. Proc. 38: 568-572.

Lomen, D.O. and A.W. Warrick. 1976. Time dependent linearized moisture flow solutions for surface sources. In System Simulation in Water Resources. G.C. van Steenkiste (Ed.). North Holland.

Lomen, D.O. and A.W. Warrick. 1978a. Solution of the one-dimensional linear moisture flow equation with implicit water extraction functions. Soil Sci. Soc. Am. J. 42: 342-344.

Lomen, D.O. and A.W. Warrick. 1978b. Linearized moisture flow with loss at the soil surface. Soil Sci. Soc. Am. J. 42: 396-400.

Loveday, J. 1974. Methods for Analysis of Irrigated Soils. Tech. Comm. No 54. CAB. Farnham - Royal.

Maaledj, M. and L. Malavard. 1973. Resolutions analogiques et numeriques do problems d'irrigation des sols par canaux equidistants. C.R. Acad. Sci. Paris Ser. A 276: 1433-1436.

McNaughton, K.G., B.E. Clothier and J.P. Kerr. 1979. Evaporation from Land Surfaces. In Physical Hydrology - New Zealand Experience. D.L. Murray and P. Ackroyd (Eds.). N.Z. Hydrological Society.

Marshall, T.J. and G.B. Stirk. 1950. The effect of lateral movement of water in soil on infiltration measurements. Aust. J. Agric. Res. 1: 253-265.

Marshall, T.J. 1958. A relation between permeability and the size distribution of pores. J. Soil Sci. 9: 1-8.

Merrill, S.D., P.A.C. Raats and C. Dirksen. 1978. Laterally confined flow from a point-source at the surface of an inhomogeneous soil column. Soil Sci. Soc. Am. J. 42: 851-857.

Montieth, J.L. 1965. Evaporation and environment. In The State and Movement of Water in Living Organisms. G. Fogg (Ed.). Soc. of Exp. Biology Symp. No 19. Cambridge Univ. Press. 205-234.

Mostaghimi, S., J.K. Mitchell and W.D. Lembke. 1981. Effect of discharge rate on distribution of moisture in heavy soils irrigated from a trickle source. Am. Soc. Agric. Engineers Meeting (St. Johseph, Michigan).

Mualem, Y. 1976. A new model for predicting the hydraulic conductivity of unsaturated porous media. Water Resour. Res. 12: 513-521.

Nielsen, D.R., J.W. Biggar and K.T. Erh. 1973. Spatial variability in field measured properties. Hilgardia 42: 215-260.

Nye, P.H. 1979. Diffusion of ions and uncharged solutes in soils and soil clays. Adv. Agron. 31: 225-272.

Parlange, J-Y. 1971. Theory of water movement in soils: 1. One-dimensional absorption. Soil Sci. 111: 134-137.

Parlange, J-Y. 1973. Theory of water movement in soils: 3. Two and three dimensional absorption. Soil Sci. 112: 313-317.

Parlange, J-Y. 1974. Gravity correction due to a variation of pressure head within a cavity. Soil Sci. Soc. Am. Proc. 38: 15-17.

Parlange, J-Y. 1975. On solving the flow equation in unsaturated soils by optimization: Horizontal infiltration. Soil. Sci. Soc. Am. Proc. 39: 885-892.

Parr, J.F. and A.R. Bertrand. 1960. Water infiltration into soils. Advan. Agron. 12:311-363.

Passioura, J.B. 1976. Determining soil-water diffusivities from one-step outflow experiments. Aust. J. Soil Res. 15: 1-8.

Peck, A.J. and T. Talsma, 1968. Some aspects of two dimensional infiltration. Trans. 9th. Int. Congr. Soil. Sci. (Adelaide). I: 11-21.

Penman, H.L. 1948. Natural evaporation from open water, bare soil and grass. Roy. Soc. London Proc. Ser. A 193: 120-146.

Philip, J.R. 1957. The theory of infiltration: 1. The infiltration equation and its solution. Soil Sci. 83: 345-347.

Philip, J.R. 1966. Absorption and infiltration in two- and three-dimensional systems. Proc. UNESCO/Netherland Govt. Symp. "Water in the Unsaturated Zone" Wageningen. 1: 503-525.

Philip, J.R. 1968a. Extended techniques of calculation of soil-water movement, with some physical consequences. Trans. 9th. Int. Cong. Soil Sci. (Adelaide). I: 1-9.

Philip, J.R. 1968b. Steady infiltration from buried point sources and spherical cavities. Water Resour. Res. 4: 1039-1047.

Philip, J.R. 1969. Theory of infiltration. Advan. Hydrosci. 5: 215-296.

Philip, J.R. 1971. General theorem on steady infiltration from surface sources with application to point and line sources. Soil Sci. Soc. Am. Proc. 35: 867-871.

Philip, J.R. 1972. Steady infiltration from buried surface, and perched point and line sources in heterogeneous soils.I. Analysis. Soil Sci. Soc. Am. Proc. 36: 268-273.

Philip, J.R. 1973. On solving the unsaturated flow equation: 1. The flux-concentration relation. Soil Sci. 116: 328-335.

Philip, J.R. and J.H. Knight. 1974. On solving the unsaturated flow equation: 3. New quasi-analytical technique. Soil Sci. 117: 1-13.

Philip, J.R. and R.I. Forrester. 1975. Steady infiltration from buried, surface and perched point and line sources in heterogeneous soils: II. Flow details and discussion. Soil Sci. Soc. Am. Proc. 39: 408-418.

Philip, J.R. 1980. Field heterogeneity. Water Resour. Res. 16: 443-448.

Pollok, J.A. 1975. A comparitive study of certain New Zealand and German soils formed from loess. Ph.D. Thesis. Friedrich-Wilhelms-Universitat, Bonn.

Priestly, C.H.B. and R.J. Taylor. 1972. On the assessment of surface heat flux and evaporation using large scale parameters. Monthly Weather Rev. 100: 81-92.

Raats, P.A.C. 1970. Study infiltration from line sources and furrows. Soil Sci. Soc. Am. Proc. 34: 709-714.

Raats, P.A.C. 1971. Steady infiltration from point sources, cavities and basins. Soil Sci. Soc. Am. Proc. 35: 689-694.

Raats, P.A.C. 1972. Steady infiltration from sources at arbitrary depth. Soil Sci. Soc. Am. Proc. 36: 399-401.

Raats, P.A.C. 1974. Steady flows of water and salts in uniform soil profiles with plant roots. Soil Sci. Soc. Am. Proc. 38: 717-722.

Raats, P.A.C. 1976. Analytical solutions of a simplified flow equation. Trans. ASAE 19: 683-689.

Raats, P.A.C. 1977. Laterally confined, steady flow of water from sources and to sinks in soils. Soil Sci. Soc. Am. J. 41: 294-304.

Raats, P.A.C and A.W. Warrick 1980. Soil water dynamics. In Design and Operation of Farm Irrigation Systems, M.E. Jensen (Ed.). Am. Soc. Agron. Eng. Michigan.

Rawlins, S.L. 1973. Principles of managing high frequency irrigation. Soil Sci. Soc. Am. Proc. 37: 626-629.

Rawlins, S.L. and P.A.C. Raats. 1975. Prospects for high frequency irrigation. Science 188: 604-610.

Rogowski, A.S. 1972. Watershed physics: Soil variability criteria. Wat. Resour. Res. 8: 1015-1023.

Rose, C.W., W.R. Stern and J.E. Drummond. 1965. Determination of hydraulic conductivity as a function of depth and water content for a soil in situ. Aust. J. Soil Res. 3: 1-9.

Roth, R.L. 1974. Soil moisture distribution and wetting pattern from a point source. Proc. 2nd. Inter. Drip Irrig. Congr. (San Diego) 246-251.

Rubin, J. 1966. Theory of rainfall uptake by soils initially drier than their field capacities and its application. Water Resour. Res. 2: 739-749.

Salter, P.J. and J.E. Goode. 1967. Crop Responses to Water. CAB. Farnham - Royal.

Scotter, D.R. 1976. Field capacity and available soil water. Proc. Soil and Plant Water Symp. (Palm.Nth) 3-11.

Scotter, D.R. 1978. Preferential solute movement through larger soil voids: I. Some computation using simple theory. Aust. J. Soil Res. 16: 257-267.

Scotter, D.R., B.E. Clothier and R.B. Corker. 1979. Soil water in a Fragiaqualf. Aust. J. Soil Res. 17: 443-453.

Shalhevet, J., A. Mantell, H. Bielorai and D. Shimshi. 1976. Irrigation of Field and Orchard Crops under Semi-Arid Conditions. Int. Irrig. Inform. Centre. Bet Dagan.

Sharma, M.L., D.R. Williamson and A.J. Peck. 1980a. Characterization of Soil Hydraulic Properties of a Catchment. Land and Stream Salinity Seminar (Murdoch University, Australia) 23.1-23.3.

Sharma, M.L., G.A. Gander and G.G. Hunt. 1980b. Spatial variability of infiltration in a watershed. J. Hydrol. 45: 101-122.

Sisson, J.B., A.H. Ferguson and M. Th. van Genuchten. 1980. Simple method for predicting drainage from field plots. Soil Sci. Soc. Am. J. 44: 1147-1152.

Slatyer, R.O. 1969. Physiological significance of internal water relations to crop yield. In Physiological Aspects of Crop Yield. J.D. Eastin, F.A. Haskins, C.Y. Sullivan, C.H.M. van Bavel(Eds.). Am. Soc. Agron. Wisconsin.

Soil Survey Staff. 1975. Soil Taxonomy. Handbook No 436. U.S.D.A. Washington.

Sojka, R.E. and L.H. Stolzy. 1980. Soil oxygen effects on stomatal response. Soil Sci. 130: 350-358.

Swartzendruber, D. and T.C. Olsen. 196la. Sand-model studies of buffer effects in a double-ring infiltrometer. Soil Sci. Soc. Am. Proc. 25: 5-8.

Swartzendruber, D. and T.C. Olsen. 1961b. Model study of the double-ring infiltrometer as affected by depth of wetting and particle size. Soil Sci. 92: 219-225.

Talsma, T. 1969. Infiltration from semi-circular furrows in the field. Aust. J. Soil Res. 7: 277-284.

Talsma, T. 1970. Some aspects of three-dimensional infiltration. Aust. J. Soil Res. 8: 179-184.

Talsma, T. and P.M. Hallam. 1980. Hydraulic conductivity measurement in forest catchments. Aust. J. Soil Res. 30: 139-148.

Tanner, C.B. 1960. Energy balance approach to evapotranspiration from crops. Soil Sci. Soc. Am. Proc. 24: 1-9.

Thomas, A.W., E.G. Kruse and H.R. Duke. 1974. Steady infiltration from line sources buried in the soil. Trans. ASAE 17: 115-128.

Thomas, A.W., H.R. Duke, D.W. Zachman and E.G. Kruse. 1976. Comparisons of calculated and measured capillary potentials from line sources. Soil Sci. Soc. Am. J. 40: 10-14.

Thomas, A.W., H.R. Duke and E.G. Kruse. 1977. Capillary potential distribution in root zones using subsurface irrigation. Trans. ASAE 20: 62-67.

Thomas, G.W. and R.E. Phillips. 1979. Consequences of water movement in macropores. J. Environ. Qual. 8: 149-152.

Tsipori, Y. and D. Shimshi. 1979. The effect of trickler line spacing on yield of tomatoes. Soil Sci. Soc. Am. J. 48: 1225-1228.

Veihmeyer, F.J. and A.H. Hendrickson. 1927. Soil moisture conditions in relation to plant growth. Plant Physiol. 2: 71-78.

Vieira, S.R., D.R. Nielsen and J.W. Biggar. 1981. Spatial variability of field-measured infiltration. Soil Sci. Soc. Am. J. 45: 1040-1048.

Warrick, A.W. 1974. Time-dependent linearized infiltration: I. Point sources. Soil Sci. Soc. Am. Proc. 38: 383-386.

Warrick, A.W. and D.O. Lomen. 1976. Time-dependent linearized infiltration: III. Strip and disc sources. Soil Sci. Soc. Am. Proc. 40: 639-643.

Warrick, A.W. and A. Amoozergar-Fard. 1977. Soil-water regimes near porous cup water samplers. Water Resour. Res. 131: 203-207.

Warrick, A.W. and D.O. Lomen. 1977. Flow from a line source above a shallow water table. Soil Sci. Soc. Am. J. 41: 849-852.

Warrick, A.W., G.J. Mullen and D.R. Nielsen. 1977. Predictions of the soil water flux based on field measured soil-water properties. Soil Sci. Soc. Am. J. 41: 14-19.

Warrick, A.W., A. Amoozergar-Fard and D.O. Lomen. 1979. Linearized moisture flow from line sources with water extraction. Trans. ASAE 22: 549-553.

Warrick, A.W. and D.R. Nielsen. 1980. Spatial variability of soil physical properties in the field. In Applications of Soil Physics. D. Hillel (Ed.). Academic Press, N.Y.

Watts, F.C., H.F. Huckle, and R.F. Paetzold. 1982. Field vs. laboratory determined hydraulic conductivities of some slowly permeable horizons. Soil Sci. Soc. Am. J. 46: 782-784.

White, I. 1979. Measured and approximate flux-concentration relations for absorption of water by soils. Soil Sci. Am. J. 43: 1074-1079.

Wooding, R.A. 1968. Steady infiltration from a shallow circular pond. Water Resour. Res. 4: 1259-1273.

Zachman, D.W. and A.W. Thomas. 1973. A mathematical investigation of steady infiltration from line sources. Soil Sci. Soc. Am. Proc. 37: 495-500.

Zangar, C.N. 1953. Theory and Problems of Water Percolation. Bur. Reclaim. Eng. Monograph No. 8. Colorado.

Zur, B. and D. Savaldi. 1977. Infiltration under a pulsed water application I. The nature of the flow system. Soil Sci. 124: 127-134.